

Biochemical and Functional Characterization of  
the Mitochondrial Immune Signaling Protein Complex

Yu Lei

A dissertation submitted to the faculty of the University of North Carolina at Chapel Hill  
in partial fulfillment of the requirements for the degree of Doctor of Philosophy in the  
Curriculum of Oral Biology, School of Dentistry.

Chapel Hill

2011

Approved by,

Mentor: Dr. Jenny P.-Y. Ting, Ph.D.

Reader: Dr. Joseph A. Duncan, M.D., Ph.D.

Reader: Dr. Patrick M. Flood, Ph.D.

Reader: Dr. Mark T. Heise, Ph.D.

Reader: Dr. Steven Offenbacher, D.D.S., Ph.D.

**©2011  
YU LEI  
ALL RIGHTS RESERVED**

## **ABSTRACT**

### **YU LEI: Biochemical and Functional Characterization of the Mitochondrial Immune Signaling Protein Complex (Under the Direction of Dr. Jenny P.-Y. Ting)**

The mitochondrion has emerged as a crucial organelle where key anti-viral responses including apoptosis, type 1 interferon (IFN-I) production and autophagy are regulated. A prime example is the intersection of the mitochondrial protein MAVS with the RLR (RIG-I-like receptors) to induce IFN-I. Here we show that MAVS is a pro-apoptotic protein independent of its function in initiating IFN-I production. Viral proteins such as NS3/4A encoded by HCV and NSP15 encoded by SARS-CoV inhibit this response. MAVS-mediated IFN-I is tightly regulated by an NLR (nucleotide-binding domain, leucine-rich repeats containing) protein NLRX1. More in-depth analysis utilizing cells from gene-deletion mice indicates that NLRX1 not only attenuates IFN-I production, it additionally promotes autophagy during viral infection. This dual regulatory function of NLRX1 parallels the previously described functions of Atg5-Atg12, although NLRX1 does not associate with Atg5-Atg12. High throughput quantitative mass spectrometry and biochemical analysis revealed a novel NLRX1-interacting partner, mitochondrial Tu translation

elongation factor (TUFM/P43/EF-Tu/COXPD4/ EF-TuMT), which does interact with Atg5-Atg12. Similar to NLRX1, TUFM potently inhibits RLR signaling and promotes autophagy during a viral infection. This thesis demonstrates the dual roles of MAVS in controlling both IFN-I and apoptosis, and establishes the first link between an NLR protein and a viral-induced autophagic machinery via TUFM.

*This work is dedicated to my father*

**Dr. Lin Lei, M.D.**

## **ACKNOWLEDGEMENT**

Being trained at Dr. Jenny P.-Y. Ting's laboratory and the curriculum of Oral Biology is certainly a privilege, which has benefited me tremendously since the first day of my graduate school and will enlighten my entire career in the forthcoming years. I am very grateful for my mentor Dr. Ting, who is also a wonderful mother of two successful and caring daughters. I not only benefit from your insightful vision and great knowledge as a pioneer in science but also the vast latitude you allow me to explore. You have tailored my graduate training to be highly individualized and efficient. I would not achieve anything without the time and efforts you dedicated to my training. I appreciate your continuous encouragement and highly value your enthusiastic endeavor in nurturing the next generation scientists in academic medicine. It is a great pleasure and honor to be your student.

I feel very fortunate to have a superb thesis committee including top-notch immunologists, virologists, dentist-scientist and physician-scientist. Drs. Joseph A. Duncan, Patrick M. Flood, Mark T. Heise, Steven Offenbacher have not only helped me to develop my potential and succeed in graduate school but also set up role models for me in various disciplines. When I feel confused about career choice, I never panic because I know they have given me an answer by being passionate scientists,

visionary leaders, knowledgeable teachers, caring doctors and honorable persons. Their insightful guidance, wise advice, generous support and encouragement are invaluable assets that I am fortunate enough to possess.

Some work presented in this dissertation has been published or in press, I appreciate the highly collaborative research environment at UNC-Chapel Hill. I would like to sincerely thank all the co-authors of my papers, especially Dr. Haitao Wen, for your scientific expertise and enduring friendship. I very much enjoy communicating science with you and I am looking forward to many wonderful years beyond.

In the past twelve years of my dental and science education, I am fortunate to have been trained by the very best experts in each discipline. I am extremely grateful for Drs. Qianming Chen, Salvador Nares, David Paquette, Zhengyan Wang, Xuedong Zhou and Zhimin Zhu for their extensive clinical expertise and intensive training, efficient guidance, continuous career support and eternal friendship.

I am also extremely indebted to my father, who sacrificed his time dedication to his career as a physician for my education ever since I was born. I feel heartbroken to know you were diagnosed with cancer during my graduate training. I could hardly imagine how much pain you have suffered from physical disease and geographic separation with your only son. I appreciate your tremendous efforts in

allowing me to continue my graduate study although I know you need me at bedside.

I would have not achieved anything without your education and eternal love.

I am also very grateful for my mother. You never complained I did not spend much time with you because of my busy work schedule, I only spent several days with you in the past five years, your understanding and tolerance with my working habits are always with me through the up and down time in my life. I also wholeheartedly thank my step-mother, thank you so much for taking good care of my father while I am on the other end of the world. I deeply appreciate your generous care for me. Last but not least, I need to thank my little sister Xiaxi Lei, and my best friends Dr. Tao Gao, Ran Jin, Ningqi Hou, Gaoyang Liang, Shen Shen, Yuying Xie, Xingmei Yang, Shaoping Zhang, Dr. Yanping Zhang and his wife Mrs. Aiwen Jin for the joy you have brought to me.

## TABLE OF CONTENTS

LIST OF TABLES .....	xi
LIST OF FIGURES .....	xii
LIST OF ABBREVIATIONS .....	xiv
CHAPTER ONE INTRODUCTION .....	1
1.1 The evolution of mitochondria .....	2
1.2 The functions of mitochondrial protein in apoptosis .....	3
1.3 Recognition of nucleic acid species .....	5
1.4 The significance of immune adaptors trafficking in host innate antiviral responses .....	11
1.5 An overview of the NLR protein family .....	13
1.6 Functions of NLR proteins in the modulation of MAVS-RLR signaling ..	20
1.7 The regulatory components of the RLR signaling pathways .....	27
CHAPTER TWO MAVS-MEDIATED APOPTOSIS AND ITS INHIBITION BY VIRAL PROTEINS .....	39
2.1 Abstract .....	40
2.2 Introduction .....	41
2.3 Results .....	45
2.4 Conclusion .....	64

2.5	Materials and Methods	70
CHAPTER THREE NLRX1 AND TUFM FORM A MITOCHONDRIAL COMPLEX THAT REGULATES TYPE 1 INTERFERON AND AUTOPHAGY		
3.1	Abstract	77
3.2	Introduction	78
3.3	Results	80
3.4	Conclusion	100
3.5	Materials and Methods	107
CHAPTER FOUR DISCUSSION AND FUTURE DIRECTION		
4.1	Viruses can subvert MAVS-dependent type 1 IFN production	118
4.2	Viruses target apoptotic signaling	120
4.3	Tu translation elongation factors are versatile proteins	123
4.4	Future directions	128
4.5	Concluding remarks	135
REFERENCES		136

## LIST OF TABLES

Table 1.1	The modulators of RLR signaling .....	28
Table 3.1	The peptides sequences matching TUFM were identified in both NLRX1 full-length group and NLRX1 $\Delta$ LRR mutant group .....	88
Table 4.1	NLRX1 interactome .....	134

## LIST OF FIGURES

Figure 1.1	NLR proteins signal through different multimeric protein complexes	20
Figure 1.2	NLR proteins and regulation of the RLR signaling	23
Figure 1.3	NOD2 signaling bifurcates into antibacterial and antiviral effector arms	26
Figure 2.1	MAVS induces cell death	46
Figure 2.2	MAVS expression leads to apoptosis	48
Figure 2.3	The kinetics of MAVS expression and MAVS-induced apoptosis	50
Figure 2.4	Confirmation of MAVS knockout by Western Blot	51
Figure 2.5	MAVS is essential for virus-induced apoptosis in primary mouse embryonic fibroblasts	52
Figure 2.6	Distinct MAVS domains are required for apoptosis	54
Figure 2.7	Expression test of MAVS truncation mutants	55
Figure 2.8	MAVS, $\Delta$ IRIG-I and MDA5 plus Poly (I:C) induce increased transcription of <i>IFNB1</i> and <i>IFNA4</i>	57
Figure 2.9	MAVS-induced apoptosis is independent of type 1 IFNs production	59
Figure 2.10	IFN- $\beta$ neutralizing antibody is able to block the function of secreted IFN- $\beta$	60
Figure 2.11	MAVS-induced apoptosis does not depend on IRF3	62
Figure 2.12	SARS-CoV proteins were expressed in HEK293T cells	63
Figure 2.13	The SARS-CoV NSP15 protein abrogates MAVS-induced apoptosis	64
Figure 2.14	A proposed model for the dual functions of MAVS	67
Figure 3.1	Confirmation of gene deletion	81

Figure 3.2	NLRX1 inhibits VSV-induced IFN-I	82
Figure 3.3	TUFM interacts with NLRX1	84
Figure 3.4	NLRX1 interactome subcellular localization	86
Figure 3.5	Mass Spectrometry identification of the TUFM peptides	87
Figure 3.6	TUFM is ubiquitously expressed in multiple cell and tissue types	89
Figure 3.7	TUFM is evolutionarily conserved	91
Figure 3.8	Both NLRX1 and TUFM are mitochondrial proteins	92
Figure 3.9	TUFM inhibits RIG-I mediated type 1 IFN production	94
Figure 3.10	Confirmation of TUFM knockdown by shRNA	95
Figure 3.11	NLRX1 is essential for VSV-mediated autophagy	98
Figure 3.12	TUFM associates with the Atg5-Atg12 conjugate	101
Figure 3.13	Protocol for subcellular fractionation	102
Figure 4.1	Papain-like protease inhibits MAVS-mediated apoptosis	130
Figure 4.2	PLP inhibits polyubiquitination of MAVS	131
Figure 4.3	MAVS contains 14 lysine residues	132

## LIST OF ABBREVIATIONS

<b>5'-ppp dsRNA</b>	5'-triphosphate bearing double-stranded RNA
<b>ANT</b>	Adenine Nucleotide Transporter
<b>Apaf-1</b>	Apoptotic Protease Activating Factor-1
<b>Atg</b>	Autophagy-related proteins
<b>Bcl-2</b>	B-cell lymphoma 2
<b>CARD</b>	Caspases Activation and Recruitment Domain
<b>CATERPILLER</b>	caspase activation and recruitment domains [CARD], transcription enhancer, R [purine]-binding, pyrin, lots of leucine repeats
<b>CoV</b>	Coronavirus
<b>Cyt c</b>	Cytochrome c
<b>DAMP</b>	Damage-Associated Molecular Patterns
<b>DAP-3</b>	Death-Associated Protein 3
<b>DENV</b>	Dengue Virus
<b>dsRNA</b>	Double Stranded RNA
<b>EF-Tu</b>	Translation Elongation Factor Tu
<b>ER</b>	Endoplasmic Reticulum
<b>ESI-Q-TOF</b>	Electrospray-quadrupole-time of flight
<b>FACS</b>	Fluorescence-Activated Cell Sorting

<b>FBS</b>	Fetal Bovine Serum
<b>GFP</b>	Green Fluorescent Protein
<b>HAV</b>	Hepatitis A virus
<b>HBV</b>	Hepatitis B Virus
<b>HBX</b>	Hepatitis B Virus X Protein
<b>HCV</b>	Hepatitis C Virus
<b>HSV-1</b>	Herpes Simplex Virus type 1
<b>IFN</b>	Interferon
<b>IPI</b>	International Protein Index
<b>IRF3</b>	Interferon Regulatory Factor 3
<b>LC</b>	Liquid Chromatography
<b>LCMV</b>	Lymphocytic Choriomeningitis Virus
<b>LPS</b>	Lipopolysaccharide
<b>LRR</b>	Leucine Rich Repeats
<b>MAM</b>	Mitochondria-Associated ER Membrane
<b>MAVS</b>	Mitochondrial Antiviral Signaling Protein
<b>MCMV</b>	murine cytomegalovirus
<b>MDA5</b>	Melanoma differentiation-associated gene 5
<b>MDP</b>	Muramyl Dipeptide
<b>MEF</b>	Mouse Embryonic Fibroblast

**MOI** Multiplicity of Infection

**MOMP** Mitochondrial Outer Membrane Permeabilization

**NBD** Nucleotide Binding Domain

**NLR** Nucleotide binding domain, Leucine rich repeats containing proteins

**NLRX1** Nucleotide binding domain, Leucine rich repeats containing proteins  
member X1

**nt** Nucleotide

**PAMP** Pathogen Associated Molecular Pattern

**pDC** Plasmacytoid Dendritic Cells

**PRR** Pattern Recognition Receptor

**PT** Permeability Transition

**RIG-I** Retinoic-acid-inducible gene

**RLR** Rig-I-like Receptor

**ROS** Reactive Oxygen Species

**rRNA** Ribosomal RNA

**RT-PCR** Reverse Transcriptase Polymerase Chain Reaction

**SARS** Severe Acute Respiratory Syndrome

**SDS-PAGE** Sodium Dodecyl Sulfate Polyacrylamide Gel Electrophoresis

**SEC** Size Exclusion Chromatography

**SEM** Standard Error of the Mean

<b>SeV</b>	Sendai Virus
<b>shRNA</b>	short-hairpin RNA
<b>TBK1</b>	TANK-binding Kinase 1
<b>TLR</b>	Toll-like Receptor
<b>TMRE</b>	tetramethylrhodamine ethylester
<b>TUFM</b>	Tu Translation Elongation Factor, mitochondrial
<b>UPLC</b>	Ultra Performance Liquid Chromatography
<b>VDAC</b>	Voltage-Dependent Anion Channel
<b>vFLIP</b>	Viral FLICE-inhibitory Protein
<b>VSV</b>	Vesicular Stomatitis Virus
<b>WNV</b>	West Nile Virus
<b>XTT</b>	2,3-bis-(2-methoxy-4-nitro-5-sulfohenyl)-2H-tetrazolium-5-carboxanilide

## **CHAPTER ONE**

### **INTRODUCTION**

## 1.1 The evolution of mitochondria

It was about one century ago when the serial endosymbiosis hypothesis was put forth to explain the origin of mitochondria <sup>1</sup>, which has drawn support from numerous contemporary studies. The prokaryotic origin of mitochondrion postulated in this hypothesis makes it the cellular power plant which also sustains three basic life functions: rapid response to insults (type 1 interferons and reactive oxygen species production) <sup>2,3</sup>, adaptation to the environmental nutrition supply (autophagy) <sup>4</sup> and active self-elimination to maintain homeostasis at an organismal level (apoptosis) <sup>5,6</sup>.

It is postulated that when an ancient species of alphaproteobacteria became an endosymbiont, this novel organelle in eukaryotes is subjected to constant interactions with host factors. Through co-evolution, the genetic material of bacterial ancestor of mitochondria has been transferred to host nucleus <sup>7</sup>; similarly mitochondria incorporate the protein import system to integrate nucleus-encoded proteins <sup>8</sup>. The membranes of mitochondria not only anchor a plethora of molecules engaged in bioenergetic functions, innate immune activation, metabolic balances and apoptotic signaling, but also sustain the biogenesis of other organelles, such as autophagosomes, mitochondria-associated endoplasmic reticulum membrane structure and peroxisomes <sup>4, 9, 10</sup>. Mitochondrial membrane fusion and fission as well as their continuity and fluidity with other membrane structures are emerging as potent regulatory factors of the host defense mechanisms.

This review focuses on the immune-regulatory functions of mitochondria, which center on the cooperation between immune-activating mitochondrial adaptor proteins,

their upstream pathogen recognition receptors (PRRs) and the regulatory complexes. These regulatory proteins employ diverse mechanisms to keep the mitochondria-based immune signaling in-check. However, these mechanisms can be hijacked by various viruses to evade host immune surveillance.

## **1.2 The functions of mitochondrial proteins in apoptosis**

Mitochondria are emerging as a critical signaling platform for apoptosis, dysregulation of which is closely associated with the pathogenesis of numerous diseases such as cancer, degenerative diseases and infectious diseases. The central roles of mitochondria in apoptotic signaling have been defined by the process of mitochondrial outer membrane permeabilization (MOMP), leading to the release of proteins from the intermembrane space to the cytosol. MOMP is closely associated with the dissipation of mitochondrial inner membrane potential ( $\Delta\psi_m$ ), which marks a point-of-no-return in apoptosis<sup>11, 12</sup>. A key event in the mitochondrial apoptotic signaling pathway is the release of cytochrome c (Cyt c), which was initially identified as an activator of the initiator caspase-9<sup>13</sup>. Indeed, Cyt c-deficient MEFs (mouse embryonic fibroblasts) are resistant to a variety of apoptotic stimuli<sup>14</sup>. In this process, released Cyt c is bound to Apaf-1 (apoptotic protease activating factors) via its WD40 domains, which oligomerize and recruit caspase-9 in the presence of ATP/dATP to form a wheel-shaped multimeric protein complex coined the apoptosome<sup>15</sup>.

Several models have been proposed for the pathogenesis of MOMP<sup>12</sup>. The first is mediated by the formation of permeability transition (PT) pores in the mitochondrial

inner membrane, which allows the passage of small molecules up to around 1.5kD<sup>16</sup>. PT opening is triggered by either mitochondrial matrix swelling or  $\Delta\psi_m$  collapse. In some hypothetical models, the mitochondrial inner membrane protein, ANT (adenine nucleotide transporter), or the outer membrane protein, VDAC (voltage-dependent anion channel), may associate with multiple proteins to facilitate PT formation<sup>12</sup>. However, recent evidence also suggests either protein may be dispensable for PT-mediated apoptosis or preferentially plays a role in necrotic signaling<sup>17-19</sup>. The second is mediated by the Bcl-2 family members. The ones with multiple BH (Bcl-2 homology) domains, such as Bax and Bak, are mediators of MOMP; and their deficiency results in the failure to respond to a variety of apoptotic stimuli<sup>20</sup>.

Although the two apoptotic mechanisms involve different components of mitochondrial membranes to induce the release of Cyt c, it has been noted that the secondary rupture of mitochondrial outer membrane also could lead to PT establishment; similarly Bax-dependent, PT-independent MOMP could result in Cyt c release, which is remarkably rapid and complete<sup>21</sup>. However, the mitochondrial intermembrane space only sequesters 15-20% of total Cyt c, while a large proportion of Cyt c resides in the tubular cristae located within the mitochondrial inner membrane<sup>21</sup>. Although it is possible that Cyt c stored on the cristae could be released to the intermembrane space with PT opening, however, significant amount of Cyt c could be detected in the cytosol before mitochondrial matrix swelling<sup>21</sup>. The complete extent of Cyt c release could be partially explained by the mitochondrial ultrastructure changes during apoptosis. The

individual cristae could be fused together, resulting in the opening of inter-cristae junction. Such morphological changes are PT-dependent, however, could occur before mitochondrial matrix swelling <sup>22</sup>.

### **1.3 Recognition of nucleic acid species**

One of the primary functions of the innate defense system is to differentiate “self” from “non-self”, which heavily relies on several classes of extracellular and intracellular sensors to detect pathogen-associated molecular patterns (PAMPs) and/or other danger signals. Since Charles Janeway predicted the existence of pattern recognition receptors (PRRs) to engage their respective ligands and trigger immune activation <sup>23</sup>, the body of knowledge in innate sensing has grown exponentially. Toll-like receptors (TLRs) represent the first identified class of PRRs <sup>24</sup>, which are type I integral membrane glycoproteins that share an N-terminal extracellular leucine-rich-repeats (LRR) domain and a C-terminal cytoplasmic Toll/IL-1R (TIR) signaling domain <sup>25, 26</sup>. TLRs detect both extracellular and endosomal/lysosomal microbial threats. Among the 10 human TLRs and 12 mice TLRs, many demonstrate specificity to distinct repertoires of microbial products of bacteria, viruses and fungi. TLR3, TLR7, TLR8 (human) and TLR9 recognize nucleic acids in the endolysosomal compartment. TLR3 binds to double-stranded RNA (dsRNA), TLR7 (or human TLR8) binds to single-stranded (ssRNA) and TLR9 recognizes CpG-DNA <sup>26</sup>. However, as early as 2004, Lopez et al found that the dendritic cells (DCs) matured normally in the absence of TLR3, TLR7, TLR8 or TLR9 signaling. In addition, these TLR-deficient DCs could prime efficiently

for Th1 responses against Sendai virus (SeV) infection or influenza A virus infection <sup>27</sup>. Similarly, *Tlr3*<sup>-/-</sup> mice displayed uncompromised antiviral responses to lymphocytic choriomeningitis virus (LCMV), vesicular stomatitis virus (VSV), murine cytomegalovirus (MCMV) and reovirus infection <sup>28</sup>. Bacterial DNA causes septic shock <sup>29</sup>, and CpG DNA of *Listeria monocytogenes* can activate type 1 interferon (IFN) signaling, however, TLR signaling is dispensable for this response <sup>30</sup>. In addition, bacterial DNA activates B lymphocytes in a TLR9-independent fashion <sup>31</sup>. Finally, DNA viruses such as Herpes Simplex Virus type 1 induces type 1 IFN production in both TLR9-dependent and TLR9-independent pathways <sup>32</sup>. These compelling evidences suggest the existence of other nucleotides-sensing pathways.

One of the early searches for novel nucleotides sensors was based on the screening of an expression cDNA library from IFN- $\beta$ -treated human K562 cells, which respond poorly to viral infections unless the cells are treated with IFN- $\beta$  <sup>33</sup>. One cDNA clone has been identified to significantly augment poly (I:C)-induced IRF promoter activation and this clone encodes the N-terminal residues of the RNA helicase retinoic acid inducible gene I (RIG-I) <sup>33</sup>. Together with the structurally similar proteins melanoma differentiation-associated gene 5 (MDA5) and laboratory of genetics and physiology 2 (LGP2), these proteins constitute the RIG-I-like receptors (RLRs) family. RIG-I contains two N-terminal caspase activation and recruitment domain (CARD), a central DExD/H box-containing helicase domain and a C-terminal regulatory domain (CTD). The CARD domain is critical in mediating a homotypic interaction with the central adaptor

molecule mitochondrial antiviral signaling protein (MAVS, also known as IPS-1, VISA and Cardif)<sup>34-37</sup>. The helicase domain endows the protein with ATPase activity to drive the unwinding of dsRNA with 3'-terminal overhang (>5nt)<sup>38</sup>. Although a mutation in this region leads to the disruption of its function in antiviral response, the K270A mutant protein still recognizes both dsRNA and 5'-triphosphate-bearing (5'-ppp) RNA<sup>38</sup>. Recent structure analysis reveals that the CTD domain of RLR members forms a RNA-binding cleft despite that the binding capacity of MDA5 CTD is much weaker than that of RIG-I and LGP2<sup>38, 39</sup>. Importantly, RIG-I and MDA5 exhibit distinct preferences for the molecular features of RNA ligands and RNA viruses<sup>40</sup>. RIG-I binds to short 5'-ppp dsRNA while MDA5 recognizes long dsRNA<sup>40-43</sup>. Although it was shown that *in vitro* transcribed 5'-ppp ssRNA could also induce type 1 IFN activation<sup>43</sup>, two recent reports show that T7 RNA polymerase leads to the generation of dsRNA<sup>44, 45</sup> while synthetic 5'-ppp ssRNA has no immune activation effect<sup>43</sup>. This suggests only dsRNA could be recognized by RLRs. The 5'-ppp moiety is the signature motif that activates RIG-I<sup>41, 43</sup>, however, it has also been shown that 5'-p dsRNA and dsRNA bearing no 5'-triphosphate moiety could still potently induce type 1 IFN activation<sup>38, 46</sup>. The source of dsRNA can be traced back to viral genomes, replication intermediates, viral transcripts or self-RNA generated by RNase L<sup>43, 46, 47</sup>. All these RNA species have been proposed to have immune stimulatory potential. However, a recent study showed that only viral genome RNA could potently induce type 1 IFN activation during influenza A virus and SeV infection; and cleaved self-RNA does not induce type 1 IFN production

during the infection <sup>48</sup>. Further studies are essential to evaluate the respective contributions of dsRNA from various sources in inducing type 1 IFN production upon viral challenges.

MDA5 recognizes higher-order structure of RNA complex involving dsRNA and ssRNA <sup>49</sup>. Due to the ligand binding properties of RIG-I and MDA5, they display specificity to different viruses. RIG-I-deficient mouse fibroblasts and conventional dendritic cells (cDCs) fail to mount type 1 IFN activation in response to Newcastle disease virus (NDV), SeV, VSV, influenza A virus and Japanese encephalitis virus (JEV). However, MDA5-deficient cells respond normally to these viral challenges, yet fail to elicit immune activation upon infections by picornaviruses such as encephalomyocarditis virus (EMCV), Mengo virus and the Theiler's virus <sup>50</sup>. Some flaviviruses such as Dengue virus and West Nile virus (WNV) can be recognized by both RIG-I and MDA5 <sup>51, 52</sup>.

RIG-I-mediated type 1 IFN signaling not only respond to certain RNA species but also to DNA. Two groups have independently identified DNA-dependent RNA polymerase III as the cytosolic DNA sensor that generates 5'-ppp RNA, which engages RIG-I and activate downstream signaling <sup>53, 54</sup>. However, RIG-I-deficient cells still show competency in responding to cytoplasmic DNA, which raises the possibility that there are additional cytoplasmic DNA sensors. To qualify as an intracellular DNA sensor, it should contain a DNA-binding domain. The DNA-dependent activator of IFN-regulatory factors (DAI, also known as Z-DNA-binding protein) binds to dsDNA

and associates with TBK1 as well as IRF3. DAI is an IFN-inducible protein, and could augment type 1 IFN induction by various DNA sources when overexpressed <sup>55</sup>. In addition, knockdown of DAI by RNA interference ablates immune activation by exogenous DNA <sup>55</sup>. The dimerization of DAI results in DNA-dependent type 1 IFN production <sup>56</sup>. DAI contains two receptor-interacting protein (RIP) homotypic interaction motifs (RHIMs) and binds to RIP1 and RIP3. Knockdown of RIP1 or RIP3 abrogates NF- $\kappa$ B activation induced by immunostimulatory DNA sequences <sup>57, 58</sup>. However, DAI-deficient and wildtype control mice demonstrate no difference in DNA-dependent type 1 IFN activation in MEFs, GM-DC (bone-marrow-derived dendritic cells differentiated by GM-CSF) and FL-DC (bone-marrow-derived dendritic cells differentiated by Flt3) <sup>59</sup>. It is possible that additional intracellular DNA sensor exist so that redundant mechanisms provide host cells another layer of safe-guard against DNA stimuli.

In order to identify novel DNA sensors, several high throughput biochemical screenings have been performed to seek DNA-interacting proteins. One of the earliest identifications is the high-mobility group box (HMGB) protein family, which includes HMGB1, HMGB2 and HMGB3 and contributes to the initiation of type 1 IFN and proinflammatory cytokine responses to DNA stimuli <sup>60</sup>. Both HMGB1 and HMGB2 can be precipitated by immobilized B-DNA, and their deficiency results in impaired activation of NF- $\kappa$ B and IRF3. Furthermore, the absence of HMGBs also compromises the activation of TLR3, TLR7 and TLR9 by their cognate ligands nucleic acids <sup>60</sup>.

Another class of the intracellular DNA sensors is the PYHIN proteins, which contain two HIN DNA binding domains and one Pypin domain. Two members in this family, including IFI16 and AIM2, have been shown to be engaged with DNA and activate innate immune system<sup>61-65</sup>. Interestingly, IFI16 and AIM2 trigger separate signaling pathways despite their structural similarity and affinity to DNA. IFI16 is essential for recruiting downstream adaptor proteins to mount type 1 IFN production in response to intracellular DNA. Targeted knockdown of IFI16 results in the ablation of DNA-induced but not RNA-induced activation of both NF- $\kappa$ B and IRF3<sup>61</sup>. In contrast, AIM2 has no effect in modulating host type 1 IFN responses to DNA, rather it forms inflammasome with a critical adaptor molecule for procaspase-1 processing<sup>62-65</sup>.

The breadth of intracellular nucleic acid sensing system is also exemplified by the identification of two DExD/H-box helicases DHX36 and DHX9 in plasmacytoid dendritic cells<sup>66</sup>. Albeit these two proteins contain the DExD/H-box as RIG-I and MDA5 do, they exhibit different specificities. DHX36 primarily binds to CpG-A via the DEAH domain, while DHX9 binds to CpG-B via the DUF1605 domain. DHX36 is pivotal in activating IFN- $\alpha$  generation in response to CpG-A, while DHX9 preferentially activates NF- $\kappa$ B-dependent TNF- $\alpha$  and IL-6 production<sup>66</sup>.

Finally, the LRR (leucine-rich repeats) domain is postulated to function as ligands binding or protein-binding platforms<sup>26, 67</sup>. A screening in mouse peritoneal macrophages with a siRNA library targeting LRR-containing and LRR-interacting proteins-encoding mRNA leads to the identification of LRRFIP1, which recognizes both

exogenous RNA and DNA species to induce type 1 IFN production in a  $\beta$ -catenin-dependent fashion<sup>68</sup>.

#### **1.4 The significance of immune adaptors trafficking in host innate antiviral responses**

Two mitochondria-based adaptors have been identified in the type 1 IFN responses to intracellular RNA or DNA threats, these are MAVS<sup>34-37</sup> and Stimulator of Interferon Genes (STING, also known as MITA, MPYS and ERIS)<sup>69-71</sup>. Both proteins are ubiquitously expressed and indispensable for transducing signals detected by upstream PRRs leading to type 1 IFNs production, albeit STING is less potent than MAVS in activating NF- $\kappa$ B or IRF3 when overexpressed<sup>70</sup>. Association between the two protein has been also identified<sup>70</sup>. Importantly the integrity of this adaptor core is critical since deletion of either of these two proteins results in ablated type 1 IFNs even though the other remains intact. Some cell lines are exclusively dependent on MAVS in the cytosolic DNA-induced type 1 IFN response, yet MAVS-independent machinery has also been implicated in certain cell types such as MEF<sup>53</sup>. On the other hand, STING mediates cytosolic non-CpG DNA-induced type 1 IFN activation in MEF, BMDM (bone-marrow-derived macrophage), GM-DC and FL-DC<sup>72</sup>.

MAVS is firstly identified as a mitochondrial outer membrane protein, where it engages upstream PRRs and recruits TBK1 and IKK complexes to activate NF- $\kappa$ B and IRF3. However, it becomes detergent-resistant when cells are infected with SeV, which indicates a possible protein translocation<sup>34</sup>. Indeed, a recent study finds MAVS is also

located within peroxisomes, which are single-membrane-bound structures known to be involved in metabolic pathways. The different locations of MAVS confer distinct antiviral signaling kinetics: the peroxisomal MAVS is unable to induce type 1 IFN production, however, it launches a quick interferon-independent transcriptional program ISG (Interferon-Stimulated Genes) to establish the early antiviral state of the cells; the mitochondrial MAVS then assumes its function to activate type 1 IFN signaling, which in turn promotes the induction of ISGs <sup>73</sup>. NDV (Newcastle disease virus) triggers RIG-I-mediated type 1 IFN production, a recent report found it also induced the redistribution of MAVS to form speckle-like aggregates <sup>74</sup>. Mfn1 (Mitofusin 1), which regulates mitochondrial fission and fusion, associates with MAVS and is responsible for its virus-induced redistribution. Indeed, disruption of mitochondrial fusion processes by knocking down Mfn1 abrogates both MAVS redistribution and type 1 IFN production in response to viral infections <sup>74</sup>. These findings support the notion that it is both the biochemical properties and localization of MAVS that determine its functional outcome.

In fact, this is also true for the other adaptor STING. The initial studies on STING showed discrepant findings regarding its subcellular localization: one group found this protein predominantly resided in the endoplasmic reticulum (ER) and interacted with a member of translocon-associated protein complex TRAP $\beta$  <sup>69</sup>; while another group demonstrated STING was an exclusive mitochondrial outer membrane protein and associated with MAVS <sup>70</sup>. Microsomes comprised of ER, Golgi and vesicles are membrane structure artifacts when eukaryotic cells are homogenized. In two

subsequent studies, STING was consistently identified in the microsomes fraction <sup>72, 75</sup>. Interestingly, ER and mitochondria are not completely physically distinct organelles but are connected by the mitochondria-associated ER membrane (MAM). STING was also found in these structures, which may explain why it was also present in the mitochondrial fraction. However, upon HSV-1 (Herpes Simplex Virus-1) infection, STING was only associated with microsomes <sup>72</sup>. Furthermore STING could be degraded by a E3 ligase ring finger protein 5 (RNF5, also known as RMA1) <sup>75</sup>. Such functional interaction and regulation predominantly occur in mitochondria. Although STING is barely detectable in the ER fraction at the resting state, it becomes more abundant when cells were infected with SeV (Sendai Virus) for 6h and diminished from the ER again by 24h post-infection <sup>75</sup>. The function of STING in response to RNA virus infection was questioned by another recent report that showed STING-deficient BMDM were fully capable of producing IFN- $\beta$  in response to SeV infection <sup>61</sup>. The significance of viral specific functions and subcellular compartmentalization of these adaptors in modulating host antiviral innate immunity require further investigations.

### **1.5 An overview of the NLR protein family**

NLR (nucleotide-binding domain, leucine-rich repeats-containing) proteins (also known as CATERPILLERS, NODs, NALPs or NACHT-LRRs) in mammals share great sequence homology with the plants NBS-LRR proteins which are pivotal in delivering disease resistance <sup>76, 77</sup>. Albeit there is scarce evidence showing the direct binding of NLRs to various cytosolic PAMPs and other DAMPs (damage-associated molecular

patterns), these proteins are generally thought to be critically involved in the sensing, regulation and translation of hazardous stimuli to host proinflammatory responses including caspase-1-dependent IL-1 $\beta$  and IL-18 processing as well as NF- $\kappa$ B-dependent defensins and cytokines induction<sup>67, 78</sup>. However, as evidences begin to accumulate, NLRs are also found pivotal in modulating cell death and RLR responses.

NLRs are characterized by a central NBD (nucleotide-binding domain), a C-terminal LRR domain and an N-terminal effector domain, which could be CARD, Pyrin, BIR (baculovirus inhibitor of apoptosis repeat), AD (transactivation domain) or an X domain that cannot be categorized as any known motifs<sup>78</sup>.

One of the best characterized functions of NLRs is mediating the formation and activation of a dynamic multimeric protein complex named inflammasome<sup>79, 80</sup>. The identification of this complex is similar to that of the apoptosome, which is comprised of Apaf-1, deoxyribonucleic ATP, cytochrome c and pro-caspase-9<sup>6, 81</sup>. In the presence of cytochrome c, a wheel-shaped protein complex apoptosome is formed by Apaf-1 oligomerization, which activates caspase-9 via a proximity-induced molecular model<sup>81</sup>. Instead of activating caspase-9, inflammasome activation triggers the processing of pro-caspase-1 into caspase-1, which then generates the mature form of pro-IL-1 $\beta$  and pro-IL-18<sup>78</sup>.

The composition of inflammasome depends on the nature of proinflammatory insults, the first identification of such complex was based on the notion that an intracellular adaptor protein ASC (apoptosis-associated speck-like protein containing a CARD, also

known as PYCARD, CARD5 or TMS1), pro-caspase-1 and an NLR protein NLRP1 were eluted from at the same fraction in a HPLC (high-performance liquid chromatography) experiment <sup>82</sup>. As the body of knowledge in the field grows, several functionally distinct and relevant inflammasomes have been discovered. The proteins other than ASC and pro-caspase-1 found in the complex, including NLRP1, NLRP3, NLRC4, NLRB1, NLRP12 or AIM2, largely determine the specific agonists that activate a particular inflammasome.

**NLRP1 (also referred to as CLR17.1, CARD7, NALP1, NAC or DEFCAP) inflammasome** is the first discovered inflammasome, which can be activated by MDP (muramyl dipeptide) <sup>83</sup>. Despite of the high evolutionary conservation of NLR proteins among species, the structures of human and mouse NLRP1 are different. There are three *Nlrp1* orthologs (*Nlrp1a*, *1b*, *1c*) in mouse, and the variations in the *Nlrp1b* locus are critical for mice susceptibility to *Bacillus anthracis* lethal toxin (LT) treatment <sup>84</sup>. However, human macrophages are resistant to LT challenge <sup>85</sup>, which renders the study of human NLRP1 function in response to LT difficult. Human NLRP1 has a C-terminal CARD domain, which makes it capable of directly interacting with pro-caspase-1 without ASC although the latter augments pro-caspase-1 processing <sup>83</sup>. Mouse *Nlrp1b* inflammasome activation is independent of ASC, in contrast to human NLRP1, this mouse counterpart does not contain the Pyrin domain and is not able to associate with ASC.

**NLRP3 (also referred to as CLR1.1, Cryopyrin, NALP3, CIAS1 or PYPAF1)**

**inflammasome** responds to a group of chemically and structurally diverse stimuli such as extracellular ATP<sup>86, 87</sup>, MDP<sup>88</sup>, hyaluronan<sup>89</sup>, bacterial potassium ionophore nigericin, the marine toxin maitotoxin, listeriolysin O from *Listeria monocytogenes*, aerolysin from *Aeromonas hydrophila*<sup>86, 90</sup>,  $\alpha$ -hemolysin from *Staphylococcus aureus*<sup>91</sup>, amyloid- $\beta$ <sup>92</sup>, uric acid crystals, calcium pyrophosphate dehydrate<sup>93</sup>, silica, asbestos<sup>94, 95</sup>, alum (aluminum hydroxide)<sup>96-98</sup> and cholesterol crystals<sup>99-101</sup>. However, little evidence has shown NLRP3 is directly engaged with any of the aforementioned stimuli. A typical feature of many stimuli is the initiation of potassium efflux and decrease in cytosolic potassium concentration<sup>102, 103</sup>. One proposed mechanism underlying NLRP3 inflammasome activation is based on the findings that numerous stimuli induced intracellular oxidative stress by generating ROS (reactive oxygen species) and broad spectrum NADPH (nicotinamide adenine dinucleotide phosphate) oxidase inhibitors ablated caspase-1 activation<sup>104, 105</sup>. In fact, potassium efflux is closely associated with ROS production at the membranes in plants<sup>106</sup>. A recent study suggests oxidative stress leads to the dissociation of TXNIP (thioredoxin-interacting protein) from oxidized TRX (thioredoxin) to allow the otherwise impossible assembly of inflammasome; consistently TXNIP deficiency leads to compromised inflammasome activation in response to uric acid crystals<sup>107</sup>. Inhibition of autophagy leads to accumulation of damaged mitochondria and enhanced ROS generation. A recent study found NLRP3 and ASC co-localized with ER and mitochondria when activated; and mitochondrial dysfunction could repress both ROS and inflammasome activation<sup>108</sup>. Another proposed theory is

based on the crystal-mediated lysosomal membranes damage model, in which silica, alum and amyloid- $\beta$  challenges would lead to lysosomal membrane rupture and release Cathepsin B to activate inflammasome<sup>92,95</sup>. It is unclear whether these two models are parallel to each other or have causal relationships, more studies are required to address how these biochemically diverse stimuli initiate the same NLRP3 inflammasome assembly and activation.

**NLRC4 (also referred to as CLR2.1, IPAF, CARD12 or CLAN) inflammasome** responds to Gram-negative bacteria, which encode either type III or type IV secretion system (T3SS or T4SS), such as *Salmonella typhimurium*<sup>109-111</sup>, *Shigella flexineri*<sup>112</sup>, *Legionella pneumophila*<sup>113</sup> and *Pseudomonas aeruginosa*<sup>114</sup>. In contrast to the NLRP1 inflammasome, NLRC4 inflammasome is dependent on ASC for activating caspase-1. NLRC4 associates with pro-caspase-1 via the CARD:CARD homotypic interaction, however, whether NLRC4 interacts with ASC remains unclear<sup>79</sup>. Notably, although ASC is critical for NLRC4 inflammasome-dependent IL-1 $\beta$  production, it seems dispensable for NLRC4 inflammasome-dependent yet caspase-1-independent cell death. There are both flagellin-dependent and flagellin-independent mechanisms underlying the activation of NLRC4. *Salmonella typhimurium* and *Legionella pneumophila* strains that lack the genes encoding flagellin are unable to activate inflammasome<sup>109, 111, 115, 116</sup>. In fact, transfection of flagellin into the cytosol induces caspase-1 activation in a NLRC4-dependent fashion<sup>109, 111</sup>. The T3SS or T4SS has been proposed to be responsible for injecting flagellin directly into the cytosol<sup>114, 117</sup>. Some studies have

demonstrated that flagellin-deficient *Shigella flexneri* and *Pseudomonas aeruginosa* can still activate NLRC4 inflammasome<sup>112, 114</sup>, while some other studies found *Pseudomonas aeruginosa* lacking flagellin failed to induce pro-caspase-1 cleavage<sup>118, 119</sup>.

In addition to mediating the assembly of inflammasome and activating caspase-1, many NLRs assume inflammasome-independent functions, such as the modulation of canonical or non-canonical NF- $\kappa$ B pathways, transcription of MHC Class I and Class II genes, defensins and chemokine production, type 1 IFN induction as well as ribonuclease L activity<sup>67</sup>. NOD1 and NOD2 are two of the first studied NLR proteins. These two proteins activate both the NF- $\kappa$ B signaling pathway and the MAPK (mitogen-activated protein kinase) p38, ERK pathway in response to the bacterial products during the synthesis and/or degradation of peptidoglycan<sup>120</sup>. NOD1 detects the dipeptide  $\gamma$ -D-glutamyl-*meso*-diaminopimelic acid (iE-DAP), which is generated by most Gram-negative and some Gram-positive bacteria. NOD2 detects MDP, which is a common component of peptidoglycans. Neither NOD1 or NOD2 has been shown to bind to iE-DAP or MDP directly, however, the LRR domain is essential to confer the responsiveness, suggesting this domain either binds to their respective peptidoglycan ligands or a *bona fide* sensor of the bacterial products<sup>67</sup>. Similar to the adaptors of RLR signaling, the subcellular translocation and their relationships with membranes structures predict the functional outcomes<sup>121</sup>. NOD2 relies on its C-terminus, which is critical for its association with plasma membranes, to activate NF- $\kappa$ B signaling in response to MDP; in fact, a Crohn's disease-associated NOD2 variant NOD2 3020insC lacking the

C-terminus of the protein has been found unable to mount proinflammatory response to MDP <sup>122</sup>. In addition, NOD1 has also been found enriched at plasma membranes structure at the bacterial entry sites, and disruption of such localization pattern compromises its downstream signaling <sup>123</sup>. Despite of the structural homology among the 22 human NLRs, their significance in disease pathogenesis are diverse, and even one protein could assume different functions depending on the stimuli (Fig. 1.1).

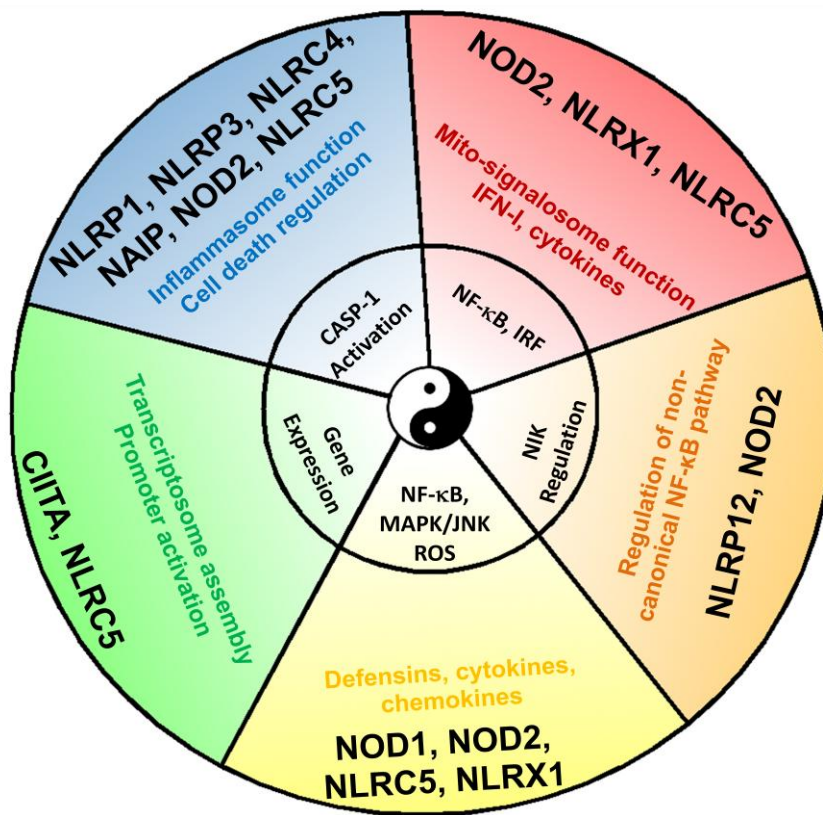


**Figure 1.1 NLR proteins signal through different multimeric protein complexes.** NLR signaling modules include the NLRC5/CIITA transcriptosome regulating the transcription of MHC Class I and II genes, the caspase-1-activating inflammasomes, the IFN/cytokine-inducing RLR signaling complex, the NF-κB/MAPK-activating NOD1/2 complex, and the non-canonical modulation of NF-κB via NIK. This figure depicts the concept that one NLR can serve multiple functions, whereas multiple NLRs can also serve similar functions.

### 1.6 Functions of NLR proteins in the modulation of MAVS-RLR signaling

NLRX1 is a unique NLR not only because of its mitochondrial localization but also its modes of functioning<sup>2, 124</sup>. Instead of direct participation in response to microbial invasion, NLRX1 modulates the functions of a MAVS-dependent multimeric protein complex which could be  $\geq 600\text{kDa}$  in its quiescent state<sup>125</sup>. This complex is pivotal in

activating type 1 IFNs upon engagement with either RNA or DNA, which then leads to the mitochondrial recruitment of TRAF3 and TRAF6 to induce type 1 IFNs production. NLRX1 is a non-canonical NLR member in that its N-terminal effector domain does not share homology to any well-conserved motifs yet it contains a mitochondrial targeting sequence, and that its central nucleotide binding domain does not have a Walker A motif found in other NLRs. Overexpression of NLRX1 inhibits RIG-I- or MDA5-mediated activation of NF- $\kappa$ B-, IRF3-dependent and *IFNB1* promoter activity in a dose-dependent fashion. In addition, NLRX1 also inhibits *IFNB1* mRNA transcription upon RLR activation. Knockdown of NLRX1 by siRNA results in an enhanced type 1 IFN signaling and thus confers resistance to Sindbis virus infection <sup>124</sup>. NLRX1 is located on the outer membrane of mitochondria and interacts with the adaptor MAVS. Exogenous NLRX1 expression potently represses SeV-induced homotypic CARD:CARD interaction between RIG-I and MAVS <sup>124</sup>. Interestingly, the inhibitory function of NLRX1 is specific to mitochondrial MAVS rather than peroxisome-localized MAVS <sup>73</sup> (Fig. 1.2). The role of NLRX1 in impeding MAVS-RIG-I interaction and the subsequent type 1 IFN induction has been further confirmed in gene deletion mice (manuscript under review). However, a recent study suggests that NLRX1 can be localized to the mitochondrial matrix and interacts with a matrix protein UQCRC2, although the physiological significance of such interaction is now known <sup>126</sup>. NLRX1 has been shown to be involved in the ROS production during *Shigella flexneri* and *Chlamydia trachomatis* infection <sup>127, 128</sup>. The discrepancy in localization may be due to the multi-faceted nature

of NLRX1 function in response to different stimuli. As the RLR signaling adaptors and some NLRs rely on the membrane structure to modulate host responses, the trafficking and localization of NLRX1 in the presence of virus needs further investigation.

In a recent screening of five NLR proteins including NOD1, NOD2, NLRC4, NAIP and NLRC3, Sabbah et al.<sup>129</sup> found that overexpression of NOD2 but not other NLRs endowed HEK293 cells with the capability to activate IRF3 in response to ssRNA. Interestingly, the endogenous level of NOD2 in A549 cells was shown to be inducible by viral infection. The authors also showed that depletion of NOD2 resulted in ablated IFN- $\beta$  production upon viral challenge. Furthermore immunoprecipitation of over-expressed NOD2 led to the recovery of RSV nucleocapsid protein specific RNA, which was substantiated in a cell-free system using HA-NOD2 bound-agarose beads as the bait (Fig. 1.3). Although it has been shown NLRP3 is involved in the recognition of influenza A virus<sup>130, 131</sup>, this finding represents the first piece of evidence that NLR can associate with viral ssRNA and activate the RLR signaling. However, it's still premature to define NOD2 as a *bona fide* PRR. Immunoprecipitation of NOD2 would be very likely to pull down NOD2-interacting proteins. Since the adaptor MAVS (mitochondrial antiviral signaling protein) associates with NOD2 and MAVS interacts with RIG-I, it is also possible that the recovery of RSV-specific RNA was the results of co-immunoprecipitation of RIG-I. In addition, the exact molecular features that activate NOD2 are still unknown.

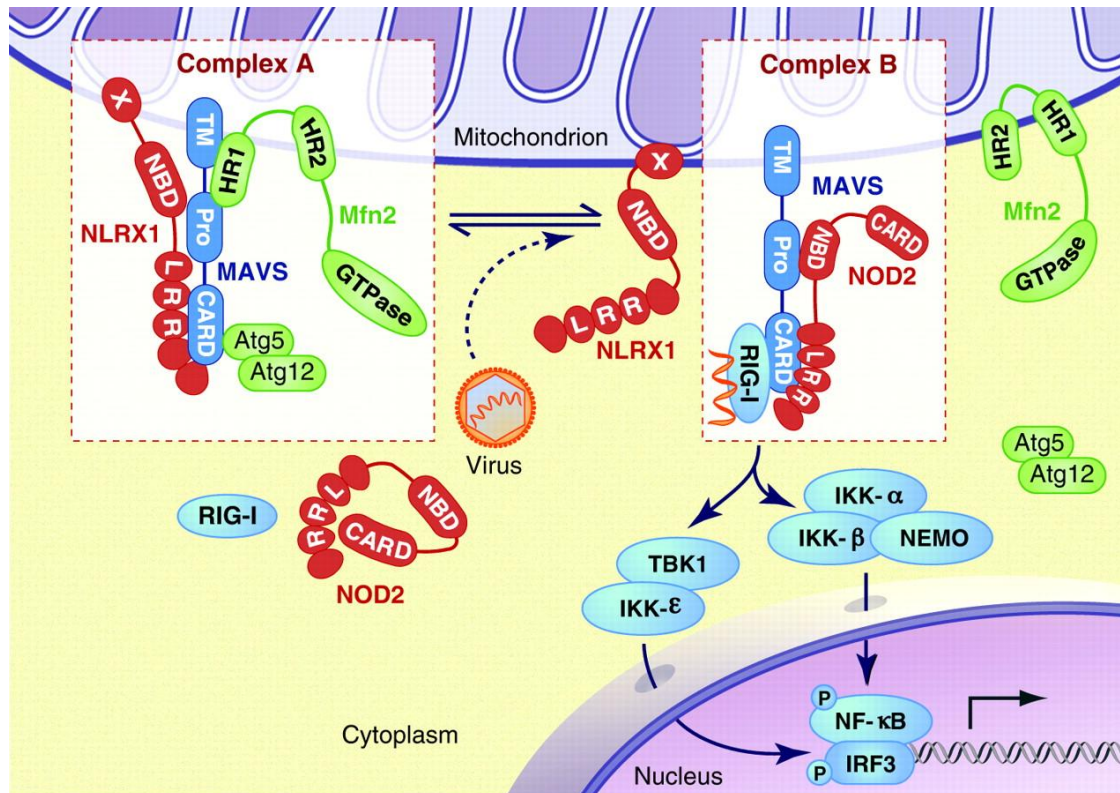


**Figure 1.2 NLR proteins and regulation of the RLR signaling.** In the quiescent state (complex A), the CARD-CARD homotypic interaction between MAVS and RIG-I is prevented by MAVS association with NLRX1 and/or Atg5-Atg12 conjugate, perhaps by steric hindrance. Mfn2 interacts with the C terminus and the transmembrane region of MAVS to abolish its immune-activating function. The three regulatory proteins target different regions of MAVS to execute the “molecular brake.” In the presence of cytosolic 5′-triphosphate, ssRNA, or dsRNA, these brakes are released, which renders the assembly of the active form of mito-signalosome (complex B), in which MAVS interacts with NOD2 and RLRs, such as RIG-I, which directly interact with viral nucleic acid to trigger type 1 IFN production.

For example, is the 5′-triphosphate moiety a necessity in this recognition? Does dsRNA interact with NOD2? Does NOD2 require ATP or GTP to associate with RNA? To demonstrate the direct binding of NOD2 to cytosolic RNA species and map the domain for such recognition, recombinant protein of full length NOD2 and its domain truncation mutants should be used in a cell-free binding assay. Unfortunately many of the NLRs

become aggregated and thus insoluble in a mammalian or insect cells expression system, which renders the evaluation of direct binding technically challenging. More sensitive assays such as protein-induced fluorescence enhancement (PIFE) or fluorescence resonance energy transfer (FRET) might shed light in resolving the conundrum. Evidences of direct binding would be compelling to establish the structural basis to group NOD2 into PRR.

The fact that certain NLR protein expression is inducible by viral infection also raises the possibility that NLRs are actively involved in the antiviral signaling modulation. A novel cytoplasmic NLR member NLRC5 has been recently characterized by several independent groups<sup>132-136</sup>. NLRC5 is highly expressed in the hematopoietic cells and lowly expressed in epithelial cells. Two groups noticed NLRC5 expression was upregulated by poly (I:C) treatment, SeV or Cytomegalovirus (CMV) infection<sup>134, 136</sup>. In fact, *NLRC5* contains the IFN- $\gamma$ -responsive elements in its promoter region; and among a variety of treatments, including LPS, EGF (epidermal growth factor), TNF- $\alpha$  (tumor necrosis factor- $\alpha$ ), Flagellin, TGF- $\beta$  (transforming growth factor- $\beta$ ), MDP, *Listeria monocytogenes* and IFN- $\gamma$ , only IFN- $\gamma$  induces the expression of NLRC5<sup>137</sup>. Overexpression of NLRC5 leads to the activation of the IFN-responsive regulatory promoter elements and the upregulation of antiviral target genes, such as *IFN- $\alpha$* , *OAS1* and *PRKRIR*<sup>137</sup>. However, one group showed that overexpression of NLRC5 alone was not sufficient to activate type 1 IFN signaling, yet knockdown of NLRC5 reduced SeV- and poly (I:C)-mediated type 1 IFN induction in both THP-1 cells and human primary

dermal fibroblasts<sup>136</sup>. NLRC5 was also found to be critically involved in inflammasome activities<sup>138,139</sup>. In contrast to these reported immune-activation effects, two other groups found that NLRC5 was a negative regulator of NF- $\kappa$ B and type 1 IFN signaling pathways<sup>132,133</sup>. NLRC5 associated with RIG-I and MDA5 via the CARD domain to preclude their interaction with MAVS. Reduction of NLRC5 level by RNA interference significantly increased type 1 IFN production. In addition, NLRC5 also sequestered the IKK $\alpha$ /IKK $\beta$  complex to abolish their phosphorylation upon LPS challenges<sup>133</sup>. In agreement with the fact that NLRC5 overexpression inhibits NF- $\kappa$ B activity, reduction of NLRC5 leads to enhanced proinflammatory responses<sup>132,133</sup>. However, all these experiments relied on overexpression and RNA interference approaches. A gene-deletion model has not been able to verify these findings<sup>139</sup>, yet instead suggests a role for NLRC5 in inflammasome activation. Our own study in human cell lines and primary monocytes also agrees with this finding<sup>138</sup>.

Inflammasome and RLR signaling complexes are two independent molecular machineries mediating caspase-1 and type 1 IFN activation. Some nucleic acids sensors can only specifically activate one pathway but not the other<sup>62-65</sup>. However, RIG-I is also shown to associate with the inflammasome adaptor ASC to induce pro-caspase-1 cleavage in a MAVS-, CARD9- and NLRP3-independent fashion. In addition the activation of inflammasome by EMCV infection depends on MDA5, CARD9 and NLRP3<sup>140</sup>. The interaction between these pathways suggests that the assembly of either macromolecular complex depends on the characteristics of insults.

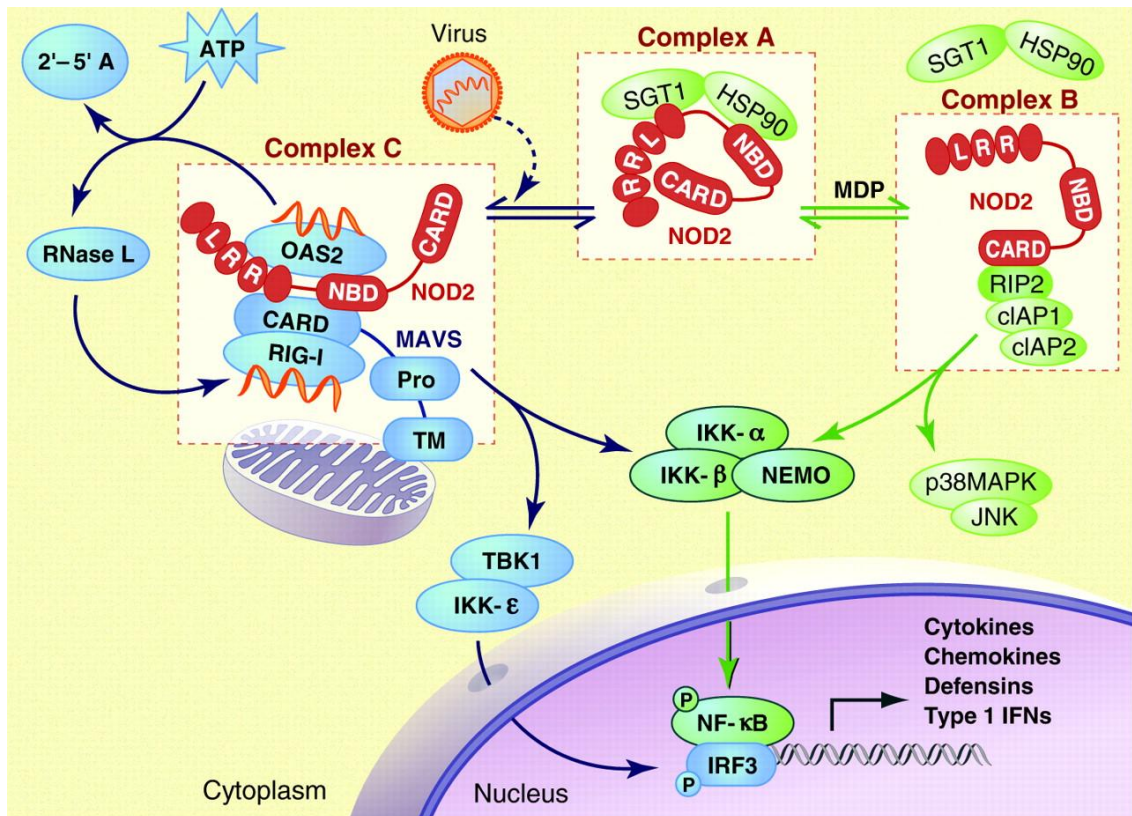


**Figure 1.3 NOD2 signaling bifurcates into antibacterial and antiviral effector arms.** A model of NOD2 signaling is presented in which NOD2 is bound to the chaperonin–ubiquitin ligase pair, HSP90 (heat shock protein 90) and SGT1 (suppressor of G2 allele of skp1), in the basal state (complex A). This is thought to hold the inactive NOD2 in a signaling-competent form. Upon stimulation with MDP, NOD2 binds to RIP2 and activates NF- $\kappa$ B and MAPK (p38 and JNK) through recruitment of several intracellular proteins, including cIAP1 and cIAP2 (complex B). This leads to the induction of chemokines, cytokines, and defensins, which mediate the antimicrobial responses. Similarly, viral infection can activate NOD2, leading to its translocation to the mitochondria, association with mitochondrial antiviral signaling protein (MAVS), and induction of the antiviral cytokine type I IFN (complex C). NOD2 also interacts with the dsRNA-binding protein OAS2. Overexpression of NOD2 can activate the RNase L pathway, providing a positive feedback mechanism for the mito-signalosome in response to RNA viruses. (complex C). RIG-I is depicted because it is the PRR that binds to viral nucleic acids, whereas TANK-binding kinase 1 (TBK1) and I $\kappa$ B kinase- $\epsilon$  (IKK- $\epsilon$ ) lie downstream of MAVS to activate IRF-3.

## 1.7 The regulatory components of the RLR signaling pathways

Given the great potential of MAVS and/or STING-mediated RLR signaling activation, this pathway is subjected to meticulous check mechanisms. Thirteen host proteins have been identified up to date in the negative regulatory module of this complex including NLRX1, NLRC5, Atg5-Atg12 conjugate, gC1qR, Mfn2, RNF5, LGP2, CYLD, PCBP2, AIP4, A20, Triad3A and PSMA7<sup>75, 124, 125, 133, 141-149</sup> (Table 1.1). RNAi-based reduction of these proteins levels results in enhanced type 1 IFN production in response to certain RNA viruses. The complexity of this regulatory module safeguards against overzealous immune activation. Although these proteins are functionally redundant, they primarily target RLR signaling via distinct mechanisms including molecular steric hindrance, autophagy as well as poly-ubiquitin (PUB) -mediated destabilization of adaptors and signaling modifications. To be noted, one regulatory protein could employ different mechanisms to function and structurally diverse proteins could fall into the same regulatory mechanism category.

**The molecular steric hindrance hypothesis** is based on the notion that some regulatory proteins could associate with the key molecules in the RLR signaling pathways, such as the PRRs, adaptors or downstream kinases; and such interaction competes them against their immune-activating engagement possibly by steric hindrance. This model has been supported by insights into the inhibitory mechanisms of NLRX1, NLRC5, LGP2, Atg5-Atg12 conjugate and Mfn2, all of which inhibit MAVS-mediated

Regulatory Mechanisms		Regulators					
Molecular Steric Hindrance	Targeting MAVS CARD	NLRX1	NLRC5	Atg5-Atg12 conjugate	NOD2		
	Targeting MAVS C-terminus	Mfn2	LGP2				
Autophagy Disturbance	Deficiency in autophagy	Mfn2	Atg5	Atg5-Atg12 conjugate			
Ub-mediated modulation	Proteosomal degradation	A20	PCBP2	AIP4	PSMA7	RNF5	Triad3A
	Signaling modification	CYLD	DUBA	Unanchored PUB chain	TRIM23	TRIM25	
Unknown mechanism		gC1qR					

**Table 1.1 The modulators of RLR signaling.** The regulators of RLR signaling could be classified into three categories based on their functioning mechanisms. The molecular steric hindrance hypothesis is based on the notion that some regulatory proteins could associate with the key molecules in RLR signaling to compete against their immune-activating engagement. Autophagy disturbance has been implicated in aberrant ROS production and damaged mitochondria accumulation, which cultivates in RLR signaling modification. PUB-mediated modulation is a set of delicate regulatory mechanisms composed of both PUB-mediated destabilization of the adaptors and PUB-mediated non-proteolytic signaling modification. Red color denotes negative RLR signaling regulators; dark blue color denotes positive regulators.

induction of type 1 IFN. In agreement with this, MAVS resides in a supramolecular complex in the quiescent state, but the majority of this protein migrates into a lower molecular weight complex when activated<sup>125</sup>. One possible explanation for the difference in signaling complex assembly could be attributed to the release of these molecular brakes. In fact, overexpression of NLRX1 abolishes the interaction between RIG-I and MAVS, and knockdown of NLRX1 results in higher resistance to Sindbis virus,

which induces type 1 IFN production in a RIG-I-dependent manner<sup>124</sup>. Similarly, NLRC5 preferentially binds to the CARD domain of RIG-I and strongly competes with MAVS for engagement. NLRC5 does not interact with MAVS, IKKi, TBK1, TRIF, TRAF3 or IRF3, which underlies the fact that NLRC5 potently inhibits RIG-I- and MDA5-induced *IFNB1* promoter activation yet only shows weak effect on MAVS- and TBK1-induced RLR signaling induction<sup>133</sup>. The accessibility to the CARD domain of PRR by either regulatory proteins or adaptor proteins determines the functional outcome RLR signaling. It is not surprising to see another regulatory component that employs the same mechanism to keep this pathway in-check. The Atg5-Atg12 conjugate intrudes between RIG-I and MAVS to abolish the homotypic CARD interactions and inhibits type 1 IFN production<sup>141</sup>. The proper functioning of MAVS depends on the integrity of both CARD and its C-terminus, in fact, the truncation of the transmembrane domain completely ablates its capacity to mount type 1 IFN production. Another “molecular break” Mfn2, targets the C terminal region of MAVS instead of the N-terminal CARD for modulation; and reduction of Mfn2 by siRNA leads to a decrease in the MAVS apparent molecular mass<sup>125</sup>. This strategy is also shared by a unique RLR member LGP2, which has a DExD/H domain as RIG-I and MDA5 do, yet lacks the CARD domain. LGP2 also interacts with the C-terminus of MAVS and precludes its interaction with downstream IKKi<sup>145, 150</sup>. However, in the gene-deletion mouse model, *Lgp2*<sup>-/-</sup> cells demonstrate impaired ability to mount type 1 IFN production in response to picornavirus infection; in addition the ATPase activity of LGP2 is essential for its facilitation of host

antiviral responses against encephalomyocarditis virus<sup>151</sup>. In the current model, these regulatory proteins target different regions of MAVS for steric preclusion of its engagement with immune-activating molecules. Interestingly, the molecular steric hindrance mechanism can also be presented by the splice variants of the adaptor itself. A recent report identified two MAVS splice variants: MAVS1a lacking exon 2 and MAVS1b lacking exon 3<sup>152</sup>. During the excision of exons, a frame shift occurs. Both splice variants possess the CARD domain, which is essential to engage with upstream RLRs. However, MAVS1a does not have the essential signaling domains to transduce RLR interaction to downstream effector activation. Meanwhile MAVS1b could interact with FADD and RIP1 to selectively induce type 1 IFN production<sup>152</sup>. Hence, MAVS1a functions as a steric blockade for full length MAVS to recruit downstream signaling complexes.

**Macroautophagy (referred to as autophagy)-related mechanisms** represent a group of novel host strategies in keeping RLR signaling from over-reacting. Besides mitochondria, ER, MAM and peroxisomes, another membrane bound structure that has been emerging to be a platform for antiviral signaling modulation is autophagosome. Autophagy is an evolutionarily conserved cellular function to recycle nutrients and maintain homeostasis. This process together with the proteasome-dependent mechanisms constitutes the major intracellular degradation system. It not only recycles damaged or aged organelles, misfolded proteins but also sequesters invading microorganisms as a primary host defense strategy. Autophagy disturbance has been

implicated in cellular components turnover, development, differentiation, tissue remodeling and numerous diseases such as cancer, muscular disorders, neurodegeneration and infectious diseases<sup>153, 154</sup>.

Autophagy has been artificially categorized into four phases: (1) vesicle nucleation, in this phase the double-membrane structure begins to form and sequesters part of the cytoplasm and damaged organelles; (2) vesicle elongation, in this phase, the membranes continue to grow until they reach the next phase; (3) docking and fusion, autophagosome formation is complete at this stage where the ends of isolated vesicles finally meet; (4) vesicle fusion and content breakdown, the autophagosome fuses with lysosome to deliver cargo into the newly formed autolysosome for content and inner membrane degradation<sup>154</sup>.

Inhibition of the TOR kinase is a major stimulus that activates autophagy<sup>155, 156</sup>, which involves Atgs (Autophagy-related Genes encoded proteins). Among about 30 Atgs identified to date, there are two essential conjugation systems centering on Atg12 and Atg8 (also referred to as LC3 in mammals) for autophagosome formation. Similar to ubiquitin, Atg12 and Atg8 have conserved ubiquitin-fold regions despite their lack of amino acids sequence homology to ubiquitin<sup>157, 158</sup>. Once activated, Atg12 will be transferred to Atg5 with the assistance of E1-like enzyme Atg7 and E2 enzyme Atg10. The Atg5-Atg12 conjugate also interacts with Atg16 to form a protein complex. Atg8 is conjugated to phosphatidylethanolamine (PE) (Atg8-PE or LC3-II) during autophagosome membrane expansion<sup>159</sup>. Hence biochemical detection of LC3-II is

widely accepted as a measurement for autophagy<sup>160</sup>.

Besides being actively involved in autophagosome biogenesis, Atg5-Atg12 conjugate has been recently found to associate with RIG-I and MAVS via the CARD domain and inhibit downstream type 1 IFN signaling activation. Overexpression of Atg5-Atg12 results in dampened NF- $\kappa$ B and IRF3 activation; and *Atg5*<sup>-/-</sup> MEFs are more resistant to VSV infection due to enhanced type 1 IFN production<sup>141</sup>. The deficiency of autophagy itself could lead to the accumulation of damaged mitochondria, which results in the buildup of MAVS and enhanced levels of intracellular ROS. Either of such effect leads to the induction of type 1 IFN<sup>142</sup>.

The functions of autophagy in antiviral innate immune response are cell type specific. Plasmacytoid dendritic cells (pDCs) primarily rely on TLRs to recognize viral PAMPs in a MAVS-independent fashion. Autophagy is essential for the transport of cytosolic viral replication intermediates into the endosomal/lysosomal compartment for TLR7 engagement<sup>161</sup>. In pDCs, absence of autophagy results in compromised antiviral innate immune response in contrast to the hyperactive type 1 IFN production in MEFs, which utilize the RLR axis to respond to the viral infections.

Mitochondria are closely associated with autophagosomes, and many proteins in both organelles have been linked to functional regulation of the other. For example, autophagic proteins Atg5 and Atg9 can be transiently localized onto mitochondria<sup>162, 163</sup>; similarly mitochondrial proteins Bif-1 and Sirt1 are essential for autophagy<sup>164, 165</sup>. A recent study shows that both Atg5 and LC3 can be temporarily localized to punctae on

mitochondria. Importantly, mitochondria provide membranes for the biogenesis of autophagosomes<sup>4</sup>. Mfn2 is responsible for tethering mitochondria to ER, and deficiency in Mfn2 leads to the disruption of the transfer of lipids from ER, which is necessary for proper mitochondrial functioning. Indeed *Mfn2*<sup>-/-</sup> cells have severely impaired autophagosome formation<sup>4</sup>. Given the fact that reduction of Mfn2 also leads to enhanced RLR signaling, it is plausible that Mfn2 not only contributes to the molecular steric hindrance in blocking MAVS association with downstream IKK complexes, but also inhibits this pathway via autophagy-mediated mechanism. However, further study is needed to understand how Mfn2 deficiency-mediated autophagy defects contribute to the RLR signaling modulation.

Although the molecular explanations of fasting or calories restriction favor its beneficial role in lowering the risks of obesity and reasonably prolonging human life expectancy<sup>154</sup>, it might not be salutary for the innate defense system. As the caspases system is generally considered to be the initiators and executioners of programmed cell death, Atgs are pivotal in the biogenesis of autophagosomes as well; to be noted, there are a plethora of non-caspase proteins that have been identified up to date to have pro-apoptotic functions in a caspase-dependent fashion, intensive search for additional factors that are critical in mediating virus-induced autophagy needs to be performed to gain deeper insight into the mechanisms by which host cells use to modify autophagy-related innate immune responses.

**Polyubiquitin (PUB)-mediated modulation** has emerged as an important regulatory

mechanisms of RLR signaling, which involves both polyubiquitination-mediated destabilization of the adaptors and PUb chain-mediated non-proteolytic signaling modification. Ubiquitin conjugation system is composed of a three-step program, in which an ubiquitin-activating enzyme (E1) activates the globular ubiquitin protein by forming an E1~Ub thioester bond in an ATP-dependent fashion. Activated Ub is then transferred to an Ub-conjugating enzyme (E2), which directs the reaction intermediates to the Ub ligase (E3). E3 associates with both E2 and the target protein to deliver Ub to the corresponding lysine residues. E3 alone or sometimes E2 and E3 together dictates the substrate specificity of PUb modification<sup>166</sup>. There are 2 E1 enzymes, over 40 E2 enzymes and 600 E3 enzymes in human cells. There are two classes of E3 enzymes which contain a HECT (homology to E6AP C-terminus) or a RING (really interesting new gene) domain respectively<sup>167</sup>. It is the diversity of E3 that expands the repertoire of Ub substrates. Ub can be delivered to a protein as a monomer or a PUb chain. The difference in the Ub linkage also activates distinct regulatory pathways. Ub contains 7 lysine residues including K6, K11, K27, K29, K33, K48 and K63. The protein modification via the K48 residue of Ub is frequently transported to the 26S proteasome, leading to protein degradation and Ub recycling. However, a modification of K63 residue-linked PUb chain is associated with alteration of signaling activity<sup>166</sup>.

RIG-I is heavily polyubiquitinated when transfected into HEK293T cells, however, the mutant lacking the CARD domain has no PUb modifications. A recent study identified K63 linkage of RIG-I, which raised the possibility that RIG-I function is

modulated by polyubiquitination <sup>168</sup>. In fact, a further mass-spectrometry analysis revealed an E3 ligase TRIM25 as a RIG-I-binding partner. TRIM25 contains a RING domain in addition to its B box/coiled-coil domain (B Box/CCD) and C-terminal SPRY domain, which is responsible for RIG-I-binding. Deficiency in TRIM25 not only results in diminished polyubiquitination of RIG-I, but also compromises type 1 IFN signaling <sup>168</sup>. Such polyubiquitination modification is also tightly regulated by phosphorylation at RIG-I Thr-170 site, which is in close vicinity to a primary site of K63 polyubiquitination Lys-172. A mutation of Thr-170 to Glu-170 abolishes both polyubiquitination modification of RIG-I and downstream type 1 IFN signaling <sup>169</sup>. Consistently, RIG-I-mediated RLR signaling activation is negatively regulated by a deubiquitinating enzyme tumor suppressor CYLD (cylindromatosis), which removes K63-linked PUB chains. CYLD expression level is reduced in the presence of viral infections and RNA interference targeting its mRNA leads to augmented type 1 IFN production <sup>147</sup>. Deubiquitinase also targets TRAF3, which is recruited to the MAVS upon activation. DUBA (deubiquitinating enzyme A20) is known to cleave the K63-linked PUB chains on TRAF3 to abolish its association with downstream TBK1 and subsequent type 1 IFN production. Overexpression of DUBA quenches RLR activation and reduction of DUBA augments such responses <sup>170</sup>. Similarly proper RLR signaling also depends on the polyubiquitination of NEMO (also known as IKK $\gamma$ ) at the K27 residue by an E3 enzyme TRIM23. Deficiency in TRIM23 expression impaires RLR signaling <sup>171</sup>.

The essential role of K63 polyubiquitination in activating RLR signaling is further

corroborated in an *in vitro* reconstitution experiment. RIG-I isolated from virus-infected cells can potentiate the dimerization of IRF3, which is a hallmark of RLR activation, in the presence of mitochondria and cytosolic extracts. When RIG-I and TRIM25 are incubated with E1 and a panel of E2s, Ubc5 and Ubc13 have been shown to be essential for RLR activation<sup>172</sup>. Interestingly, in addition to the K63-linked PUB chains conjugation, a recent study demonstrated an unusual function of unanchored PUB chains in the modulation of RLR signaling<sup>172</sup>. Incubation of the helicase domain truncation mutant of RIG-I ( $\Delta$ RIG-I) with a PUB chain comprised of 4 ubiquitin molecules linked via K63 potently induces IRF3 dimerization. However, the PUB chains linked via K48 or shorter PUB chains comprised of 2 ubiquitin molecules are inert in activating RLR signaling. When full length RIG-I is incubated with 5'ppp-dsRNA and K63 PUB chains, IRF3 dimerization is also potently induced as observed in experiment with the constitutively activated  $\Delta$ RIG-I. Notably endogenous K63 PUB chains concentration is approximately 300 fold higher than the EC<sub>50</sub> for RLR activation, which explains why overexpression of  $\Delta$ RIG-I is sufficient to induce type 1 IFN production. These findings identify the ubiquitin system has profound effects on the outcome of RLR activation<sup>172</sup>.

PUB-mediated destabilization represents another distinct set of mechanisms by which RLR signaling is regulated. The target proteins are either the adaptor proteins, MAVS and STING, or essential downstream signaling molecule such as TRAF3. In two independent yeast two hybrid screenings for MAVS-interacting proteins, PCBP2 and PSMA7 were identified as interacting partners. PCBP2 recruits an E3 ligase AIP4 to

mediate the proteosomal degradation of MAVS. Interestingly, the expression level of PCBP2 is induced by viral infections<sup>148</sup>, suggesting this molecule might be harnessed by certain viruses to subvert host defense system. Another protein PSMA7, which is a subunit of the 20S proteasome, also mediates the proteosomal degradation of MAVS. Reduction of PSMA7 results in enhanced type 1 IFN signaling although the precise mechanism of its function remains unclear<sup>144</sup>. STING is targeted by an E3 ligase RNF5, which adds the PUb chain to the Lys150. Despite the multiple localizations of RNF5 at ER, endosome and mitochondria, SeV infection induces local condensation of RNF5 at mitochondria accompanied by the downregulation of STING<sup>75</sup>. Another virus-inducible E3 enzyme is Triad3A, which includes TRAF-interacting motifs (TIMs). Triad3A binds to TRAF3 via TIM; and the TRAF3 Y440 and Q442 mutations disrupt such association. Triad3A negatively regulates RLR signaling by targeting TRAF3 for proteosomal degradation<sup>149</sup>. A20 is an ubiquitin-editing enzyme composed of both an N-terminal deubiquitination domain and a C-terminal ubiquitin ligase domain. Overexpression of A20 potently inhibits RLR signaling and only the ligase domain but not the deubiquitination domain is responsible for its inhibitory function. However, RIG-I is not degraded by A20, further studies are necessary to delineate the molecular mechanism of its function<sup>146</sup>.

The Mitochondrial Immune Signaling Complex is a dynamic protein complex localized in the mitochondria, whose composition is responsive to cytosolic 5'-ppp RNA, dsRNA and DNA. NLR proteins actively participate in the activation and regulation of

this complex to induce type 1 IFN production. In addition to immune modulation, the complex also contains proteins that are pivotal in autophagy<sup>141, 142</sup> and apoptosis<sup>173, 174</sup>. Further characterization of its composition and function would certainly shed light on our understanding of mitochondria as a critical platform for host-virus interaction and future strategic design of antiviral therapeutics to elicit host antiviral response to full potential.

## **CHAPTER TWO**

### **MAVS-MEDIATED APOPTOSIS AND ITS INHIBITION BY VIRAL PROTEINS**

## 2.1 Abstract

Host responses to viral infection include both immune activation and programmed cell death. The mitochondrial antiviral signaling adaptor, MAVS (IPS-1, VISA or Cardif) is critical for host defenses to viral infection by inducing type-1 interferons (IFN-I), however its role in virus-induced apoptotic responses has not been fully elucidated. We show that MAVS is a pro-apoptotic protein independent of its function in initiating IFN-I production. MAVS-induced cell death requires mitochondrial localization, is caspase dependent, and displays all of the hallmarks of apoptosis. Consistent with these data, fibroblasts from *Mavs*<sup>-/-</sup> animals are resistant to Sendai virus-induced apoptosis. A functional screen of the Severe Acute Respiratory Syndrome coronavirus (SARS-CoV) genome identified the nonstructural protein (NSP15) that inhibited MAVS-induced apoptosis, possibly as a method of immune evasion. This study describes a novel role for MAVS in controlling viral infections through the induction of apoptosis, and identifies viral proteins, which inhibit this host response.

## 2.2 Introduction

In recent years, knowledge of host cell-signaling responses to viral infection has progressed rapidly. It is known that cells of the immune system contain toll-like receptors (TLRs) capable of detecting extracellular or endosomal viral nucleic acid and activating appropriate signal transduction pathways leading to the up-regulation of immune and inflammatory cytokines. Besides detecting extracellular viral products, somatic cells can also respond to intracellular viral RNA by activating the recently identified mitochondrial antiviral signaling pathway. Following cytoplasmic detection of viral nucleic acid by the RIG-I-like helicases (RLH) family of receptors, these and other signaling proteins are recruited to the mitochondria where they interact with the mitochondrial antiviral signaling adaptor protein MAVS (IPS-1, VISA and Cardif)<sup>34-37</sup>. *In vitro* and *In vivo* experiments have revealed a critical role for MAVS and its mitochondrial localization in the activation of host antiviral responses<sup>34, 175</sup>. Although the role of MAVS in type-1 interferon (IFN-I) responses is known, the localization of MAVS to the mitochondria suggests other putative mitochondrial functions for MAVS, prominent among these is apoptosis. However, to date, there are no comprehensive studies focused on testing this hypothesis. Notably, host cell apoptosis is a successful strategy to impede viral replication and restrict virus spreading during a productive infection<sup>176</sup>.

Multicellular organisms are equipped with at least two evolutionarily conserved defensive arms to eradicate viral infections: programmed cell death and innate immune

responses. Many proteins which function in both apoptotic and inflammatory signaling cascades contain a caspase recruitment domain (CARD), which functions as a homotypic interaction motif. In fact, the biological function of the CARD domain was initially described in a subset of caspases which activate mitochondrial dependent apoptotic signaling<sup>177</sup>. For example, the CARD containing Apaf-1 (apoptosis protease-activating factor-1) protein binds to cytochrome c and forms a ternary multimeric protein structure called the apoptosome which functions to activate caspase-9 via a proximity-induced mechanism<sup>178</sup>. Other CARD-containing proteins including some members of the NLR (nucleotide-binding domain and leucine-rich repeat containing) protein family have been linked with both apoptotic and inflammatory signaling<sup>179</sup>. For example, the CARD-containing NLR, Nod1, has been shown to activate a caspase-9 dependent apoptosis and play a positive regulatory role in pathogen-induced NF- $\kappa$ B activation<sup>180</sup>. Similarly, Nod2, a protein linked with the etiology of the autoinflammatory Crohn's disease, has been reported to augment caspase-9-induced apoptosis when overexpressed<sup>181</sup>. A third CARD-containing NLR, IPAF (NLRC4), mediates cell death through a caspase-1 dependent fashion<sup>110, 182, 183</sup>.

Similar to the aforementioned proteins, MAVS contains an N-terminal CARD-like domain, in addition to a central proline-rich region and a C-terminal transmembrane (TM) domain, which targets MAVS to the mitochondrial outer membrane<sup>34</sup>. Recent crystal structure analysis reveals that the CARD-like domain of MAVS is indeed a classical CARD fold with surface charge profiles of a typical CARD domain involved in

homotypic associations<sup>184</sup>. Consequently, the presence of a CARD-like domain coupled with its mitochondrial localization suggests a putative role for MAVS in both immune and cell death responses. In fact, both the N-terminal CARD-like and TM domains are indispensable for MAVS-mediated activation of interferon regulatory factor-3 (IRF-3) and subsequent transcription of the antiviral IFN-I, suggesting that these domains are critical to MAVS function<sup>34</sup>. As a survival mechanism, it is known that some viruses have evolved strategies to inhibit MAVS function through selective targeting of these functional domains. For example, the genome of hepatitis C virus (HCV) has evolved to include a serine protease, NS3/4A, which cleaves the MAVS TM domain and dislodges MAVS from the mitochondria, thereby abrogating MAVS mediated IFN-I production<sup>37, 185</sup>. Similar to HCV, hepatitis A virus (HAV) encodes for the 3ABC protein, which localizes to the mitochondria and inhibits MAVS signaling via proteolytic cleavage<sup>2, 186</sup>. Currently, there are no reports of viral proteins targeting MAVS for inhibition of virus-induced cell death responses.

Host cell apoptosis has been reported to suppress viral replication and the subsequent production of infectious progeny viruses<sup>187</sup>. For example, adenoviruses and baculoviruses which are defective in anti-apoptotic genes are compromised in producing progeny viruses<sup>187</sup>. In addition, several viruses infectious to humans, including the coronaviruses, are known to modulate host cell apoptotic responses<sup>188, 189</sup>. In 2003, researchers from several labs identified a unique coronavirus linked with the pathogenesis of severe acute respiratory syndrome (SARS) in humans<sup>190-192</sup>. The

spread of SARS-CoV, reaching near pandemic levels, resulted in the death of over 900 individuals with a case fatality rate of 11%<sup>193</sup>. Since that time, the sequencing of the complete SARS-CoV genome has allowed scientists to study the function of each SARS-CoV encoded protein in greater details. Phylogenetic analyses revealed that SARS-CoV was not closely related to any other characterized coronaviruses<sup>194, 195</sup>. The distinct nature of the SARS-CoV genome suggests possible unique strategies employed by this virus to subvert host defense mechanisms. Notably, unlike other common human respiratory viral infections, such as influenza A virus, the viral loads in the upper airway of SARS patients progressively increase, reaching a peak around 10 days after the initial onset of symptoms<sup>196</sup>. This indicates that at least during the initial stages of SARS-CoV infection, this virus might suppress host defensive responses. In fact, several SARS-CoV proteins have been shown to inhibit host IFN-I responses<sup>188, 189, 197</sup>. Although the fact that certain clinical manifestations of SARS such as lymphopenia and cell death in the lung or liver are thought to be related to the ability of SARS-CoV to induce apoptosis in specific cell types and that several pro-apoptotic proteins have been found in SARS-CoV genome<sup>198-200</sup>, the early pathogenesis of SARS is poorly understood and how apoptosis contributes to the initial pathological changes is largely unknown. In addition, the replication of SARS-CoV seems to be restrained to the first two weeks upon symptom onset with little evidence of continued replication after this time window<sup>201</sup>. Clearly, the temporal and cell-type specific expression of SARS-CoV proteins could account for the dynamics of SARS-CoV infection and given that host cell fate decisions

are a part of overall host responses to any pathogen, it is conceivable that like SARS-CoV inhibitory effects on IFN-I responses, this virus could employ proteins which function as inhibitors of host cell death. In this report, we describe a novel function of MAVS in mediating virus-induced apoptosis, and identify a SARS-CoV protein which inhibits this response.

## **2.3 Results**

### **MAVS induces caspase-dependent apoptosis.**

Transient expression of MAVS protein causes HEK293T cells to crenate and lose adherence, suggesting that MAVS is cytotoxic (Fig. 2.1A). Although some cell death was observed at 24 hours post-transfection, it was most evident at 48 hours post-transfection, which was quantitated by the Trypan blue exclusion test of cell viability. In this assay, we observed a dose-dependent increase in the percentage of Trypan blue positive cells at 48 hours post-transfection with MAVS plasmid (Fig. 2.1B). This result was confirmed by measurements of cell viability via XTT assay. MAVS-induced cell death is potent as 10ng of MAVS plasmid was sufficient to decrease cell viability by 40% (Fig. 2.1C).

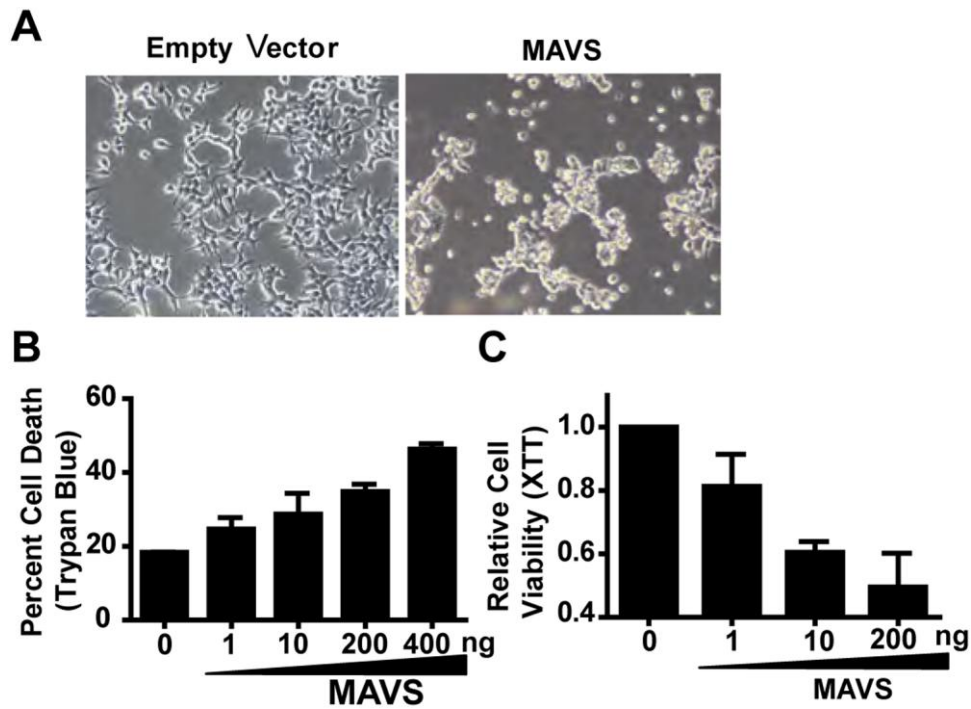


**Figure 2.1 MAVS induces cell death.** (A) MAVS overexpression in HEK293T cells results in cell death. (B) MAVS-induced cell death displays dose dependency determined by Trypan blue exclusion cell counting. Cells were harvested for Trypan Blue counting 48 h post-transfection. (C) In the XTT cell viability assay,  $1.0 \times 10^4$  HEK293T were plated in 96-well plate, and increasing doses of MAVS from 0 ng/well to 200 ng/well were transfected and total amount of plasmids for each well was maintained at 400 ng by mixing pcDNA3 and MAVS plasmids together. XTT assays were performed 48 hours post-transfection. Error bar represents standard deviation of triplicates of biological samples and each graph represents three individual experiments.

MAVS contains a N-terminal CARD-like domain, which is well conserved from human to pufferfish<sup>34</sup>; and the CARD domain of other proteins has been shown to mediate the activation of caspases, facilitating apoptosis<sup>202</sup>. Therefore, we next sought to test the hypothesis that MAVS induces apoptosis through a caspase-dependent mechanism. It is well known that blockade of caspase activity will inhibit the intrinsic apoptotic pathway<sup>203</sup>. Thus, we treated HEK293T cells with a pan-caspase inhibitor (Z-VAD-FMK) followed by transfection of increasing amounts of MAVS plasmid. As expected, transient MAVS expression in untreated cells resulted in a significant loss of cell viability as measured by XTT assay (Fig. 2.2A, black bars); and application of the pan-caspase inhibitor resulted in a complete reversal of MAVS-induced cell death (Fig. 2.2A, grey bars). It is known that caspase-dependent apoptosis can cause Poly (ADP-ribose) Polymerase (PARP) cleavage, thus we investigated the effect of MAVS expression on the triggering of PARP cleavage. HEK293T cells were transfected with two different doses of MAVS plasmid and both adherent and floating cells were harvested

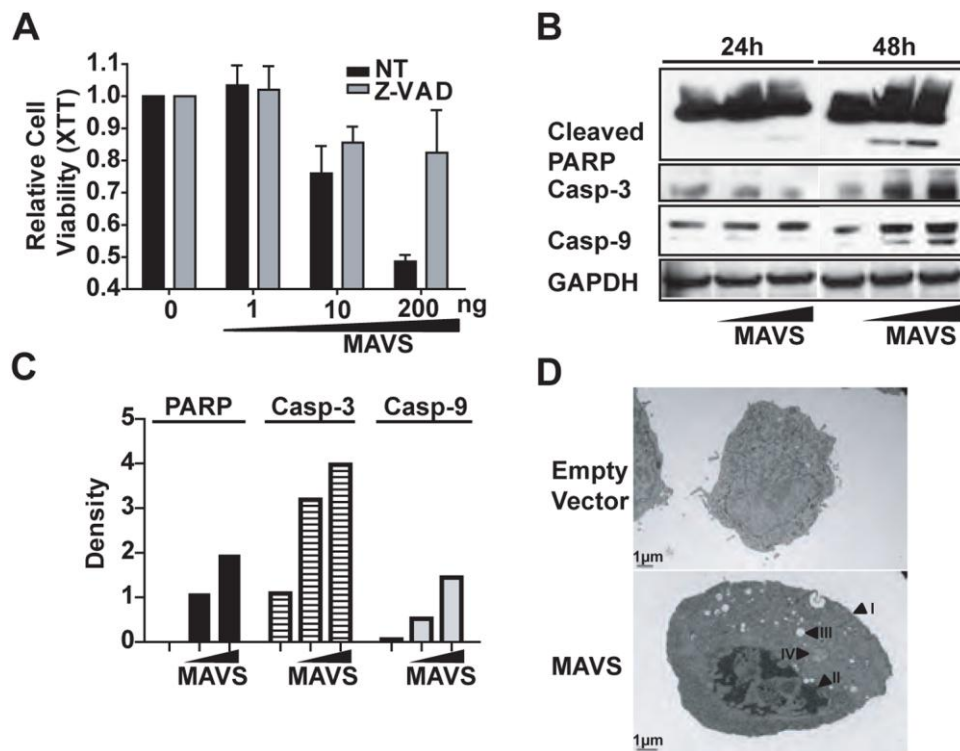


**Figure 2.2 MAVS expression leads to apoptosis.** (A) MAVS-induced cell death is caspase-dependent. HEK293T cells were treated with a pan-caspase inhibitor z-VAD-FMK before transfection with a titration doses of MAVS, and cell viability was measured by XTT assay. (B) MAVS triggers PARP cleavage as well as the activation of caspase-3 and caspase-9. One million HEK293T cells were transfected with 1 μg or 3 μg of MAVS-expressing plasmids and harvested 24 h or 48 h post-transfection. Cell extracts were immunoblotted for PARP, caspase-3 and caspase-9. (C) Densitometry analysis on the Western blot shown in (B). (D) Apoptotic morphological features of MAVS-induced cell death. Three micrograms of MAVS plasmids were transfected into  $5 \times 10^5$  HEK-293T cells. Transmission electron microscopy (TEM) analysis was carried out 48 hours post-transfection. Arrows: (I) intact plasma membrane; (II) marginated and condensed chromatin; (III) large vacuole; (IV) swollen mitochondria. Each graph represents two individual experiments.

and lysed 24 and 48 hours post-transfection. Immunoblotting followed by densitometry measurements revealed a dose-dependent increase in PARP cleavage (Fig. 2.2B-C). In congruence with the PARP cleavage pattern, caspases-3 and caspase-9 protein levels also showed a dose-dependent increases following MAVS expression (Fig. 2.2B-C). Transmission electron microscopy examination of HEK293T cells transfected with MAVS or empty vector was performed at 48 hours post-transfection (Fig. 2.2D). Unlike the otherwise healthy cells transfected with empty vector (Fig. 2.2D, top panel), MAVS-expressing cells exhibit all of the morphological hallmarks of apoptosis including an intact plasma membrane (Fig. 2.2D, bottom panel arrow I), crenation, condensed and marginated chromatin (arrow II), large vacuoles (arrow III), cytoplasm shrinkage, membrane blebbing, an intact nuclear envelope, and swollen mitochondria (arrow IV)<sup>204</sup>. Interestingly, even though the expression of MAVS reached peak at 24h post-transfection (Fig. 2.3A), the apoptosis became apparent at later time point (Fig. 2.3B).

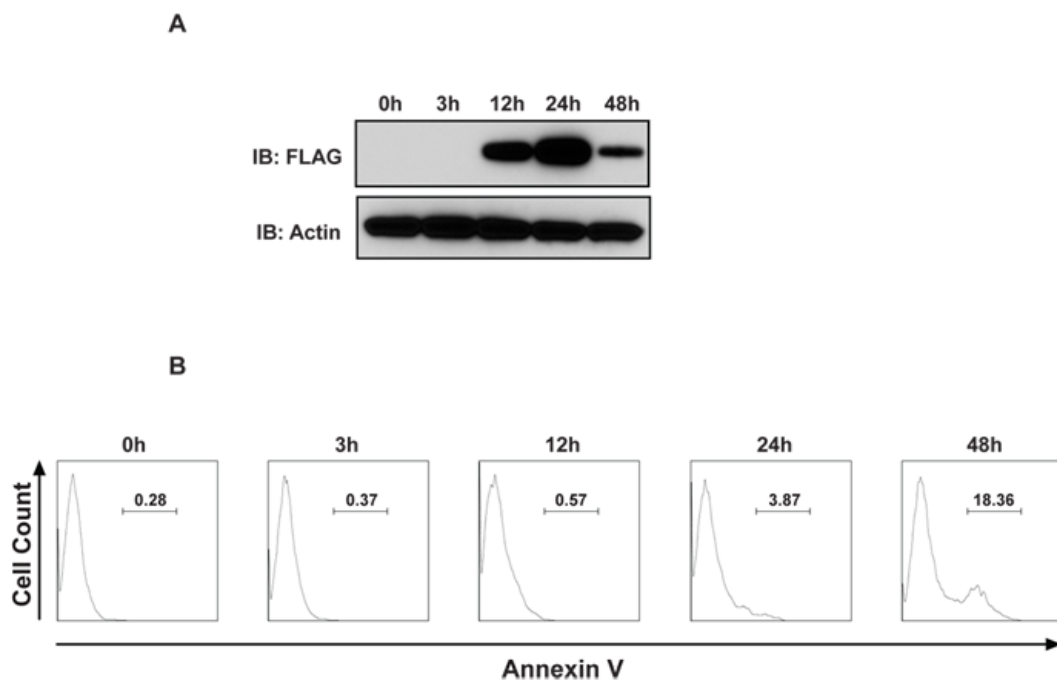


**Figure 2.3 The kinetics of MAVS expression and MAVS-induced apoptosis.** (A)  $5 \times 10^5$  HEK293T cells were plated in 6 well plate,  $3 \mu\text{g}$  MAVS plasmids were transfected at 3h, 12h, 24h and 48h prior to cell harvesting. Half of the cells were lysed in RIPA buffer and blotted with anti-FLAG to determine the protein expression kinetics. (B) The other half of the cells from each well were stained with Annexin V and analyzed by flow cytometry.

## Virus-induced apoptosis in primary mouse fibroblasts requires MAVS.

The aforementioned studies analyzed the effect of transient expression of MAVS on cell death. To explore the physiological role of endogenous MAVS in mediating

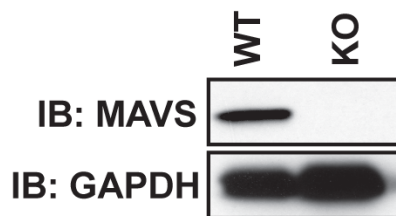


**Figure 2.4 Confirmation of MAVS knockout by Western Blot.** One million *Mavs*<sup>+/+</sup> and *Mavs*<sup>-/-</sup> MEFs were lysed in RIPA buffer containing proteinase inhibitor cocktail. Cell extracts were subjected to SDS-PAGE and Western blotting for rodent-specific MAVS.

virus-induced apoptosis, we extended these findings to investigations of recombinant Sendai virus expressing GFP (rSeV-GFP) infected mouse embryonic fibroblasts (MEFs) isolated from

MAVS knockout or wild type littermate control mice. MAVS deficiency was confirmed by Western Blot (Fig. 2.4). *Mavs*<sup>-/-</sup> and wildtype littermate control MEFs were infected with rSeV-GFP, a known inducer of apoptosis<sup>205</sup>, 48

hours post-infection, infection efficiency in both

cell lines was measured by the percentage of rSeV-GFP. No difference in infection percentage was found between wildtype and *Mavs*<sup>-/-</sup> MEFs (Fig. 2.5A, top graph). In contrast, the percentage of Annexin V positive cells was >30% among infected wildtype MEFs compared to <8% for the *Mavs*<sup>-/-</sup> MEFs (Fig. 2.5A, bottom graph). Similarly, MAVS-deficient MEFs maintained a spindle-like fibroblastic morphology (Fig. 2.5B, GFP bottom panel), while wildtype MEFs crenated and became detached from the plate. In addition, rSeV-GFP infected wildtype MEFs have higher propidium iodide/Hoechst staining ratio as compared to MAVS<sup>-/-</sup>, further indicating an increase in cell death (Fig.

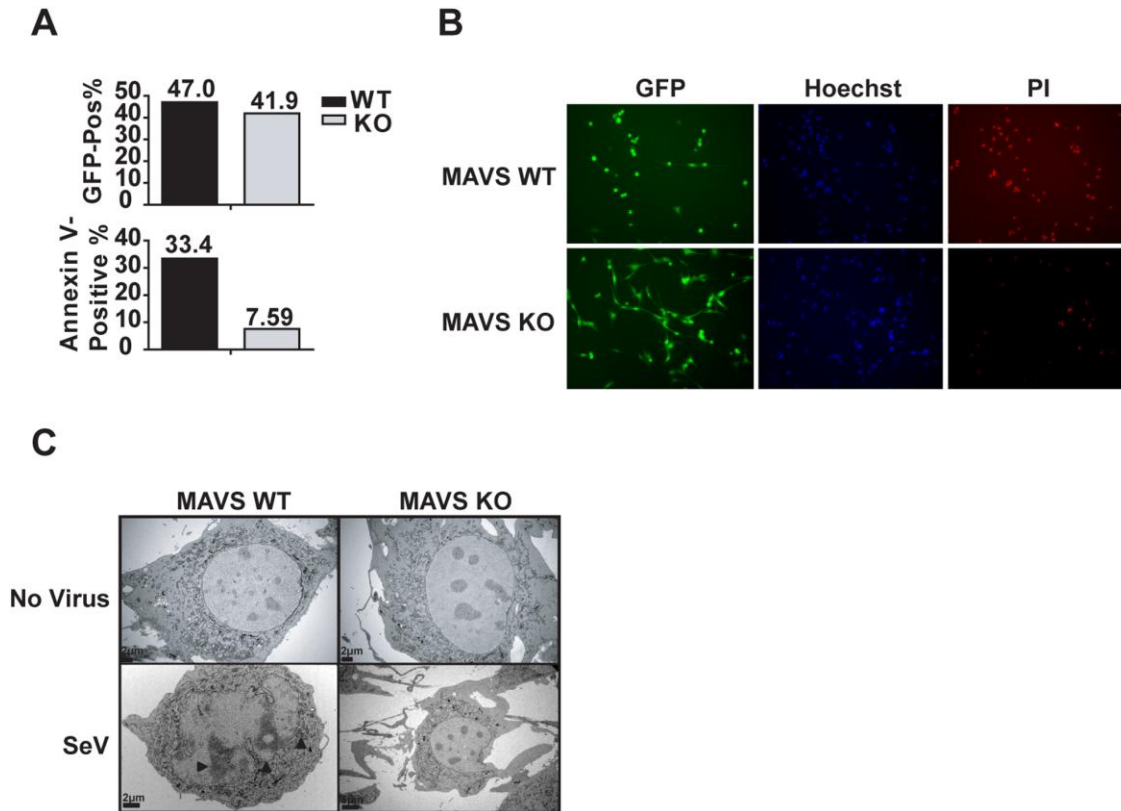


**Figure 2.5 MAVS is essential for virus-induced apoptosis in primary mouse embryonic fibroblasts.** (A) MAVS is critical for SeV-induced apoptosis. MAVS wild type and knockout MEFs were infected with recombinant Sendai virus expressing GFP at a MOI of 0.5. Forty-eight hours post-infection, GFP-positive cells were gated (top graph) and then subjected to Annexin V binding analysis (bottom graph) by flow cytometry. (B) MAVS wild type and knockout MEFs were infected with rSeV-GFP at the MOI of 0.5. Forty-eight hours post-infection, cells were stained with Hoechst blue and Propidium Iodide (PI). (C) Morphological features of MAVS wild type and knockout MEFs infected by SeV. TEM pictures were taken 48 h post-infection. While SeV infected wildtype cells displayed morphology typical of apoptotic cells, SeV infected *Mavs*<sup>-/-</sup> cells did not exhibit such morphology. Each graph represents two separate experiments.

2.5B, Hoechst and PI panels). Transmission electron micrographs taken for both cell types, with or without SeV, demonstrated that SeV infection resulted in the presence of typical apoptotic features in the wildtype MEFs (Fig. 2.5C, left panels). However, SeV infected *Mavs*<sup>-/-</sup> showed little signs of apoptosis and are indistinguishable from the uninfected controls (Fig. 2.5C, right panels).

### **Mitochondrial localization is required for MAVS-induced apoptosis.**

Previous reports have shown that the MAVS C-terminal transmembrane domain (TM) is essential to MAVS function as an adaptor in IFN-I signaling<sup>34</sup>. Therefore we sought to determine the essential domain that mediates MAVS-induced apoptosis. We expressed full length MAVS protein or three truncation mutants (Fig. 2.6A) in HEK293T cells and measured Annexin V and 7-AAD staining. The MAVS $\Delta$ TM mutant, which lacks the mitochondrial transmembrane sequence, was completely incapable of inducing apoptosis, suggesting that similar to the role of MAVS in interferon signaling, mitochondrial localization is essential to MAVS activation of apoptosis (Fig. 2.6B, top right panel). Truncation of the MAVS CARD domain (MAVS $\Delta$ CARD) significantly inhibited MAVS-induced apoptosis, but to a lesser extent than the aforementioned MAVS $\Delta$ TM mutant (Fig. 2.6B, bottom left panel). Truncation of the MAVS proline rich region (MAVS $\Delta$ Prol) had little effect on MAVS-induced apoptosis (Fig. 2.6B, bottom middle panel). All the MAVS truncation mutants were expressed well (Fig. 2.7A, 2.7B), thus the differences in the potency of inducing apoptosis are not due to the protein expression but the intrinsic ability to activate downstream pro-apoptotic signaling. To

solidify the

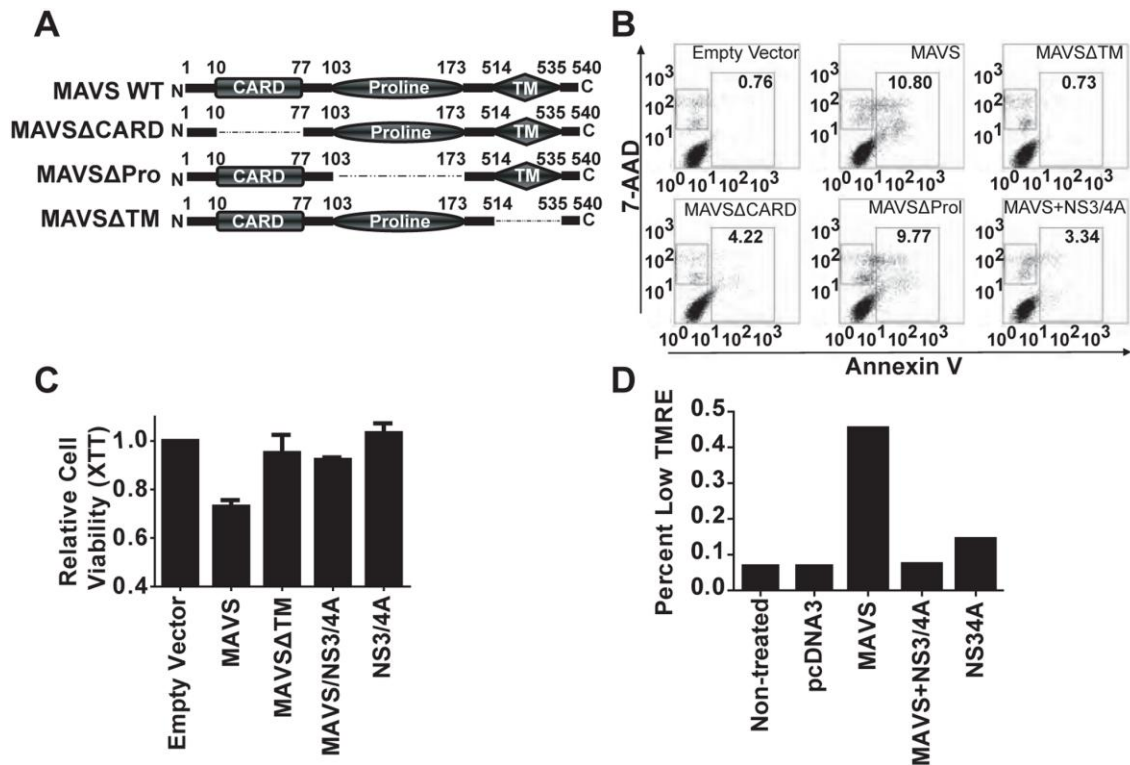


**Figure 2.6 Distinct MAVS domains are required for apoptosis.** (A) The domain structure of MAVS. MAVS contains a N-terminal CARD-like domain, a C-terminal transmembrane domain (TM) and a central proline-rich region. The cartoon shows the structure of the three truncation mutants we used in the study. (B) The TM and CARD-like domains are not dispensable for the pro-apoptotic function of MAVS. 1  $\mu$ g of wildtype MAVS and its three mutants depicted in (A) were introduced in HEK293T cells; and apoptosis was assessed by flow cytometry 48 h post-transfection using 7-AAD and Annexin V as markers of dead and apoptotic cells respectively. (C) The mitochondrial localization of MAVS is critical for its pro-apoptotic function. Cell viability was determined by XTT assay. (D) MAVS induces mitochondrial membrane potential collapse in HEK293T cells as quantified by TMRE staining. Each graph represents two separate experiments.

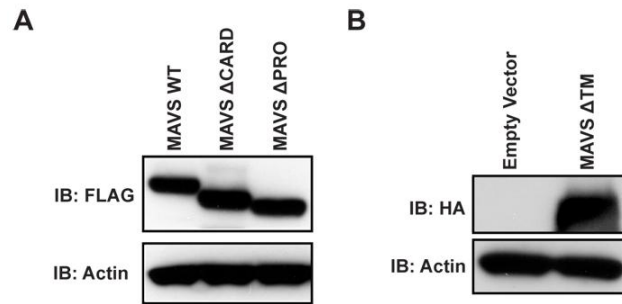


**Figure 2.7 Expression test of MAVS truncation mutants.** 3  $\mu$ g FLAG-MAVS wild type, FLAG-MAVS $\Delta$ CARD, FLAG-MAVS $\Delta$ pro and HA-MAVS $\Delta$ TM plasmids were transfected to  $5 \times 10^5$  HEK-293T cells seeded in 6 well plate. Cell were harvested 24 h post-transfection and blotted with anti-FLAG or anti-HA antibody to confirm protein expression efficiency.

mitochondrial dependency of MAVS-induced cell death, we co-expressed MAVS with the hepatitis C virus (HCV) protein NS3/4A. NS3/4A is a serine protease which has been shown to target the MAVS TM domain for cleavage and subsequent inhibition of MAVS antiviral signaling<sup>37, 186</sup>. Consistent with its role in inhibiting MAVS mediated IFN-I signaling, NS3/4A inhibited MAVS induced apoptosis (Fig. 2.6B, bottom right panel). The inhibitory effects of MAVS $\Delta$ TM mutant and NS3/4A were also verified by a measurement of cell viability via XTT assay (Fig. 2.6C). Mitochondrial membrane potential collapse marks a point-of-no-return during apoptosis and occurs earlier than DNA fragmentation<sup>206, 207</sup>. Only wildtype MAVS resulted in compromised mitochondrial membrane potential as measured by TMRE staining while the addition of NS3/4A abrogated this effect (Fig. 2.6D).

### **MAVS-induced apoptosis is independent of type-1 interferon production or NF- $\kappa$ B activity.**

It has been shown that exogenous MAVS expression triggers IFN-I production<sup>34, 175</sup>. Type-1 IFNs mediate their effects by binding to cell surface receptors, activating downstream interferon-stimulated genes or ISGs, among which more than 15 genes have pro-apoptotic functions<sup>208</sup>. We sought to determine if MAVS-induced apoptosis was the result of activation of a distinctive signaling pathway or as a consequence of IFN production. First, we induced IFN-I production in HEK293T cells by ectopic expression of upstream signaling molecules that activate MAVS-mediated IFN production. As previously reported, a helicase domain truncation mutant of RIG-I<sup>33</sup>,

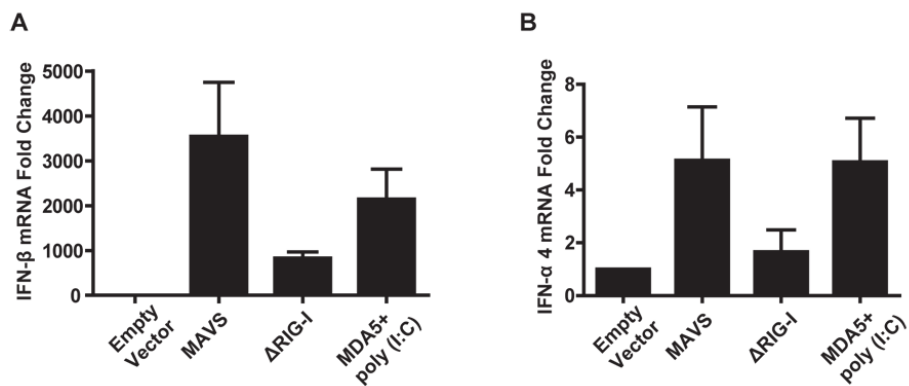


**Figure 2.8** MAVS, ΔRIG-I and MDA5 plus Poly (I:C) induce increased transcription of *IFNB1* and *IFNA4*.  $5 \times 10^5$  HEK293T cells were seeded in 6-well plates and grown overnight. 1 μg of MAVS and ΔRIG-I plasmids were transfected into the cells the next day, similarly 1 μg MDA5 and 100 ng poly (I:C) were co-transfected into the cells as well. RNA samples were extracted from each group of cells 24 h post-transfection and subjected to real time RT-PCR analyses on the transcripts of *IFNB1* and *IFNA4*.

full-length MAVS<sup>34</sup>, or MDA-5 in conjunction with its ligand poly(I:C)<sup>209</sup> are all potent IFN-I inducers (Fig. 2.8A, 2.8B). Neither  $\Delta$ RIG-I nor MDA-5 plus poly(I:C) induced any observable cell death or Annexin V-positive cells (Fig. 2.9A, bottom panels). Only full-length MAVS triggered apoptosis as quantified by Annexin V and 7-AAD staining (Fig. 2.9A, top right panel). To explore the role of IFN- $\beta$  in MAVS-induced apoptosis, HEK293T cells were treated with 200 neutralization IU/ml IFN- $\beta$  antibody prior to transient expression of MAVS followed by XTT measurements. We found that blocking IFN- $\beta$  from binding to its cell surface receptor had no effect on MAVS-induced apoptosis (Fig. 2.9B) even though the antibody efficiently blocked the function of secreted IFN- $\beta$  (Fig. 2.10). In congruence with these findings, GFP-Sendai virus infections of the interferon- $\alpha/\beta$  receptor (IFNAR) knockout and wildtype MEFs demonstrated that this receptor is not required for SeV-induced cell death as visualized by PI staining (Fig. 2.9C). Although to a lesser extent than IFN-I responses, MAVS is also capable of inducing the transcription factor NF- $\kappa$ B, which is known to activate a wide array of genes linked to immune, inflammatory, and cell-fate processes<sup>210</sup>. To test the involvement of NF- $\kappa$ B in MAVS-induced apoptosis, we co-expressed MAVS with the non-degradable super-repressor form of I $\kappa$ B $\alpha$ . This super-repressor is a known potent inhibitor of NF- $\kappa$ B activation and as expected inhibited MAVS-induced NF- $\kappa$ B activation (Figure S6)<sup>211</sup>. However, transient expression of MAVS in HEK293T cells induced apoptosis even in the presence of the NF- $\kappa$ B super-repressor (Fig. 2.9D). There are 14 subtypes of type-1 interferons, and a plethora of other secreted soluble factors induced by MAVS

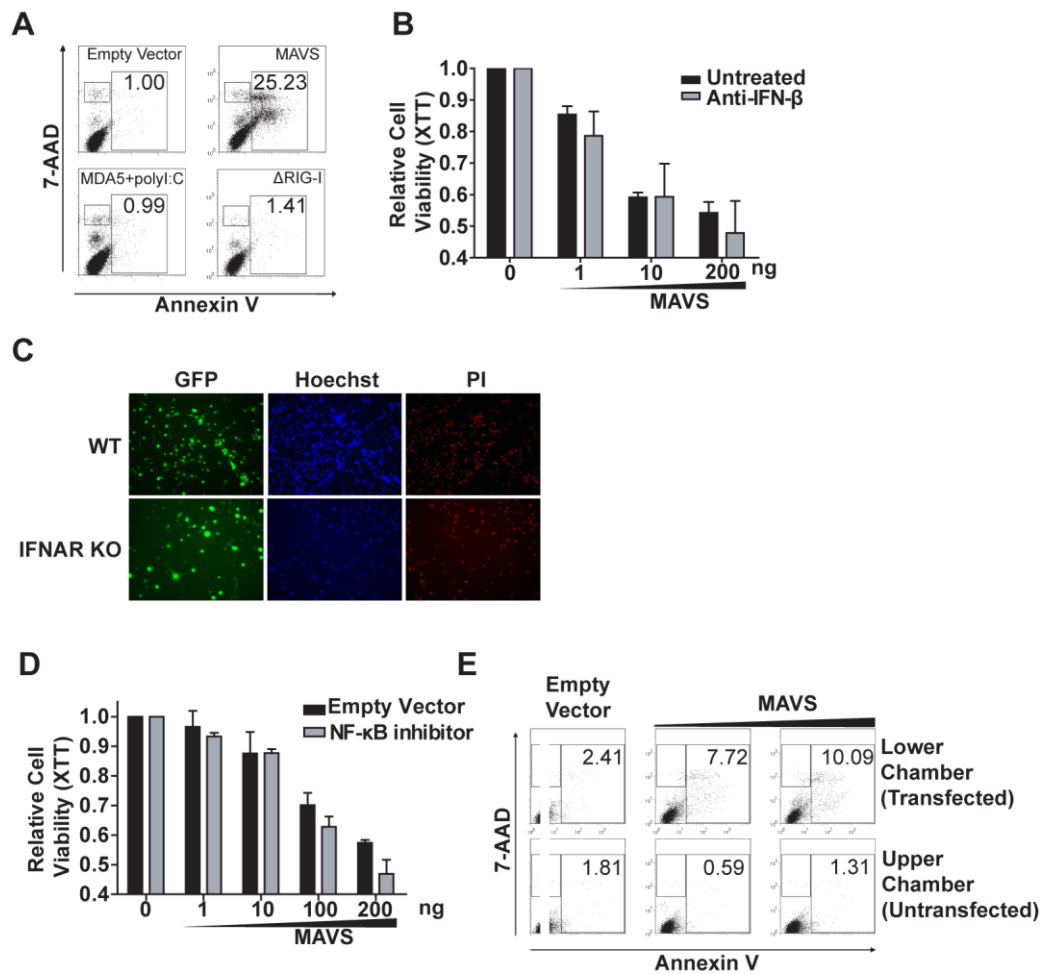


**Figure 2.9 MAVS-induced apoptosis is independent of type I IFNs production.** (A) Three molecules ( $\Delta$ RIG-I, MDA5 and MAVS) that activate the production of type I IFNs were introduced into HEK293T cells; only MAVS is able to induce apoptosis. (B) Anti-IFN- $\beta$  antibody was added to the medium at the final concentration of 200 neutralization units/ml to prevent secreted IFN- $\beta$  binding to IFNAR, this neutralization process did not inhibit MAVS-induced apoptosis. (C) SeV-induced apoptosis is IFN-I-independent. MEFs from both C57BL/6 wild type and *Ifnar*<sup>-/-</sup> mice were infected with rSeV-GFP. Cells were stained with Hoechst and PI 48 h post-infection. (D) The non-degradable form of I $\kappa$ B was co-expressed with different doses of MAVS, yet cell viability loss was not restored. (E) HEK293T cells were plated at both the lower chamber and upper chamber of the transwell plate separated by an insert filter membrane with 0.4  $\mu$ m pore size. 1  $\mu$ g of MAVS-containing plasmid was transfected into the cells in the lower chamber and all cells were harvested 48 h post-transfection for flow cytometry analysis.

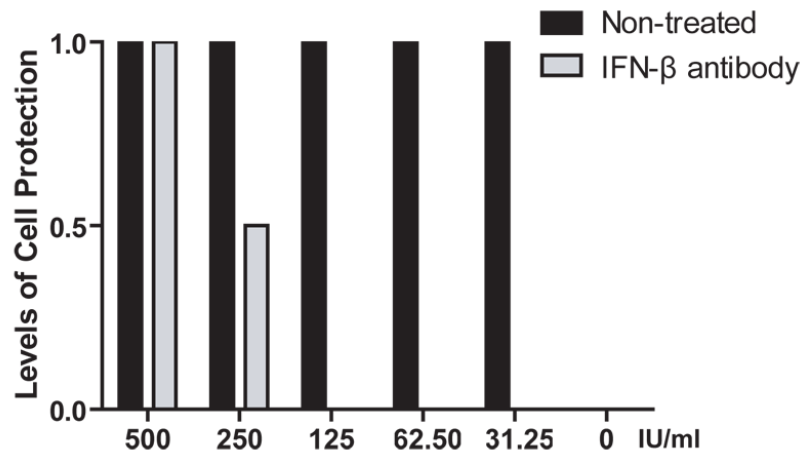


**Figure 2.10 IFN- $\beta$  neutralizing antibody is able to block the function of secreted IFN- $\beta$ .** A549 cells were seeded in 96-well plate at the density of  $2 \times 10^4$  per well, 1  $\mu$ l of media or anti-IFN- $\beta$  antibody was added to reach the final concentration of 200 neutralization IU/ml the next day. One hour after incubation with the antibody, recombinant IFN- $\beta$  was added to culture at a series of doses from 31.25 to 500 IU/ml. Cells were infected with Encephalomyocarditis virus (EMCV) at  $4 \times 10^6$  pfu/ml 16 h after IFN treatment. The plates were blind scored 24 h post-infection using “1” as maximal protection (most cells are protected by IFN), “0.5” as about 50% of the cells were not protected by IFN, and “0” as no IFN protection (most cells are dead).

expression. Therefore, we performed a transwell assay designed to definitively answer if MAVS-induced cell death was intrinsic to the host cell or caused by some unknown secretory factor. HEK293T cells were plated in two different chambers (top and bottom) separated by an insert filter membrane, permissive to all secretory cytokines but impermeable to FuGENE6:DNA complexes. In this experiment, only the lower chamber was transfected with MAVS. Cells in the upper chamber were not transfected with MAVS, but were exposed to the same cytokine milieu. As expected, MAVS induced cell death in the lower chamber (transfected cells); however the upper well (untransfected cells) remained healthy and unchanged from controls (Fig. 2.9E). This

indicates that the MAVS-induced death is not caused by an undefined secretory product(s) which includes the interferon family members. IRF3 is a critical transcription factor for IFN-I production and can be activated by MAVS. Therefore we intended to determine whether MAVS-induced apoptotic signaling depends on IRF3. HEK293T cells were plated in 96-well plate and endogenous IRF3 was knocked down by transfecting a pool of four siRNA into the cells, MAVS was introduced 24 hours after siRNA transfection. Cell viability was measured by XTT assay 48 hours after MAVS or control empty vector plasmids transfection. Depletion of IRF3, however, did not restore MAVS-induced cell viability loss (Fig. 2.11A, 2.11B). In order to further strengthen these findings, we repeated our experiments in 6 well plates and harvested cells 48 hours after plasmids transfection. Half of the cells from each well were stained for Annexin V and analyzed by flow cytometry, and the other half of the cells were lysed in RIPA buffer for Western blotting analyses on IRF3. As expected we were able to deplete above 90% of the endogenous IRF3, yet MAVS-induced apoptosis was not abrogated (Fig. 2.11C, 2.11D).

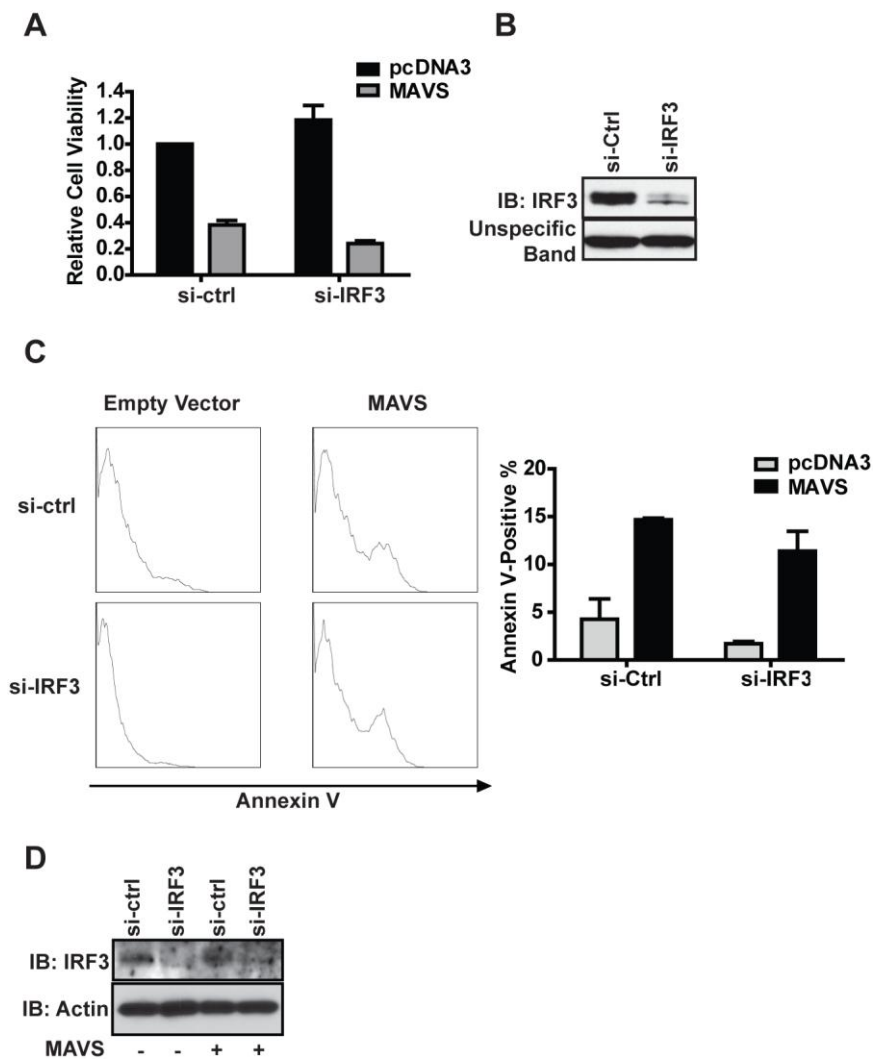


**Figure 2.11 MAVS-induced apoptosis does not depend on IRF3.** (A)  $1.0 \times 10^4$  HEK293T cells were plated in 96-well plates, a pool of four siRNA targeting IRF3 or control siRNA were added to each well, 24 hours later 200 ng MAVS or empty vector plasmids were transfected into the cell. XTT assay was performed 48 hours thereafter. Error bars shown in the plot represents three biological replicates. (B) The same IRF3-targeting and non-targeting siRNA transfection reagents used in (A) were applied to  $5.0 \times 10^5$  cells, and all cells were lysed in RIPA buffer 48 hours post-transfection and subjected to Western blotting to confirm knockdown. (C)  $5.0 \times 10^5$  HEK293T cells were plated in 6-well plates and treated with IRF3 or control siRNAs, 24 hours later 3  $\mu$ g of MAVS expression plasmid or empty vector plasmids were introduced into the cells. Half of the cells from each well were harvested 48 hours thereafter and stained with Annexin V. The plot represents two separate experiments and the percentages of Annexin V positive cells were averaged for quantification. (D) The other half of the cells described in (C) were lysed in RIPA buffer and subjected to western blot analyses to confirm IRF3 knockdown.

### The SARS-CoV non-structural protein 15 inhibits MAVS-induced apoptosis.

While host response that elicits apoptosis may function as an antiviral strategy, viruses have also evolved diverse mechanisms to evade these host antiviral responses. Therefore we performed a functional screen of 12 SARS-CoV-encoded proteins to identify any potential modulators of MAVS-induced apoptosis. Each of these SARS-CoV genes were cloned into an expression vector and co-expressed with MAVS plasmid followed by XTT cell viability measurements. Protein expression was verified by an immunoblot (Fig. 2.12). Of the 12 tested proteins, only one SARS-CoV protein,

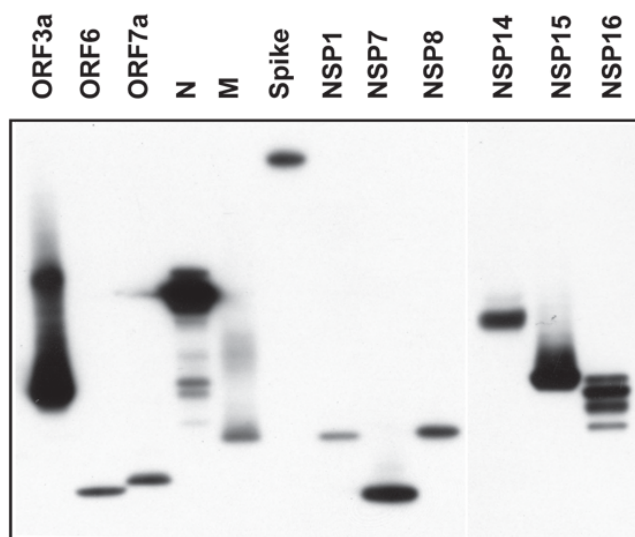


**Figure 2.12 SARS-CoV proteins were expressed in HEK293T cells.** Twelve SARS-CoV protein-encoding sequences were cloned into expression vectors with an HA tag. HEK293T cells were seeded in 6-well plate and transfected with 1  $\mu$ g plasmid of each protein when cells reached 60% confluence, all cells were harvested and lysed 24 h post-transfection for Western blotting analysis with anti-HA antibody.

NSP15, significantly altered MAVS-induced apoptosis of HEK293T cells (Fig. 2.13A). Further examination shows that NSP15 significantly inhibited MAVS induced apoptosis in a dose-dependent manner (Fig. 2.13B). The anti-apoptotic function of NSP15 shows specificity since it did not inhibit staurosporine-induced apoptosis (Fig. 2.13C). We sought to investigate if the anti-apoptotic function of NSP15 was specific for SARS-CoV or shared by other coronaviruses. When the NSP15 protein encoded by the SARS-CoV,

HKU1 or NL63 genome was coexpressed with MAVS, only SARS-CoV NSP15 inhibited MAVS-mediated apoptosis as measured by Annexin V and 7-AAD staining, while the others showed little effect on cell viability (Fig. 2.13D).

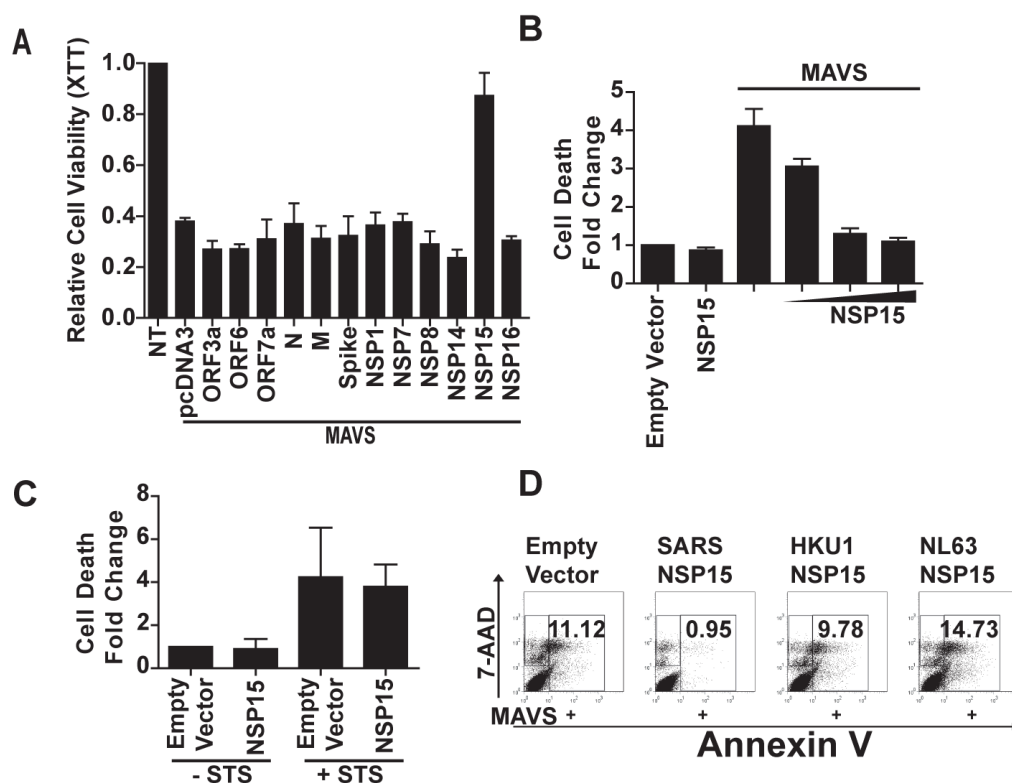


**Figure 2.13 The SARS-CoV NSP15 protein abrogates MAVS-induced apoptosis.** (A) Twelve of the SARS-CoV proteins were co-expressed with MAVS and NSP15 is the only one that exhibited a potent inhibitory effect on MAVS-induced apoptosis as assessed by XTT cell viability assay. (B) The inhibitory effect of NSP15 displays dose-dependency. Cell death was measured by an adenylate kinase activity assay. (C) The anti-apoptotic function of NSP15 does not extend to staurosporine-induced cell death. NSP15-expressing plasmid or empty vector were transfected in HEK293T cells seeded on 96-well plate, cells were treated with 500 nM staurosporin or PBS 24 h post-transfection, cell death fold change was evaluated by the adenylate kinase activity assay. (D) The inhibitory effects of NSP15 is unique to SARS-CoV. MAVS was co-expressed with NSP15 encoded by SARS-CoV, HKU1 and NL63. Flow cytometry analysis of 7-AAD/Annexin V stained cells was performed 48 h post-transfection. The results represent two separate experiments.

## 2.4 Conclusion

Host cellular response to virus infection involves the concomitant activation of

parallel signaling pathways leading to the transcription of a plethora of cytokine genes, prominent among these are the genes encoding type-1 interferons (IFN-I). It is the autocrine and paracrine action of these and other cytokines which encompasses the comprehensive host immune response designed to defend against viral infection. This is accompanied by a reciprocal activation of programmed cell death in infected host cells, which is also known to reduce viral load. Apoptosis has been suggested to play a protective role at the organismal level in preventing the virus from completing its replication and producing infectious progeny viruses<sup>187</sup>. Consequently, the exact mechanisms underlying both virus-induced apoptotic signaling in addition to viral strategies to subvert these responses is currently a topic of intensive research. While pathways that govern IFN-I have been extensively investigated, the molecular mediators that activate host cell apoptosis during viral infection are less known. In this study we have identified a role for MAVS in the initiation of virus-induced apoptosis (Fig. 2.14). Furthermore, we have identified a viral gene encoded by the SARS-CoV which functions as an inhibitor of MAVS-mediated apoptosis.

It is known that MAVS is a potent inducer of IFN-I responses and that IFN-I can activate host apoptotic responses, therefore it was important to determine whether the cell death responses observed in the current study were a consequence of IFN-I secretion. In fact, IFN-I consist of several species including IFN- $\alpha$ , IFN- $\beta$ , IFN- $\omega$  and IFN- $\kappa$  and these cytokines bind to surface receptors leading to the activation of the Jak-Stat signal transduction pathway resulting in the transcriptional activation of virtually hundreds of

IFN-stimulated genes (ISGs), whose protein products play pivotal roles in a plethora of biological events, including but not limited to immunomodulation, cell differentiation, anti-angiogenesis and programmed cell death. For example, type-1 IFN induction of apoptotic responses can be mediated by a multitude of ISGs, illustrated by the finding that more than 15 ISGs pro-apoptotic functions<sup>208</sup>. In addition, the involvement of proteins on IFN axis in virus-induced host cell apoptosis has been implicated in another previous report, in which MAVS has been shown to be critical for reovirus-triggered caspase-3/7 activation in HEK293T cells<sup>212</sup>, however, the study did not evaluate whether MAVS mediates virus-induced apoptosis and what roles type 1 IFNs play in MAVS-mediated apoptosis.. Using a multi-pronged approach we demonstrate that MAVS-mediated apoptosis is not a consequence of IFN-I induction by MAVS. We show that (a) the over-expression of RNA helicases that induce IFN-I does not lead to apoptosis; (b) anti-IFN- $\beta$  antibodies does not ablate MAVS-induced apoptosis; (c) the targeted deletion of IFN receptor does not alter MAVS-induced apoptosis; (d) the co-culture of MAVS-transfected cells with nontransfected cells separated by a trans-well membrane does not induce apoptosis in the latter, indicating that a soluble secretory factor is likely not responsible for the apoptosis-inducing activity.

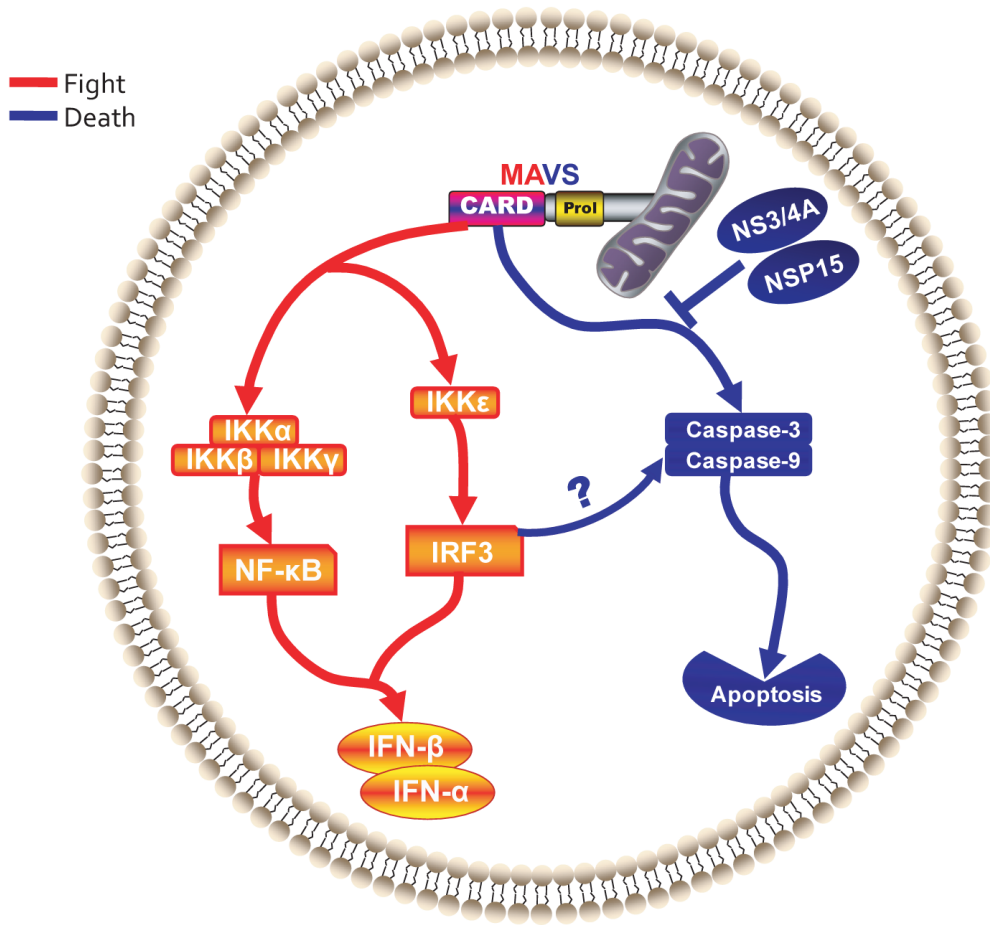


**Figure 2.14 A proposed model for the dual functions of MAVS.** MAVS is engaged in two distinct host protective responses to viral infections. Upon activation by RNA viruses, MAVS initiates type 1 IFN signaling by activating the nuclear translocation of NF-κB and IRF3. In addition, host cells could mount apoptotic responses to viruses such as SeV via MAVS. Notably MAVS is targeted by viruses not only for abrogating IFN-I production but also inhibiting host apoptosis. For example, HCV NS3/4A and SARS-CoV NSP15 proteins abrogate MAVS-mediated apoptosis.

IRF3 is downstream of MAVS in inducing IFN-I transcription, and exogenous expression of MAVS could lead to its phosphorylation and nuclear translocation<sup>34</sup>. In addition, it's been shown that expression of the constitutively active form of IRF3 is toxic and wild type IRF3 expression can augment SeV-induced apoptosis<sup>205, 213</sup>. We evaluated if MAVS-induced apoptosis depends on the presence of IRF3. However we found that depletion of endogenous IRF3 by means of RNAi did not reverse MAVS-induced cell

viability loss. Together with our findings that MAVS-induced apoptosis is IFN-I-independent, we believe that the MAVS-induced apoptotic signaling pathway is different from the classical MAVS-mediated antiviral signaling and that the reported pro-apoptotic effects of the constitutively active form of IRF3 might be independent of its transcriptional activity in inducing IFN-I production. In fact our data suggests other IFN-I signaling molecules such as the constitutively active form of RIG-I and MDA5 does not result in apoptosis despite of their potency in inducing IFN-I. However, the exact mechanisms of MAVS activation of caspases remain unclear.

The dual function of MAVS in virus-induced IFN-I and apoptosis highlights this molecule as a putative target for viral evasion strategies designed to escape host immunity. For example, it is already known that Hepatitis C Virus (HCV) produces a serine protease, NS3/4A, which disrupts IFN-I production through the targeted cleavage of the MAVS transmembrane region and the subsequent dislodging of MAVS from the mitochondria<sup>37, 185</sup>. In fact, we found that loss of MAVS mitochondrial localization through mutation of the transmembrane domain, also completely abolished its pro-apoptotic effects. Consistent with these results, when HCV NS3/4A protein was co-expressed with MAVS, this viral protein completely inhibited MAVS-induced cell death. This result would suggest that the host immune evasion strategies of the HCV NS3/4A protein may be extended to inhibition of MAVS-mediated apoptosis. Similarly hepatitis A virus (HAV), a picornavirus, employs a cysteine protease 3ABC to abrogate type-1 IFNs production by targeting MAVS<sup>186</sup>. Therefore, it is likely that other uncharacterized viral mechanisms

target MAVS for modulation of host cell death responses.

One novel strategy described in this study is employed by the SARS-CoV. Similar to SARS-CoV abilities to inhibit IFN-I responses, we have found that this virus is also capable of interfering with host cell death responses by targeting MAVS. We showed that among the 12 SARS-CoV proteins tested, NSP15 alone can completely abrogate MAVS-induced apoptosis. The underlying mechanism is currently unclear since the function of NSP15 is not yet fully defined. However, an earlier report indicates that this protein is indeed important for SARS pathogenesis in that it is essential for viral replication<sup>214</sup>. However, until we understand the exact temporal expression patterns of each of the SARS-CoV proteins during the course of an infection, the relative contributions of each to the evasion of host immunity and apoptosis will not be fully understood. Further studies are needed to determine the exact mechanism of action for NSP15 on inhibiting MAVS-induced cell death. Since SARS-CoV replication is limited to the first two weeks after symptom onset and NSP15 is critical for its replication<sup>201, 214</sup>, this would support the theory that NSP15 may function as an inhibitor of host cell death during this time, which would possibly benefit viral replication. Further studies are ongoing to determine how NSP15 and other SARS-CoV proteins contribute to overall viral evasion strategies.

The finding that MAVS mediates virus-induced apoptosis posits a new mechanism by which mitochondria serves as a *bona fide* intracellular sentinel for antiviral and apoptotic responses. It is well established that the permeabilization of the mitochondria

outer membrane by the pro-apoptotic Bcl-2 family member BAK results in the activation of caspase-9 in a classical Apaf-1-dependent or an alternative Apaf-1-independent pattern<sup>215</sup>. Furthermore, it is known that proteins localized in the mitochondria are targeted by viruses to modulate host responses. For example, the cytomegalovirus RNA can interact with the mitochondrial enzyme complex I (reduced nicotinamide adenine dinucleotide–ubiquinone oxido-reductase) to modulate the classical mitochondria-mediated apoptosis<sup>216</sup>. Recent discoveries also underscore the mitochondria as a platform orchestrating host antiviral type-1 IFNs through the mitochondrial-localized MAVS protein. This study describes, for the first time, a duality of function for the MAVS protein in regulating both IFN-I and apoptotic antiviral responses from within the mitochondria and suggests that MAVS is a pivotal molecule in the bifurcation of host responses following viral challenge. Furthermore, the identification of SARS-CoV NSP15 as an inhibitor of host apoptotic responses reveals both novel host defense mechanisms as well as viral immune-evasion mechanisms that might serve as useful templates for the development of anti-viral drug strategies.

## **2.5 Materials and Methods**

### **Cells and Plasmids**

HEK293T cells, MAVS<sup>+/+</sup>, MAVS<sup>-/-</sup>, IFNAR<sup>-/-</sup> mouse embryonic fibroblasts were maintained in DMEM media supplemented with 10% FBS, 1% penicillin and 100 µg/ml streptomycin. Cells were passed every three days and grown at 37 °C in 5% CO<sub>2</sub>.

The mammalian expression plasmids of NS3/4A, wild type MAVS and truncation

mutants were kindly provided by Dr. Zhijian Chen at the University of Texas southwestern medical center. HA-tagged SARS-CoV proteins expression plasmids, HKU1 NSP15 and NL63 NSP15 expression plasmids were gifts of Drs. Ralph Baric and Matthew Frieman at the University of North Carolina.

### **Transfections and Viral Infections**

HEK293T cells were seeded in 96-well or 6-well plates, and the total DNA transfected into these cells was 400ng/well and 1 µg/well, respectively. Standard transfection protocol was performed using FuGENE6 (Roche Applied Science) according to the commercial protocol. Cells were incubated for the indicated times prior to assay.

rSeV-GFP is a recombinant Sendai virus expressing GFP and was originally made by Dr. Daniel Kolakofsky. For viral infections,  $1.6 \times 10^4$  MEFs were plated into 12-well plate one day prior to Sendai virus (SeV) infection. Viral infections were performed when cells reached 60% confluence. MEFs were incubated with SeV for 1h in serum-free DMEM supplemented with 0.5% trypLE Select at the MOI of 0.5. Serum-free DMEM supplemented with 0.5% trypLE Select was used for mock infection. Virus inoculum was removed and cells were replenished with complete media supplemented with 0.5% trypLE Select following incubation with virus.

### **Cell Viability Assays**

XTT salt (Sigma, St. Louis, MO) (1mg/ml) was dissolved in serum-free media and phenazine methosulfate (PMS) (5mM) (Sigma, St. Louis, MO) solution was prepared fresh. For activated XTT solution, PMS and XTT solutions were mixed at a ration of

5:1, respectively. 50 µl of activated XTT solution was added to each 96 well ( $1 \times 10^4$  cells/well), incubated at 37 °C for 4 hours and absorbance read at a wavelength of 450nm. An adenylate kinase non-destructive cytotoxicity assay was performed utilizing the ToxiLight bioassay kit (Lonza) following the manufacturers standard protocol for adherent cells in a 96 well plate. For Trypan blue exclusion test of cell viability, 10 µl of cell suspension was mixed with 10 µl of 0.4% Trypan blue solution (Sigma, St.Louis, MO), and both unstained (viable) and stained (dead) cells were counted on the hemacytometer. The percent of dead cells was calculated by dividing the number of stained cells by the total number of cells.

### **Flow Cytometry**

Cells were harvested and washed in cold FACS buffer (5% FBS in  $1 \times$  PBS) twice and once using  $1 \times$  Annexin V binding buffer (BD Bioscience, San Diego, CA). Cells were transferred into 96-well plate and resuspended in 45 µl Annexin V binding buffer. Cells were stained according to standard cell staining protocol<sup>217</sup> using Annexin V conjugated to FITC or APC (BD Biosciences, San Diego, CA). Cells were washed in FACS buffer and stained with 7-AAD (Invitrogen, Carlsbad, CA) for 10 min at room temperature. Cells were washed twice and resuspended in FACS buffer containing 1 µg/ml Actinomycin D. After 5 min incubation, all samples were fixed in 500 µl 1% EM grade formaldehyde (Polysciences, Warrington, PA) for immediate flow cytometry analyses. For the rSeV-GFP infected samples, GFP positive cells were gated and Annexin V and 7-AAD quantitated.

Mitochondrial membrane potential  $\Delta\psi$  was assessed by flow cytometry analysis on a  $\Delta\psi$ - sensitive fluorophore tetramethylrhodamine ethylester (TMRE) (Molecular Probes, Eugene, OR). After treatment, HEK-293T cells were incubated with TMRE at the concentration of 10nM per  $1 \times 10^6$  cells for 40min at 37 °C. Immediate flow cytometry analysis was performed after staining.

All flow cytometry data were collected on either a FACSCalibur (BD Biosciences, San Jose, CA) or CyAn flow cytometer (Dako North America, Carpinteria, CA) and then analyzed by FlowJo software (Tree Star, Ashland, OR)

### **Imaging**

Transmission electron microscopy examination was performed as described <sup>124</sup>. MEFs or HEK293T cells were harvested and fixed in glutaraldehyde and all samples were post-fixed in 1% OsO<sub>4</sub> for transmission electron microscopy examination. Cells were embedded in London Resin White and sections were analyzed using a LEO EM-910 transmission electron microscope (LEO Electron Microscopy Inc., Thornwood, NY). Hoechst and Propidium Iodide (PI) dual staining was used to evaluate SeV-induced cell death. Samples were photographed using a Leica DMIRB inverted fluorescence microscope (Leica Microsystems Inc., Bannockburn, IL) with a digital camera (MicroPublisher, Q-Imaging, Burnaby, BC, Canada) -

### **Immunoblotting**

Cells were lysed in RIPA lysis buffer (1% Triton X-100, 0.25% DOC, 0.05% SDS, 50mM Tris pH8.0, 150mM NaCl and 50mM NaF) containing proteinase inhibitor

cocktails (Roche) for 30min at 4°C. Whole cell lysates were suspended in Laemmli's sample buffer and loaded onto NuPAGE Bis-Tris 4-12% gradient pre-cast gels (Invitrogen, Carlsbad, CA) for SDS-PAGE and subsequent immunoblotting for PARP, caspase-3 and caspase-9 (Abcam, Cambridge, MA), IRF3 (Santa Cruz Biotechnology, Santa Cruz, CA), rodent specific MAVS (Cell Signaling, Danvers, MA). Densitometry was performed using ImageJ analysis software.

### **Caspase and Interferon inhibition treatments**

HEK293T cells were incubated with 50µM Z-VAD-FMK to inhibit caspase activity. HEK293T cells were treated with human IFN-β neutralizing antibody (GeneTex, San Antonio, TX) at the concentration of 200 neutralization units/ml.

### **Depletion of endogenous IRF3**

HEK293T cells were transfected with a pool of four targeting siRNA according to the manufacturer's protocol (Dharmacon, Chicago, IL). The sequences are: (1) sense 5'-CGAGGCCACUGGUGCAUAAUUU, antisense 5'-PAUAUGCACCAGUGGCCU CGUU; (2) sense 5'-CCAGACACCUCUCCGGACAUU, antisense 5'-PUGUC CGGAGAGGUGUCUGGUU; (3) sense 5'-GGAGUGAUGAGCUACGUGAUU, antisense 5'-PUCACGUAGCUCAUCACUCCUU; (4) sense 5'-AGACAUUCU GGAUGAGUUAUU, antisense 5'-PUAACUCAUCCAGAAUGUCUUU. A pool of 4 non-targeting siRNA were used as control. Empty vector or MAVS expression plasmids were introduced into the cells 24 hours after the transfection of siRNA.

### **Transwell Assay**

HEK-293T cells were seeded on the bottom of both chambers in a HTS 24-well transwell plate with 0.4µm pore polycarbonate membrane (Corning Incorporated Life Sciences, Lowell, MA). MAVS expression plasmid DNA was transfected into the cells on the bottom of lower chamber and flow cytometry analysis on apoptosis was performed 48h post-transfection on cells grown in each chamber.

## **CHAPTER THREE**

### **NLRX1 AND TUFM FORM A MITOCHONDRIAL COMPLEX THAT REGULATES TYPE 1 INTERFERON AND AUTOPHAGY**

### 3.1 Abstract

Mitochondria are crucial in the regulation of host innate antiviral responses. A prime example is the intersection of the mitochondrial protein MAVS/IPS-1/VISA/CARDIF with RLR (RIG-I-like receptors) to induce type 1 interferon (IFN-I). NLRX1 is a mitochondrial NLR (nucleotide-binding, leucine-rich repeats containing) protein that attenuates MAVS-RLR signaling. More in-depth analysis utilizing cells from gene-deletion mice indicates that NLRX1 not only attenuates IFN-I production, it additionally promotes autophagy during viral infection. This dual regulatory function of NLRX1 parallels the previously described functions of Atg5-Atg12, although NLRX1 does not associate with Atg5-Atg12. High throughput quantitative mass spectrometry and biochemical analysis revealed a novel NLRX1-interacting partner, mitochondrial Tu translation elongation factor (TUFM/P43/EF-Tu/COXPD4/EF-TuMT), which does interact with Atg-5-Atg12. Similar to NLRX1, TUFM potently inhibits RLR signaling and promotes autophagy during a viral infection. This study establishes the first link between an NLR protein and a viral-induced autophagic machinery via an intermediary partner, TUFM.

### 3.2 Introduction

The mitochondrion is a coordinating site for several key host responses against viral infection including apoptosis and type 1 IFN (IFN-I) signaling<sup>5, 173, 218</sup>. Upon infection with a RNA virus, virus-related RNA species are recognized by RIG-I (retinoic-acid inducible gene I)-like receptors (RLRs), including RIG-I and MDA5 (melanoma differentiation associated gene 5)<sup>218</sup>. The 5'-ppp moiety of cytosolic dsRNA is the molecular signature that activates RIG-I<sup>41, 43</sup>, and RIG-I deficiency leads to compromised IFN-I in response to VSV (vesicular stomatitis virus), SeV (Sendai virus) and NDV (Newcastle disease virus)<sup>40</sup>. The helicase domain drives the unwinding of dsRNA with 3'-terminal overhang via its ATPase activity<sup>38</sup>. Upon activation, RIG-I binds to its adaptor, the mitochondrial antiviral signaling protein (MAVS, also referred to as IPS-1, VISA or Cardif) via homotypic CARD interaction to activate IFN-I by facilitating the nuclear translocation of the transcription factors NF- $\kappa$ B and IRF3<sup>34-37</sup>. Similar to MAVS, another adaptor protein MITA (also referred to as STING, ERIS and MPYS) is ubiquitously expressed and is indispensable for inducing IFN-I upon RIG-I activation<sup>69-72, 75</sup>. Overexpression of MITA/STING is less potent than MAVS in the activation of IRF3<sup>70</sup>, and it may employ a separate mechanism via its association with components of the endoplasmic reticulum translocon-associated protein (TRAP) complex to modulate RLR signaling<sup>69</sup>.

Due to the detrimental effects of IFN-I at high levels, several molecular machineries keep the RLR pathway in-check. A unique member of the nucleotide-binding domain

(NBD) and leucine-rich-repeats (LRR)-containing proteins (NLRs), NLRX1, resides in the mitochondria and attenuates the activation of MAVS by binding to its CARD domain, possibly precluding its engagement with RIG-I<sup>124</sup>. The NLR family was first discovered by bioinformatic data mining based on the sequence of CIITA<sup>219</sup>. NLRs have diverse biological functions including formation of the caspase-1 activating inflammasome protein complex, modulation of host anti-pathogen response, regulation of gene transcription and cytokine, chemokine and defensin production<sup>67, 220</sup>. Emerging evidence suggests that NLRs actively participate in antiviral signaling pathways. For example, NLRP3 inflammasome has been shown to respond to influenza A virus, VSV and EMCV (Encephalomyocarditis virus) infection<sup>130, 131, 221, 222</sup>. NOD2 is shown to associate with MAVS to induce IFN-I<sup>129</sup>. On the other hand, NLRX1 is the first NLR found to negatively impact IFN-I production<sup>124</sup>, although the evidence was largely obtained in cell lines with transfected protein or shRNA-mediated gene reduction. Overexpression of NLRX1 inhibits  $\Delta$ RIG-I-induced NF- $\kappa$ B- and IRF3-dependent promoter activity, and a reduction of NLRX1 results in enhanced transcription of *IFNB1*<sup>124</sup>. Recent studies linked NLRC5 to IFN-I production, however conflicting evidence exists where the protein is found to be either a negative<sup>133</sup> or positive regulator<sup>134, 136</sup> of IFN-I, while a gene-deletion study shows that it has no effect on IFN-I response<sup>139</sup>. Thus the link between NLRs and IFN-I requires more in-depth analysis.

In addition to NLR-based complexes, the autophagy-related protein conjugate, Atg5-Atg12, has also been shown to regulate the RLR signaling pathway. The absence

of autophagy, which causes the degradation of misfolded proteins and cytoplasmic organelles to recycle nutrients<sup>223, 224</sup>, results in significantly higher RLR signaling, leading to more IFN-I production in mouse embryonic fibroblasts<sup>141, 142</sup>. One study showed that Atg5 deficient cells and Atg7-deficient cells, in which the Atg5-Atg12 conjugation is impeded, exhibit enhanced IFN-I response to virus<sup>141</sup>. The role of autophagy in RLR signaling appears to be cell type specific since such inhibitory effects were not seen in plasmacytoid dendritic cells<sup>161</sup>. Nonetheless, the relationship between the two regulatory functions of RLR in IFN-I and autophagic signaling remains to be studied and how NLRs might integrate these two pathways has not been addressed in the literature.

This study employs quantitative proteomics approaches and uncovered a novel regulatory mitochondrial protein platform comprised of NLRX1 and mitochondrial Tu translation elongation factor (TUFM/P43/EFTu/COXPD4/EF-TuMT). This complex regulates virus induced IFN-I activation and autophagy by engaging RIG-I and the autophagy-related proteins, Atg5-Atg12 conjugate. This shows that a novel complex comprised of NLRX1, TUFM, RIG-I and Atg5/Atg12 controls two crucial anti-viral functions: IFN-I induction and autophagy.

### **3.3 Results**

#### **NLRX1 inhibits type 1 IFN signaling in MEFs**

To assess the role of NLRX1 in modulating IFN-I signaling, we generated C57BL/6 mice deficient in the *Nlr1* gene (*Nlr1*<sup>-/-</sup>). A more thorough *in vivo* analysis

of this strain is described in a report that is currently being reviewed. *Nlr1<sup>-/-</sup>* mouse embryonic fibroblasts (MEFs) were cultured from 13.5 day embryos; and the lack of *Nlr1* transcripts was confirmed by RT-PCR (Fig. 3.1). In agreement with a previous

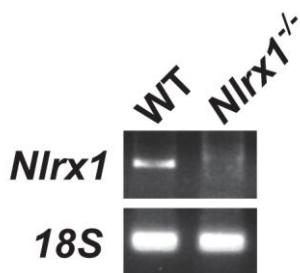


**Figure 3.1 Confirmation of gene deletion.** *Nlr1<sup>+/+</sup>* and *Nlr1<sup>-/-</sup>* MEFs were harvested for RNA extraction. *Nlr1* mRNA level was evaluated by RT-PCR. 18s mRNA level was assessed as internal control.

study where overexpressed NLRX1 in transformed cell lines was shown to inhibit IFN-I promoter activation by  $\Delta$ RIG-I<sup>124</sup>, *Nlr1<sup>-/-</sup>* MEFs showed enhanced *Ifnb1* mRNA transcription in response to the RIG-I ligand, cytoplasmic 5'-ppp-dsRNA (Fig. 3.2A). Control dsRNA without the 5'-ppp moiety failed to induce IFN-I. When MEFs from both genotypes were challenged with VSV, a deficiency in NLRX1 resulted in enhanced IFN-I production (Fig. 3.2B). We previously found that NLRX1 interacts with MAVS to impede the latter's interaction with RIG-I at a basal state, thus suggesting that NLRX1 might form an active inhibitory complex at the unstimulated state<sup>124</sup>. To further explore this possibility, we employed size exclusion chromatography and found that NLRX1 is most abundant in a higher molecular mass during the resting state, while it resides in smaller molecular complexes upon RLR activation by its known ligand, 5'-ppp-dsRNA (Fig. 3.2C, upper panels). As an internal control, the mitochondrial protein COX IV-

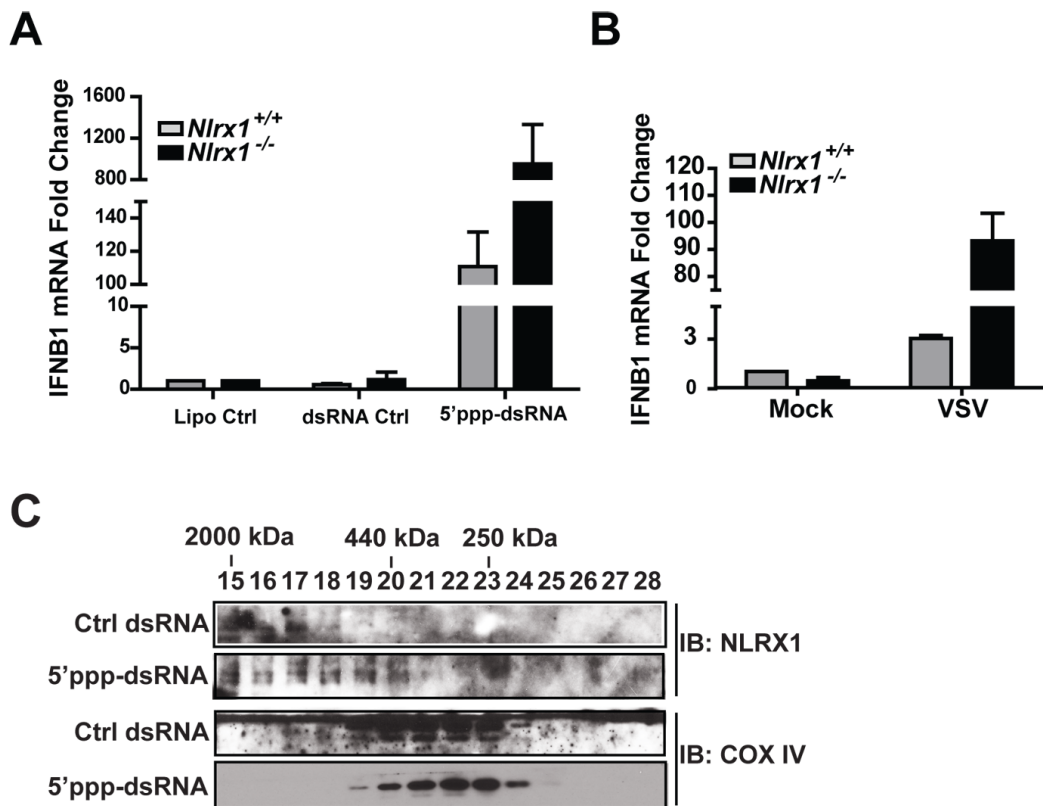


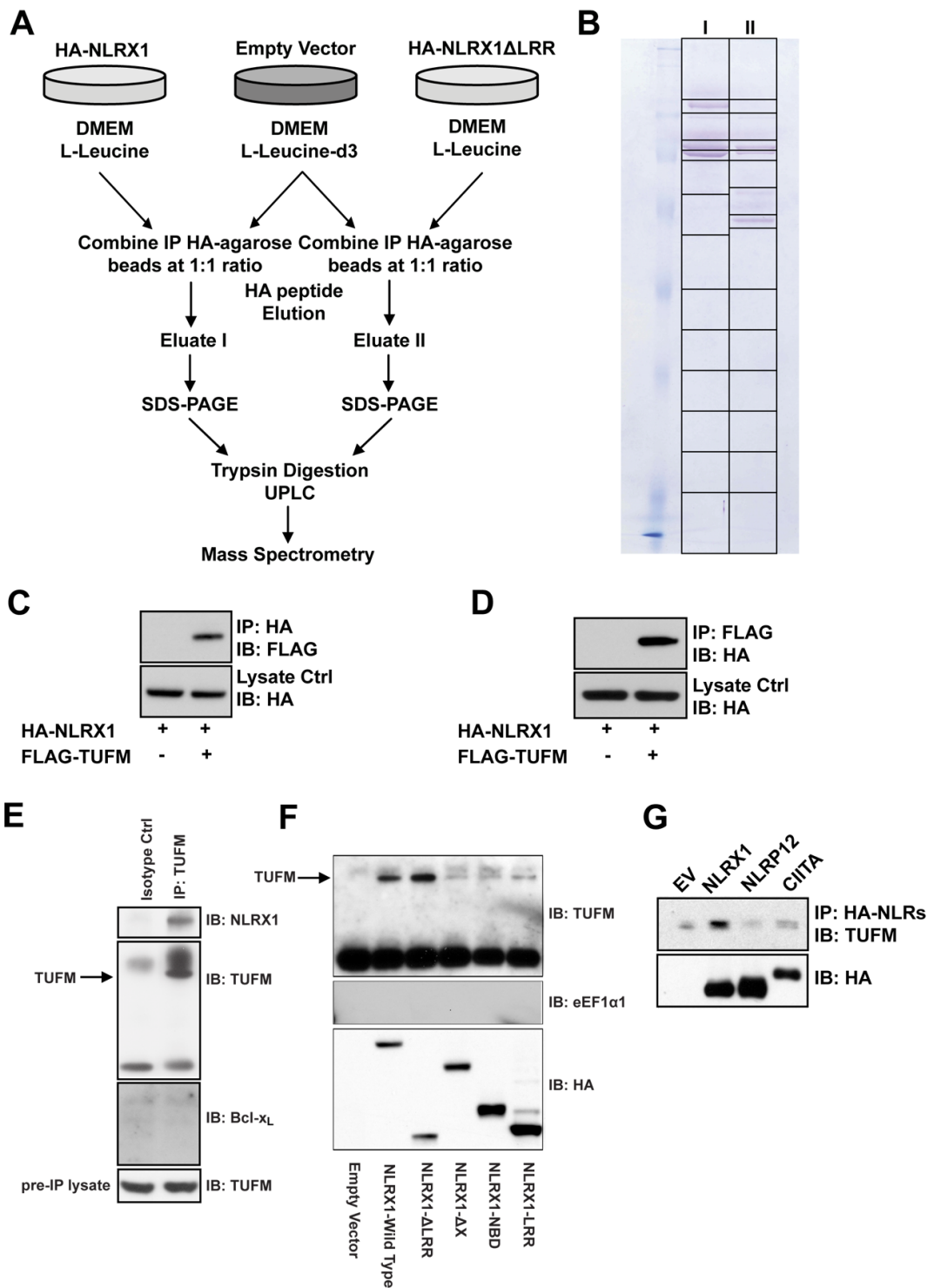
**Figure 3.2 NLRX1 inhibits VSV-induced IFN-I response.** (A) *Nlrp1*<sup>+/+</sup> and *Nlrp1*<sup>-/-</sup> MEFs were transfected with control dsRNA or 5'ppp-dsRNA, and *IFNB1* mRNA levels were assessed by real time PCR. *Nlrp1*<sup>-/-</sup> cells produced approximately 9× more *IFNB1* mRNA than controls. (B) *Nlrp1*<sup>+/+</sup> and *Nlrp1*<sup>-/-</sup> MEFs were mock treated or infected with VSV (MOI of 0.1), and *IFNB1* mRNA levels were assessed by real time PCR. *Nlrp1*<sup>-/-</sup> cells produced approximately 30× more *IFNB1* mRNA than WT controls. (C) Five million HEK293T cells were transfected with 5'ppp-dsRNA or control dsRNA, cells were harvested and homogenized in hypotonic lysis buffer 16h post-transfection. Protein extractions were then separated by size exclusion chromatography, and collected fractions were subjected to western blotting against NLRX1 and COX IV.

containing complex did not display an altered size profile in response to 5'-ppp dsRNA challenge (Fig. 3.2C, lower panels).

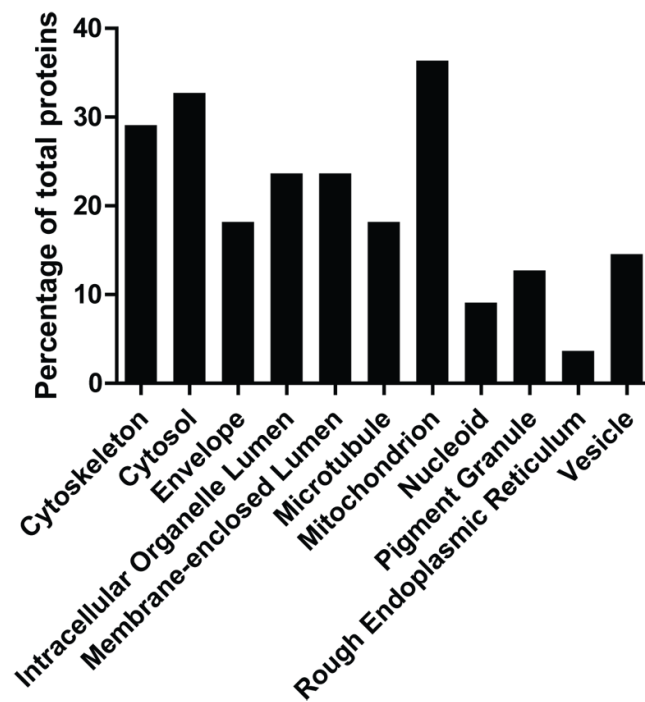
### **TUFM associates with NLRX1**

Fig. 3.2 indicates that NLRX1 is a component of a larger molecular complex. To identify additional molecules which might be a component of the NLRX1 complex, we employed the amino acid-coded mass tagging (AACT, also known as SILAC)-assisted quantitative mass spectrometry to identify NLRX1-interacting proteins<sup>225, 226</sup> (Fig. 3.3A). The N-terminal domains of NLRs are considered to mediate protein-protein interaction while LRRs are considered inhibitory<sup>124, 227</sup>. Hence, we constructed vectors encoding full-length NLRX1 and a mutant lacking the LRR domain, and used these as baits to identify interacting partners. Eluted proteins from both groups (Eluates I and II) (Fig. 3.3A) were separately fractionated by SDS-PAGE (Fig. 3.3B) followed by high-performance liquid chromatography and mass spectrometry. A subcellular compartment localization analysis of the NLRX1 interactome revealed that a high percentage of interacting partners are mitochondrial proteins (Fig. 3.4). Among these, peptide profiles that matched the mitochondrial Tu translation elongation factor (TUFM) with ion scores of >39 were identified in both eluates (Fig. 3.5A-D). This indicates with >95% certainty that these peptides represent TUFM (Table 3.1). Similar to NLRX1<sup>124</sup>, TUFM is ubiquitously expressed in multiple tissue and cell types (Fig. 3.6).

To further validate these findings, reciprocal co-immunoprecipitation experiments were performed to show interaction between ectopically expressed NLRX1 and TUFM



**Figure 3.3 TUFM interacts with NLRX1.** (A) Scheme of AACT/SILAC mass spectrometry identification of NLRX1-interacting partners. (B) Immunoprecipitated proteins were eluted by HA-peptide and separated by SDS-PAGE, the gel was continuously sliced as indicated for further high performance liquid chromatography and mass spectrometry analyses. (C) HA-tagged NLRX1 was co-transfected with either empty vector or FLAG-tagged TUFM. Cells were lysed and immunoprecipitated proteins were blotted for FLAG-TUFM. (D) HA-tagged NLRX1 was co-transfected with empty vector or FLAG-tagged TUFM and immunoprecipitated with anti-FLAG-agarose beads, and immuno-blotted for HA-NLRX1. (E) HEK293T cells were lysed and immunoprecipitated with either isotype control antibody or anti-TUFM antibody and immuno-blotted for NLRX1, TUFM and Bcl-x<sub>L</sub>. (F) Full-length NLRX1 or its truncation mutants were expressed in HEK293T cells, and protein samples were immunoblotted for endogenous TUFM and eEF1α1. (G) Over-expressed NLRX1, NLRP12 and CIITA were immunoprecipitated from HEK293T cells, and immuno-blotted for endogenous TUFM. Results represent 2-3 independent repeats.



**Figure 3.4 NLRX1 interactome subcellular localization.** NLRX1-interacting proteins were annotated on their subcellular localization based on the Gene Ontology database. The number of proteins that reside in the same compartment was divided by the total number of proteins to calculate the percentage.

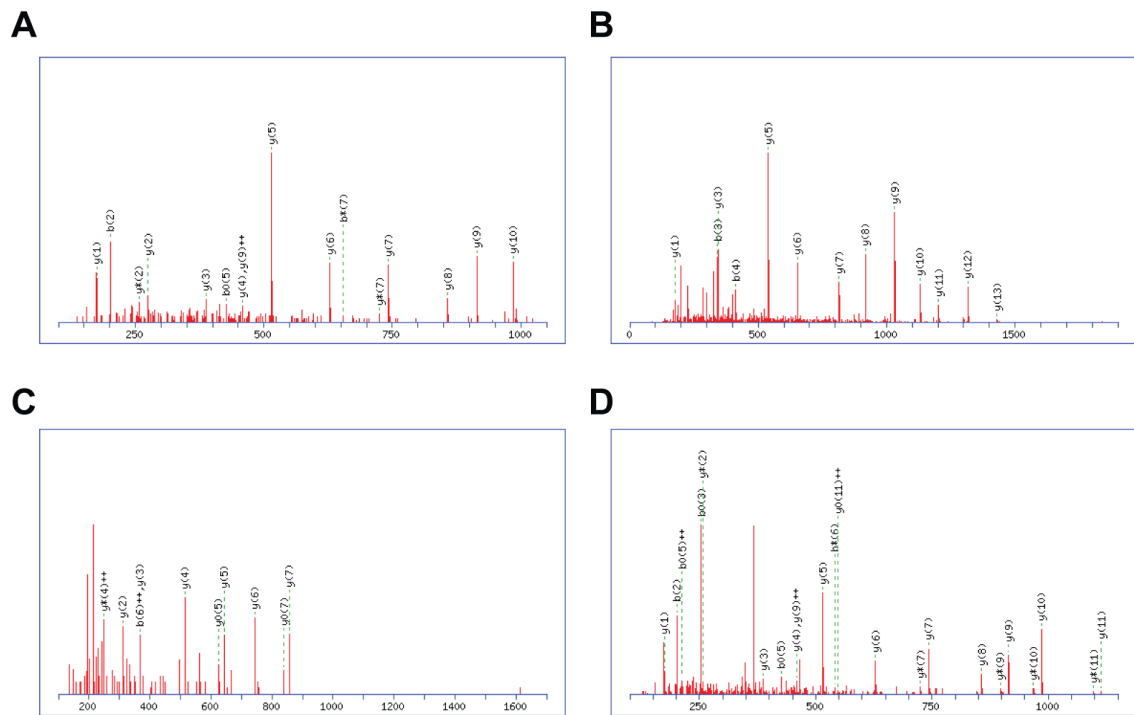


**Figure 3.5 Mass Spectrometry identification of the TUFM peptides.** (A, B) MS/MS spectrum of the peptides AEAGDNLGALVR and LLDAVDTYIPVPAR were captured from those derived from the interacting partners with NLRX1 full-length protein. (C, D) MS/MS spectrum of the peptides ELLTEFGYK and AEAGDNLGALVR were captured from those derived from the interacting partners with NLRX1 $\Delta$ LRR protein. These peptides are further shown in Table S1.

Bait	Observed Mass	Sequence	Ion Score
NLRX1	(A) 593.2867	AEAGDNLGALVR	69
NLRX1	(B) 771.8945	LLDAVDTYIPVPAR	107
NLRX1 $\Delta$ LRR	(C) 550.3176	ELLTEFGYK	39
NLRX1 $\Delta$ LRR	(D) 593.3447	AEAGDNLGALVR	42

**Table 3.1** The peptides sequences matching TUFM were identified in both NLRX1 full-length group and NLRX1 $\Delta$ LRR mutant group. Peptides were eluted from NLRX1 or NLRX1 $\Delta$ LRR. Two unique peptides with at least five consecutive amino acids sequences which matched sequences in IPI database were found in each eluate. The ion scores for all peptides shown are equal or greater than 39, which indicates a greater than 95% possibility that the peptides detected represent TUFM protein ID in the International Protein Index database.

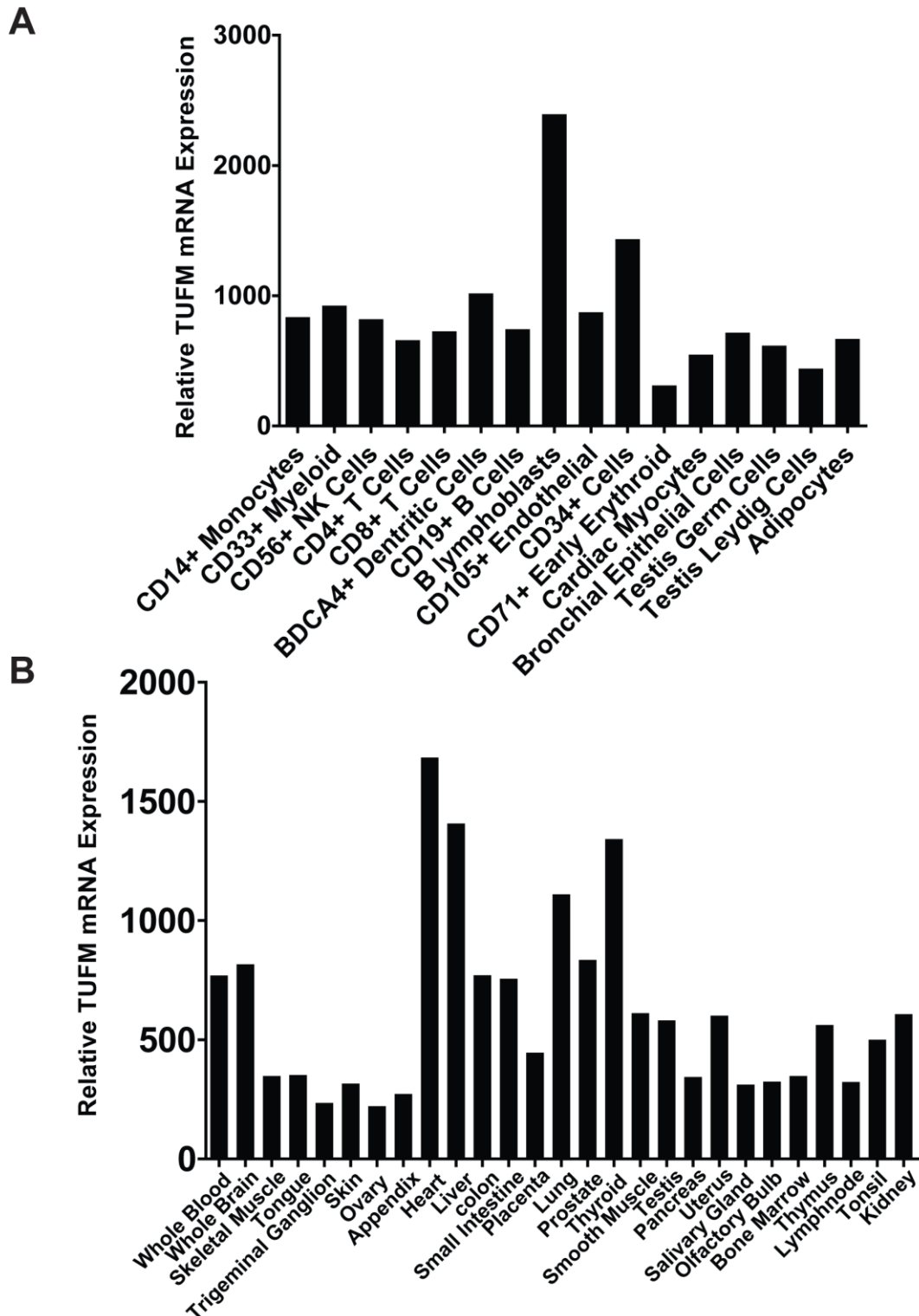


**Figure 3.6 TUFM is ubiquitously expressed in multiple cell and tissue types.** The mRNA expression data of human TUFM is made available by the BioGPS project (<http://biogps.gnf.org/>), which is funded by the Genomics Institute of the Novartis Research Foundation. TUFM was used as the key identification word.

(Fig. 3.3C-D). More importantly, endogenous TUFM co-immunoprecipitated with endogenous NLRX1 (Fig. 3.3E). As a negative control, TUFM did not co-immunoprecipitate with another mitochondrial protein Bcl-x<sub>L</sub>. NLRX1-TUFM interaction requires the N-terminus of NLRX1 as its deletion (NLRX1-ΔX) abolished this interaction (Fig. 3.3F). Deletion of the LRR domain (NLRX1-ΔLRR) slightly increased this interaction while constructs expressing NBD or LRR alone (NLRX1-NBD, NLRX1-LRR) did not interact with TUFM. As negative controls, NLRX1 did not bind to the cytoplasmic homolog of TUFM, eEF1α1 (Fig. 3.3F). Furthermore, TUFM did not co-precipitate with other NLRs such as NLRP12 and CIITA (Fig. 3.3G).

### **Both NLRX1 and TUFM are mitochondrial proteins**

NLRX1 is a highly conserved protein, thus we also evaluated the evolutionary conservation of TUFM. TUFM is conserved from humans to its bacterial counterpart. The bacterial elongation factor Tu (EF-Tu) serves as a PAMP (pathogen-associated molecular pattern) in plant cells to elicit immune activation<sup>228, 229</sup>. However, despite this general sequence homology, the key activating sequence of bacterial EF-Tu KxKfxR no longer exists in the human counterpart; instead the N-terminus of TUFM has undergone drastic changes (Fig. 3.7). Previously, we investigated the localization of NLRX1 using sucrose gradients similar to the ones used to localize MAVS<sup>34</sup>. However, a separate study reported NLRX1 as a matrix protein<sup>126</sup>. To clarify this issue, we used an additional approach to study mitochondrial proteins. We isolated crude mitochondria from cell homogenates and treated the preparation with increasing doses of digitonin

```

Arabidopsis thaliana MASVVLRNPSKRLVPFSSQIYSRCGASVTSSYSISHSIGGDDLSSTFGTSSFWRSMAT 60
Listeria monocytogenes -----MAKEK 5
Homo sapiens ----MTTMAAATRATPHFSGLAAGRTFLLQLLRLLKAPALPLLCRG-----LAVEAKKT 51
: .

Arabidopsis thaliana FTRNKPHVNVGTIGHVDHGKTTLTAAITKVLAEEGKAKAIAFDEIDKAPEEKRGITIIAT 120
Listeria monocytogenes EDKSKPHVNI GTIGHVDHGKTTLTAAITVLAKKGYADAQAYDQIDGAPEERERGITIIST 65
Homo sapiens YVRDKPHVNVGTIGHVDHGKTTLTAAITKILAEGGGAKFKKYEIDNAPEERARGITINA 111
: * .*****:*****:***: * * . :::** *****: ***** :

Arabidopsis thaliana AHVEYETAKRHYAHVDCPGHADYVKNMITGAAQMDGGILVVSFGPDGMPQTKEHILLARQ 180
Listeria monocytogenes AHVEYQTD SRHYAHVDCPGHADYVKNMITGAAQMDGAILVVSADGMPQTR EHI LLSRQ 125
Homo sapiens AHVEYSTAARHYAHTDCPGHADYVKNMITGTAPLDGCILVVAANDGMPQTR EHL LLARQ 171
***** . * ***** .*****:***: * * *****: . *****:***:***:

Arabidopsis thaliana VGVPSLVCFLNKVDVDDPELLELVEMELRELLSFYKFPGD D IPIIRGSALSALQGTNDE 240
Listeria monocytogenes VGVPIVVF MNKCDMVDDEELLELVEMEIRDLLTEYEFPGDDIPVIKGSALKALQGEADW 185
Homo sapiens IGVEHVVVVYV NKADAVQDSEMVVELVELEIRELLTEFGYKGEETPVIVGSALCALEGRDPE 231
: ** : * : : * * * * * : : *****:***:***: : : : * : * * * * * : *

Arabidopsis thaliana IGRQA I LK LMDAVDEYIPDPVRVLDKPF LMPIEDVFSIQGRGT VATGRIEQGVIKVGE EV 300
Listeria monocytogenes EAK--IDELMEAVDSYIPTPERD TDKPFMMPVEDVFSITGRGT VATGRVERGQVKVGDEV 243
Homo sapiens LGLKSVQKLLDAVD TYIPV PARDLEKPFLLPVEAVYSV PGRGT VVTGTLERGI LKKGDEC 291
. : : * : * * * * * : * * * : * * * : * * * . * * : * * : * * *

Arabidopsis thaliana EILGLREGGVPLKSTVTGVEMFKKILDNGQAGDNVGLLLRGLKREDIQRGMVIAKPGSCK 360
Listeria monocytogenes EVIGIEEE--SKKVVVTGVEMFRKLLDYAEAGDNIGALLRGVAREDIQRGQVLAKPGSIT 301
Homo sapiens ELLGHSKN---IRTVVTGIEMFHKSLERAEAGDNLGALVRGLKREDLRRGLVMVKPGSIK 348
* : * : : * * * : * * * : * * * : * * * : * * * : * * * : * * * .

Arabidopsis thaliana TYKKFEAEIYVLTKEEGRRHTAFFSNYRPQFYLR TADITGKVELPENVKMVM PGDNVTAV 420
Listeria monocytogenes PHTNFKAETYVLTKEEGRRHTPFNNYRPQFYFR TTDVTGIVTLEPGTEMVMPGDNIELA 361
Homo sapiens PHQKVEAQVYILSKEEGRRHKPFVSHFMPVMFSLTWDMACRIILPPEKELAMPGEDLKFN 408
. : : * : * * * : * * * . * . : : * : * * : : * * : : * * : : * * : :

Arabidopsis thaliana FELIMPVPLETGQRFALREGGRTVGAGVVSQVMT----- 454
Listeria monocytogenes VELIAPIAIEDGTFKSIREGGRTVGAGVVSNI SK----- 395
Homo sapiens LILRQPMILEKGRFTLRDGNRTIGTGLVTNTLAMTEEEKNIKWG 453
. * * : : * * : * * : * * : * * : * * : * * : * * :

```

**Figure 3.7 TUFM is evolutionarily conserved.** The protein sequences of human TUFM (Accession: AAH01633), mitochondrial EF-Tu in *A. thaliana* (Accession: AAH01633) and EF-Tu in *L. monocytogenes* (Accession: YP\_002759310) were aligned using ClustalW2 software. The essential N-terminal immune-activating sequence KXXFXXR of the *L. monocytogenes* EF-Tu is highlighted and missing in the plant and human sequences.

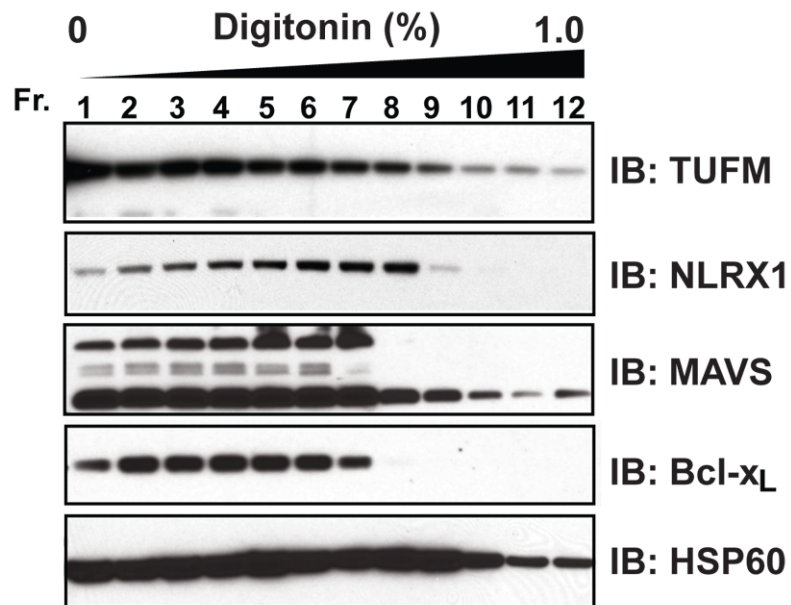


**Figure 3.8 Both NLRX1 and TUFM are mitochondrial proteins.** Isolated mitochondria were treated with increasing doses of digitonin (0-1.0%) and then subjected to SDS-PAGE and immunoblotted with the indicated antibodies. Results represent 2 independent repeats.

which gradually extracted mitochondrial proteins from the less detergent-resistant outer membrane fraction to the more detergent-resistant inner membrane/matrix fraction<sup>75</sup> (Fig. 3.8). MAVS (upper band) displayed a profile similar to Bcl-x<sub>L</sub>, a well-accepted mitochondrial outer membrane protein. Consistent with the initial identification of MAVS<sup>34</sup>, the anti-MAVS antibody also recognized a smaller, detergent-resistant portion (lower band) (Fig. 3.8). The extraction profile of NLRX1 more closely resembled that of Bcl-x<sub>L</sub> and the higher molecular weight MAVS protein, but not the mitochondrial matrix protein HSP60. On the other hand, a portion of TUFM appeared to be in the inner membrane/matrix compartment, however it can not be ruled out that TUFM also resides in the outer-membrane.

### **TUFM potently inhibits RIG-I signaling**

Given the interaction of NLRX1 with TUFM and previous findings that NLRX1 attenuates MAVS and RIG-I induced IFN-I production and NF- $\kappa$ B signaling<sup>124</sup>, we analyzed the role of TUFM in these same pathways. Similar to NLRX1, TUFM inhibited ISRE-, NF- $\kappa$ B-dependent and *IFNBI* promoter activation by  $\Delta$ RIG-I in a dose-dependent fashion (Fig. 3.9A-C). IFN-I signaling in response to cytosolic viral PAMPs is also regulated by the adaptor MITA/STING<sup>69,70,72</sup>. However, neither TUFM nor NLRX1 affected ISRE activation by MITA/STING (Fig. 3.9D, E). In addition to reporter assays, TUFM squelched  $\Delta$ RIG-I-induced *IFNBI* mRNA production, similar to NLRX1 (Fig. 3.9F). RNA interference targeting of TUFM (si-TUFM) partially reduced TUFM expression and increased IFN- $\beta$  mRNA induction by  $\Delta$ RIG-I (Fig. 3.9G, 3.10A).

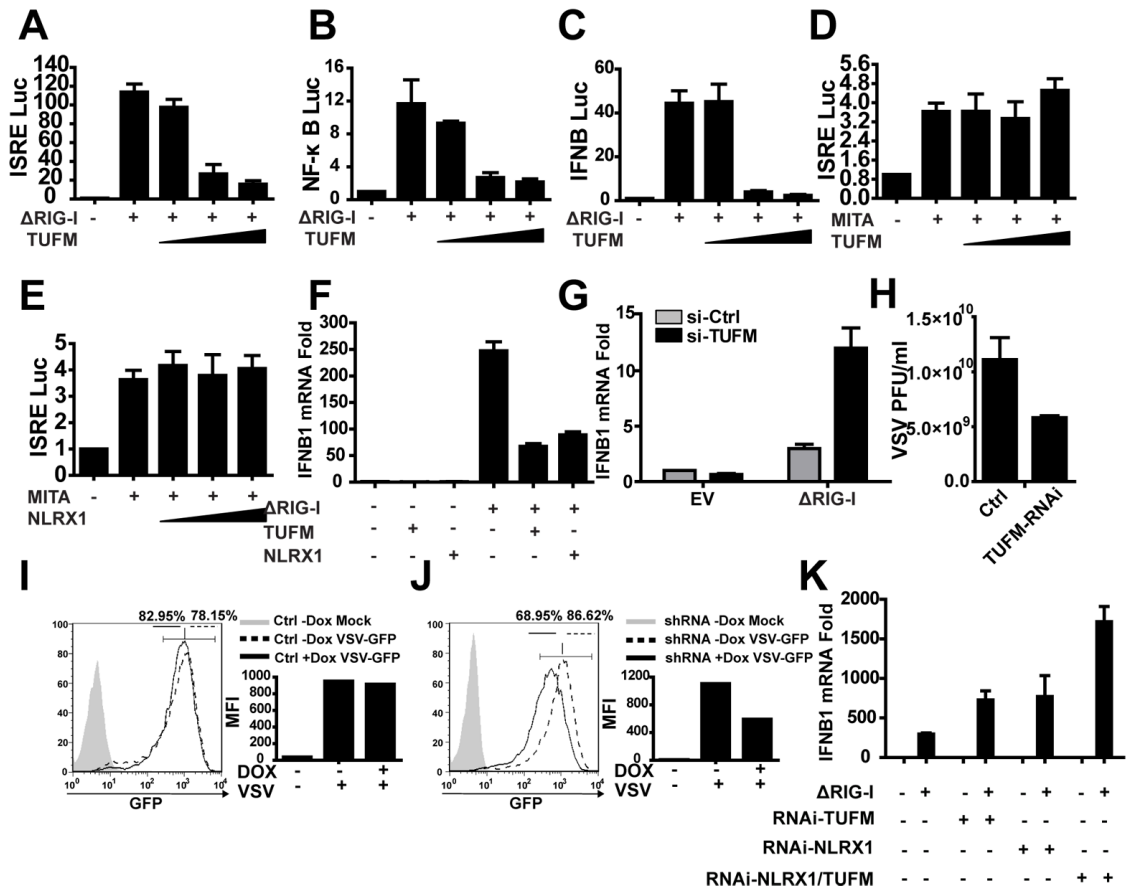


**Figure 3.9 TUFM inhibits RIG-I mediated type I IFN production.** (A-E) HEK293T cells were transfected with  $\Delta$ RIG-I or MITA/STING expression plasmid plus luciferase reporter plasmids for ISRE, NF- $\kappa$ B or IFNB1 activation. FLAG-TUFM plasmid was titrated into the system and cells were lysed 24h post-transfection for luciferase assays. (F)  $\Delta$ RIG-I was co-transfected with either TUFM or NLRX1 into HEK293T cells; and cells from all groups were harvested for real time PCR analysis 24h post-transfection. (G) Endogenous TUFM was partially reduced by transfecting a pool of 4 targeting siRNA into the cells;  $\Delta$ RIG-I was transfected to induce *IFNB1* mRNA as measured by real time PCR. (H) HEK293T cells with reduced TUFM expression and control cells were challenged with VSV, and plaque assay was performed to assess the viral titers. (I) HEK293T cells were transduced with control lentiviruses and infected with VSV-GFP (MOI of 0.1) for 16h and analyzed by flow cytometry for GFP as a marker for VSV. (J) HEK293T cells transduced with sh-TUFM were treated and analyzed as described in (I). (K) HEK293T cells transduced with scrambled control shRNA or sh-NLRX1 were treated with control or siRNA pool targeting TUFM. Cells were then harvested 16h post transfection of either empty vector control or  $\Delta$ RIG-I plasmid. *IFNB1* mRNA abundance was analyzed by real time PCR. Results of all panels are representative of three independent experiments.

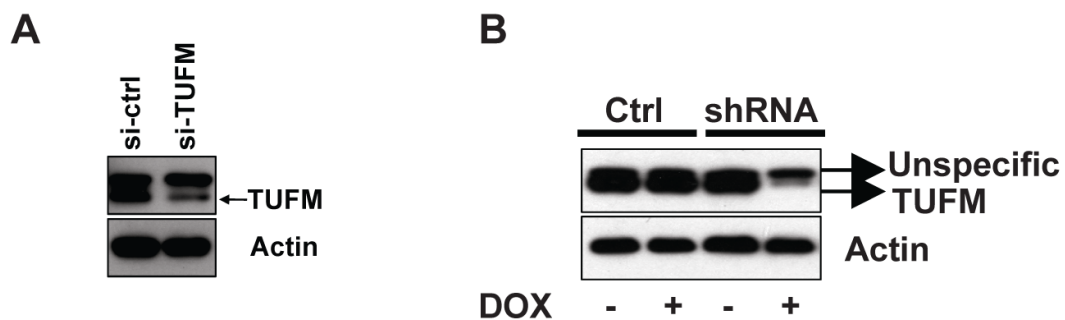


**Figure 3.10 Confirmation of TUFM knockdown by shRNA.** HEK293T cells were transduced with lentiviruses containing either tetracycline-inducible TRIPZ™ control vector or shRNA targeting TUFM. One  $\mu\text{g/ml}$  doxycycline was added to cell culture and incubated for 48h before cells were harvested for protein extraction. Samples were subjected to SDS-PAGE and immunoblotting for TUFM.

Reduction of TUFM expression level also resulted in lower viral plaque forming units (PFU) compared to control cells (Fig. 3.9H). As an additional approach to assess the IFN-I-regulatory function of TUFM, GFP-expressing VSV was used to infect HEK293T cells stably transduced with a doxycycline-inducible shRNA lentivirus (Fig. 3.10B). In the control group, doxycycline did not affect the percentage of infected cells and viral infection as assayed by the GFP-positive population and mean fluorescence intensity (MFI) (Fig. 3.9I). By contrast, induction of TUFM shRNA reduced both signals (Fig. 3.9J). These results indicate that TUFM is similar to NLRX1 in attenuating RLR signaling. In fact, by reducing the expression of both NLRX1 and TUFM, the transcription of *IFNBI* was further enhanced, suggesting a complementary effect of these two proteins in attenuating RIG-I induced IFN-I activation (Fig. 3.9K).

### **NLRX1 is essential for VSV-mediated autophagy**

Another key host response that is elicited by virus is autophagy. In addition to IFN-I induction, VSV is known to induce autophagy<sup>141, 230</sup> during which the light chain 3 (LC3) protein is converted from a cytosolic form (LC3B-I) to a LC3B-lipidated, membrane-associated form (LC3B-II) and displays a punctate appearance<sup>231, 232</sup>. We next explored the role of NLRX1 in autophagy. VSV-infected wild type (WT) MEFs displayed punctate LC3B staining while *Nlr1<sup>-/-</sup>* cells exhibited a diffuse cytoplasmic staining pattern, implicating for the first time a role for NLRX1 in autophagy (Fig. 3.11A). VSV-infected WT and *Nlr1<sup>-/-</sup>* MEFs were further assayed for LC3B-II level by immunoblot, and LC3B-II level relative to  $\beta$ -actin was greatly reduced in the *Nlr1<sup>-/-</sup>* cells

(Fig. 3.11B). Rapamycin, an inhibitor of the mTOR signaling, is a common inducer of autophagy. Rapamycin-treated *Nlrp1*<sup>-/-</sup> MEFs showed a modest reduction in LC3B-II compared to WT cells (Fig. 3.11B), while a more dramatic reduction was observed in VSV-treated samples. Transmission electron microscopy<sup>160</sup> confirmed that VSV infection resulted in more autophagosomes in WT than *Nlrp1*<sup>-/-</sup> cells (Fig. 3.11C). To extend these findings to human cells, lentiviral vector harboring shRNA targeting human NLRX1 and its controls were produced. HEK293T cells with sh-NLRX1 construct showed reduced endogenous NLRX1 expression and reduced LC3B-II level relative to  $\beta$ -actin compared to controls (Fig. 3.11D). The association of the Atg5-Atg12 conjugate with MAVS has been shown to inhibit MAVS-mediated IFN-I production<sup>141</sup>. Thus we explored the interaction of Atg5-Atg12 with NLRX1, but we failed to detect any association of NLRX1 and Atg5-Atg12 under stringent lysis and wash conditions (Fig. 3.11E). Given the fact that *Nlrp1*<sup>-/-</sup> MEF resembles *Atg5*<sup>-/-</sup> MEF in increasing type 1 IFN production and both proteins associate with MAVS, we hypothesized that an additional member exists to engage with both proteins and stabilizes a regulator protein complex. Thus we explored if TUFM might constitute such a protein.

### **TUFM associates with Atg5-Atg12 conjugate**

To test our original hypothesis that TUFM engages with both NLRX1 and Atg5-Atg12 conjugate, we performed co-immunoprecipitation analysis and revealed strong interaction between TUFM and Atg5-Atg12 (Fig. 3.12A), in contrast with the earlier failure to detect NLRX1:Atg5-Atg12 interaction. MAVS also displayed

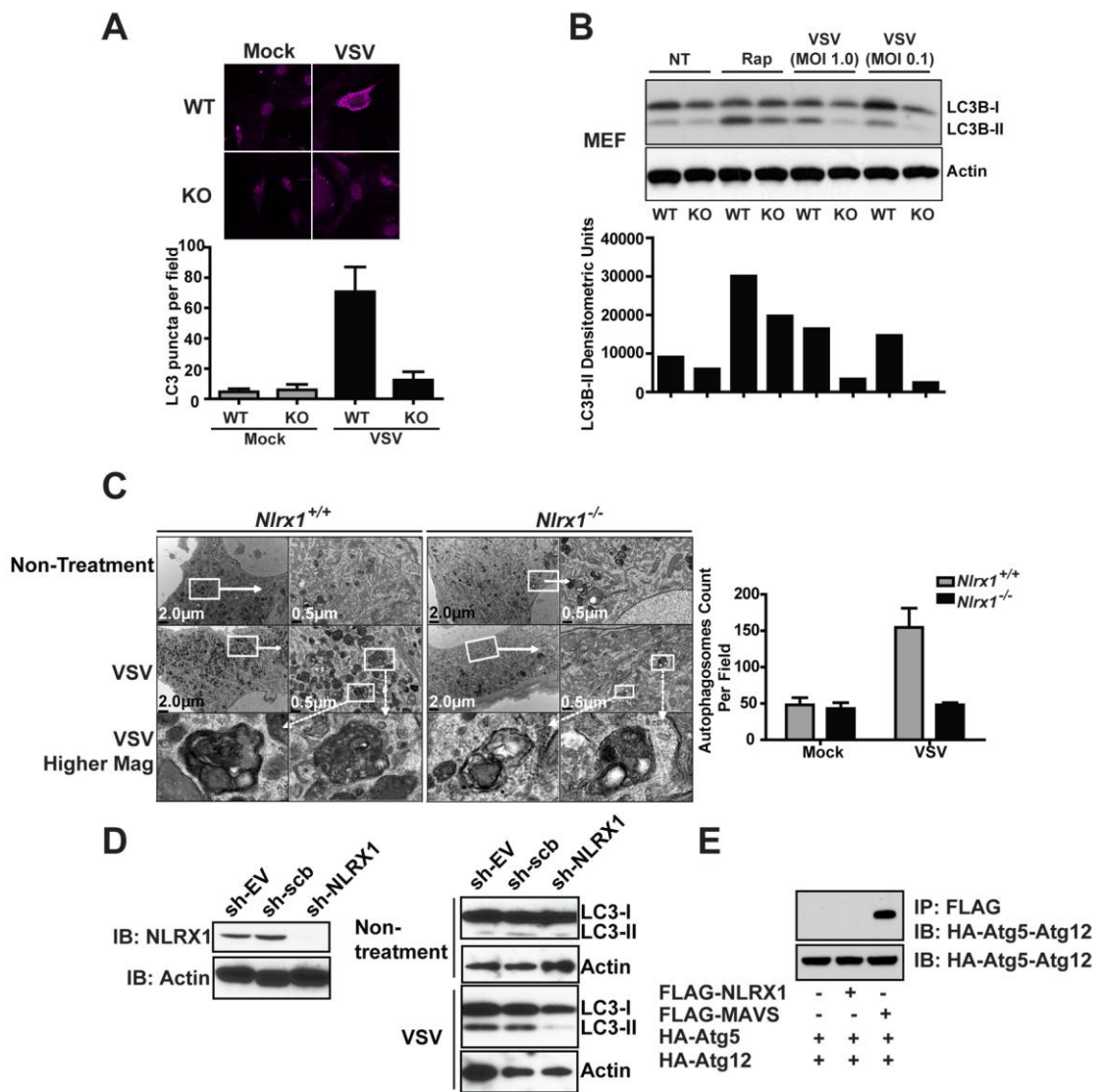


**Figure 3.11 NLRX1 is essential for VSV-mediated autophagy.** (A) WT and *Nlrp1*<sup>-/-</sup> MEFs were infected with VSV (MOI of 0.1), fixed and stained for LC3B 4h post-infection and examined by confocal imaging. Quantitation is shown below. (B) WT and *Nlrp1*<sup>-/-</sup> MEFs were infected with VSV and harvested 16h post-infection, or treated with rapamycin and harvested 2h post-stimulation. Protein samples were immuno-blotted for LC3B. Densitometry analysis (below) of the bands representing LC3B-II was performed using ImageJ. (C) WT and *Nlrp1*<sup>-/-</sup> MEFs were infected with VSV (MOI of 1.0) for 16h and examined by electron microscopy for autophagosomes. Quantitation is based on counting the number of autophagosomes present in 2-3 fields per treatment. (D) HEK293T cells were transduced with control lentiviral sh-EV, sh-scrambled or sh-NLRX1 (left). The cells were then challenged with VSV and harvested 16h post-infection for LC3B immunoblot (right). (E) FLAG-tagged NLRX1 or MAVS and HA-tagged Atg5, Atg12 expression plasmids were transfected into HEK293T cells. Cell extracts were harvested 24h post-transfection and subjected to co-immunoprecipitation as indicated. Results of all experiments are representative of at least 2-3 repeats.

interaction with Atg5-Atg12 as reported <sup>141</sup>, while MITA/STING did not (Fig. 3.12A).

A previous study has shown that Atg5-Atg12 can be transiently localized to the mitochondria <sup>4</sup>. If so, a model can be evoked where MAVS, NLRX1, TUFM and Atg5-Atg12 association takes place within the mitochondria. To assess this, we prepared mitochondria-enriched fractions using the protocol shown in Fig 3.13. We detected Atg5-Atg12, NLRX1, TUFM and MAVS but not the endoplasmic reticulum proteins KDEL and calreticulin in the mitochondrial fraction, which is also enriched for mitochondrial COX IV and Bcl-x<sub>L</sub> (Fig. 3.12B). To map the essential domains for the Atg5-Atg12 conjugate recruitment, TUFM truncation mutants were generated (Fig. 3.12C). The N-terminal domain I of TUFM was required for optimal interaction with Atg5-Atg12, while domains II and III were not as critical (Fig. 3.12D). To explore the physiological significance of such interaction, we utilized the TUFM stable knockdown cells described above to investigate if TUFM also affects autophagy. Lentiviral vector transduced HEK293T cells were challenged with VSV, which induced LC3B-II formation. However, cells with sh-TUFM displayed significantly reduced LC3B-II (Fig. 3.12E). This indicates that TUFM, similar to NLRX1, also regulates viral-induced autophagy.

### **3.4 Conclusion**

The NLR family is comprised of twenty-two proteins, and a prominent subgroup contains those that mediate inflammasome function. Our previous analysis identified a new function for NLRs and demonstrated that NLRX1 is a negative regulator of the MAVS-RIG-I induced IFN-I response. Since then, accumulative evidence has shown

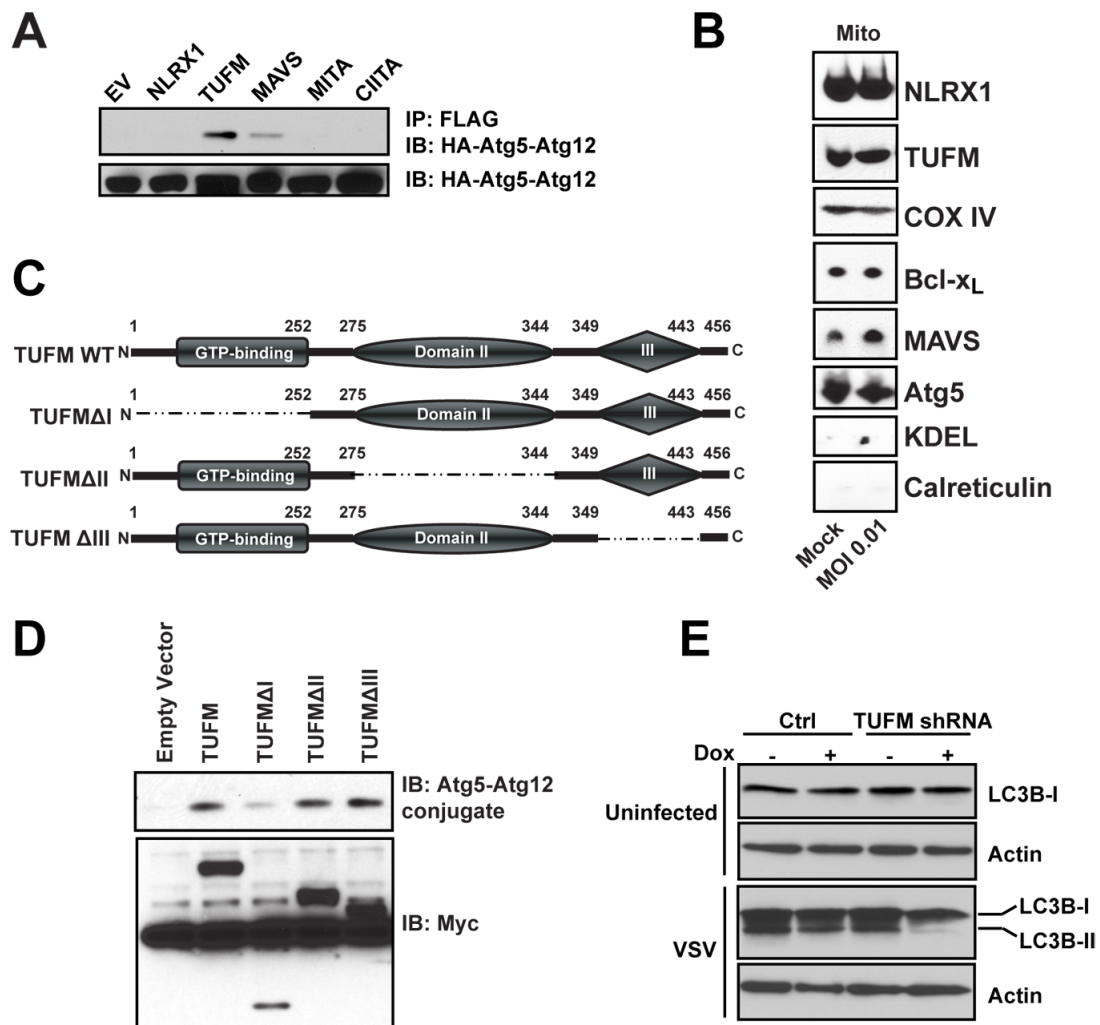


**Figure 3.12 TUFM associates with the Atg5-Atg12 conjugate.** (A) FLAG-tagged NLRX1, TUFM, MAVS, MITA or CIITA was co-transfected with HA-Atg5 and HA-Atg12; cell lysates were immunoprecipitated with anti-FLAG M2 affinity gel and then immuno-blotted for the HA-Atg5-Atg12 conjugate. (B) Crude mitochondria were isolated from cells mock treated or infected with VSV using protocol described in Figure S6. All samples were subjected to SDS-PAGE and immunoblot. (C) Domain structures of TUFM and truncation mutants. (D) FLAG-tagged TUFM wildtype and domain truncation mutants were co-transfected with HA-Atg5 and HA-Atg12 into HEK293T cells, cell extracts were immunoprecipitated with anti-FLAG and immuno-blotted for HA-Atg5-Atg12 conjugate. (E) HEK293T cells transduced with tetracycline-inducible shRNA for TUFM and or control shRNA were infected with VSV-GFP (MOI of 0.1) and harvested for LC3B immunoblot.

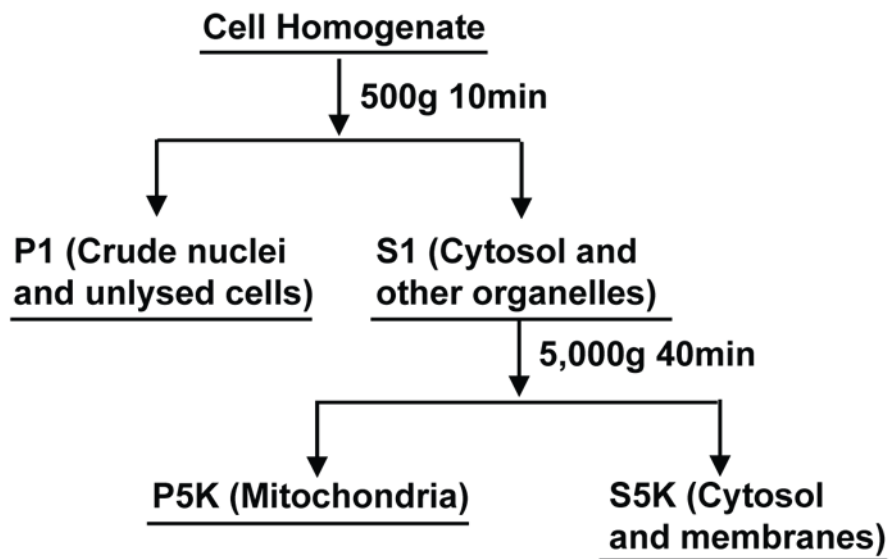


**Figure 3.13 Protocol for subcellular fractionation.** For each cell fractionation experiments,  $5 \times 10^7$  cells were lysed in hypotonic lysis buffer with a dounce homogenizer. Then serial centrifugation was carried out to separate each compartment according to the scheme.

additional NLR proteins which can control IFN-I in both negative and positive ways. In the current study, we show an additional role for NLRX1 and demonstrated that it dually regulates IFN-I and autophagy. This involves the engagement of a new mitochondrial protein, TUFM. TUFM binds to NLRX1 and the Atg5-Atg12 conjugate in both over-expression system and via endogenous protein-protein interaction, thus it is likely to serve as an intermediary between NLRX1 and Atg5-Atg12. Similar to NLRX1, TUFM inhibits NF- $\kappa$ B-, ISRE-dependent and IFNB1 promoter activities in a dose-dependent manner and the over-expression of TUFM squelched *IFNB1* mRNA transcription. Reduction of both NLRX1 and TUFM resulted in enhanced IFN-I activation, indicating that their effects are additive. These experiments demonstrate a partnership between NLRX1 and TUFM to control host anti-viral responses.

We have previously found that endogenous NLRX1 interacts with endogenous MAVS, and that this interaction interferes with MAVS interaction with RIG-I. Domain mapping showed that the CARD domain of MAVS can interact with both NLRX1 and RIG-I<sup>124</sup>. This has led to the hypothesis that NLRX1 impedes MAVS-RLR association by steric hindrance<sup>67</sup>. The molecular steric hindrance hypothesis postulates that negative regulatory proteins can associate with molecules in the RLR signaling pathways, such as the RLRs, adaptors or downstream kinases, and this association prevents their engagement with other essential regulator such as MAVS. This model has been supported by the analysis of other inhibitory proteins including Atg5-Atg12 conjugate, Mfn2 and NLRC5<sup>124, 125, 133, 141</sup>. Among these other modulators, only Mfn2 is a

mitochondrial protein, and the rest are likely recruited to the mitochondria via association with MAVS. The association of multiple checkpoint proteins with MAVS is supported by the finding that MAVS is found to be in a supramolecular complex in the quiescent state, but a majority of MAVS migrates into a lower molecular weight complex when cells are activated<sup>125</sup>. This suggests that during viral activation, MAVS is released from these molecular brake, presumably so that it can engage the RLR protein that are themselves activated by the binding of viral RNAs.

The data in this report show that NLRX1 also resides in a larger molecular complex in the quiescent state but migrates to smaller molecular mass in response to cytosolic 5'ppp-dsRNA treatment. This led us to postulate the existence of a larger NLRX1 complex, and to identify TUFM as an NLRX1-interacting partner. To date, functional analysis of these two proteins indicates that they phenocopy each other. Thus TUFM also serves to attenuate RIG-I dependent IFN-I production. Further study would be necessary to better understand the relationship among NLRX1, TUFM and the other regulators of RLR such as Mfn2, NOD2 and NLRC5.

This report also shows that similar to NLRX1, TUFM can promote viral-induced autophagy. Autophagy has been increasingly appreciated as a central mechanism for modulating host innate antiviral responses. Several proteins are found to dually control IFN-I and autophagy, and the intersection of IFN-I and autophagy pathway has been noted in the literature. For example, Atg5 and formation of the Atg5-Atg12 conjugate are found to regulate the RLR signaling pathway and negatively impact IFN-I activation

<sup>141, 142</sup>. In MEFs, the absence of Atg5 results in enhanced IFN-I partially because of the accumulation of intracellular ROS due to a deficiency of autophagy <sup>142</sup>. Additionally, the Atg5-Atg12 conjugate has been shown to intercalate between RIG-I and MAVS, abolishing RLR-induced IFN-I gene activation <sup>141</sup>. Another protein that has been found to dually regulate autophagy and IFN-I is Mfn2. Mfn2 is a mitochondrial outer membrane GTPase and regulates mitochondrial fusion together with its close homologue Mfn1 <sup>233</sup>. Recent evidence suggests that Mfn2 is needed for autophagosome formation <sup>4</sup>, while *Mfn2*<sup>-/-</sup> cells exhibited enhanced IFN-I production <sup>125</sup>. Interestingly Mfn2 also interacts with MAVS to preclude its association with RLR, providing a plausible mechanism for how it interferes with the RLR-MAVS signaling complex <sup>125</sup>. Mechanistically, NLRX1 and TUFM resemble both Mfn2 and Atg5 in that they are all essential for virus-induced autophagy and function as molecular brakes of IFN-I. Thus the downregulation of IFN-I and induction of autophagy appear to be mediated by a group of proteins with dual functions, including NLRX1 and TUFM described here.

Although the immune function of TUFM has not demonstrated before, its bacterial homologue EF-Tu is known to function as an immune-activating PAMP in the plant system <sup>228, 229</sup>. EF-Tu homologs are found across the bacterial kingdom, thus its recognition by host cells might represent a shared pathway by which bacteria modulate host responses. The immune-eliciting activity of EF-Tu depends on its N-terminus. In fact, a short polypeptide that is comprised of the N-terminal 12 amino acids of EF-Tu plus an N-terminal acetylation is sufficient to activate immune system to its full potential.

The sequence acetyl-xKxKFxRxxxxxxxxx has been found to be the minimal sequence required to elicit an immune reaction in *Arabidopsis thaliana*<sup>228</sup>. A reverse-genetic approach identified the transmembrane protein EFR (Elongation Factor Tu Receptor) as the receptor of EF-Tu<sup>229</sup>. The endosymbiosis theory hypothesized that mitochondrion originated from the integration of alphaproteobacteria into the host cells, which then interacts with host factors<sup>1</sup>. It is possible that bacterial EF-Tu is incorporated into host cells and gradually evolves to become TUFM, while its function evolved from immune-activation to immune-suppression. In our sequence homology comparison analysis of EF-Tu and TUFM, it appears that the N-terminus of EF-Tu has undergone drastic changes, which generates a mitochondrial-targeting sequence in the mammalian homologue. Additionally, the sequence essential for immune-activation is lacking in TUFM, in agreement with the possible evolution of immune activating EF-Tu to an immunosuppressive form. In addition to immune modulation, TUFM has also been implicated in protein translation elongation, oncogenesis, oxidative phosphorylation and protein quality control<sup>234-236</sup>. More investigations are necessary to elucidate the molecular complexes involved in these distinct functions, and whether the diverse functions of TUFM are inter-related.

In summary, previous studies have shown a central role for Atg5-Atg12 in autophagy induction and IFN-I inhibition. This work identifies a novel mitochondrial protein platform which is comprised of NLRX1 and TUFM that coordinately controls these two functional outcomes through association of the latter with Atg5-Atg12. By recruiting

Atg5-Atg12 and NLRX1, TUFM serves as a nodal check point of the RIG-I-MAVS axis. These studies significantly expand our understanding of the players involved in controlling diverse mitochondria-based anti-viral responses. While NLRX1 is the first NLR linked to mitochondrial function<sup>124</sup>, there is increasing evidence of NLR proteins that regulate MAVS function as well as mitochondrial functions that regulate NLRs<sup>129, 237</sup>. Future studies are likely to reveal multiple intersections of NLRs and the mitochondria.

### 3.5 Materials and Methods

**Cell culture.** HEK293T cells were maintained in complete DMEM medium supplemented with 10% fetal bovine serum, 4.5g/L glucose, 110mg/L sodium pyruvate, 2mM L-glutamine, 1% penicillin and 100µg/ml streptomycin. *Nlr1<sup>+/+</sup>* and *Nlr1<sup>-/-</sup>* MEFs were made from 13.5-day embryos and maintained in the complete DMEM medium described above. Cells transduced with tetracycline-inducible shRNA delivery lentiviruses were cultured in DMEM complete medium containing 10% tet system approved FBS (Cat. 631105, Clontech, Mountain View, CA). All cells were grown in 37 °C incubator supplied with 5% CO<sub>2</sub>.

**Experimental animals.** The *Nlr1<sup>-/-</sup>* C57BL/6 mice were generated in conjunction with the InGenious Targeting Laboratory, Inc (Stony Brook, NY). The conventional NLRX1-targeting construct was made by replacing the genomic region including exons 4 and 5 with the Neo cassette. The genotyping primers used to confirm gene deletion are:  
AT1 forward, 5'-GGTTTGATGGCCGTACATTCACAG-3'; WT1 reverse,  
5'-AGCCGGAAGTCAAGGTTGAGG-3'; UNI reverse,

5'-AGCGCATCGCCTTCTATCGCCTTC-3'. All experimental mice were bred in a pathogen-free facility at the University of North Carolina at Chapel Hill in accordance with the National Institutes of Health Guide for the Care and Use of Laboratory Animals and the Institutional Animal Care.

**Plasmids and molecular cloning.** FLAG-tagged TUFM expression plasmid was a kind gift from Dr. Nono Takeuchi at the University of Tokyo, Japan. FLAG-tagged MITA expression plasmid and ISRE reporter plasmid were generously provided by Dr. Hongbing Shu at Wuhan University, China. The domain truncation mutants of TUFM were generated according to standard molecular cloning protocols with the following primers:

a) for TUFM $\Delta$ I, 5'-GTCGAATTCACCACAATGGCGGCCGCCACCCTGCTG-3', 5'-CTCCAGGTCCCGGGCGGGGTCGCGCACGTAAGTCTT-3', 5'-AAGACTTACGTGCGCGACCCCGCCGGGACCTGGAG-3', 5'-GTCCTCGAGTCAACCCCATTTGATATTCTTCTCCTC-3'; b) for TUFM $\Delta$ II, 5'-GTCGAATTCACCACAATGGCGGCCGCCACCCTGCTG-3', 5'-CTTGATGGAACCTGGCTTACGGCCAGGGACGGAGTA-3', 5'-TACTCCGTCCCTGGCCGTAAGCCAGGTTCCATCAAG-3', 5'-GTCCTCGAGTCAACCCCATTTGATATTCTTCTCCTC-3'; c) for TUFM $\Delta$ III, 5'-GTCGAATTCACCACAATGGCGGCCGCCACCCTGCTG-3', 5'-CTCCTCCTCAGTCATGGCGGAACCTGGCTTGACCAT-3', 5'-ATGGTCAAGCCAGGTTCCGCCATGACTGAGGAGGAG-3', 5'-

GTCCTCGAGTCAACCCCATTTGATATTCTTCTCCTC-3'; d) for TUFMΔDIΔDII, 5'-GTCGAATTCGGCACCGTGGTGACAGGTACACTAGAG-3', 5'-GTCCTCGAGTCAACCCCATTTGATATTCTTCTCCTC-3'. The TUFMR339Q point mutation was generated using the QuickChange site-directed mutagenesis kit (Stratagene, La Jolla, CA). The primer pair used was: 5'-GGGAGGACTTGCGGCAGGGCCTGGTCATGGT-3', 5'-ACCATGACCAGGCCCTGCCGCAAGTCCTCCC-3'.

**Real time RT-PCR and gene tissue expression.** Total RNA was extracted from cells using the RNeasy plus mini kit (Cat. 74134, Qiagen, Valencia, CA). cDNA was reversed transcribed using random primers and MMLV reverse transcriptase (Invitrogen, Carlsbad, CA). Real time RT-PCR was performed using SYBR green master mix (Applied Biosystems, Foster City, CA) and data was acquired by an AB Prism 7700 analyser (Applied Biosystems, Foster City, CA). All samples were run in triplicate and data were analyzed by SDS2.2.2 software (Applied Biosystems, Foster City, CA). The primer pair used for IFN-β mRNA evaluation was: 5'-CATTACCTGAAGGCCAAGGA-3', 5'-CAATTGTCCAGTCCCAGAGG-3'; the primer pair for 18s was: 5'-GCTGCTGGCACCCAGACTT-3', 5'-CGGCTACCACATCCAAGG-3'. The expression data of TUFM in multiple cell and tissue types was made available by the BioGPS project (<http://biogps.gnf.org/>), which is funded by the Genomics Institute of the Novartis Research Foundation.

**RNAi-based protein expression knockdown.** NLRX1 mRNA was targeted using a

lentiviral delivery system to stably introduce shRNA expressed from a pol III promoter. The promoter, targeting shRNA or scrambled shRNA hairpin sequence, and polyT termination signal were amplified by PCR from a U6 promoter template and cloned into the lentiviral vector FG12. A universal forward PCR primer (5'-TGGCGGCCGCTCTAGAACTAGTGGA-3') was used together with the following specific reverse PCR primers (hairpin sequences are highlighted): A) sh-NLRX1: forward 5'-CTCCGCTCGAGAAAAAGCACATCTTCCGTCGGGATTCTCTTGAAATCCCGACGGAAGATGTGCGGTGTTTCGTCCTTTCCACAAGATATATAAAGCC-3'. B) sh-scrambled: 5'-CTCCGCTCGAGAAAAAGCACATCGCTTCTCGGGATTCTCTTGAAATCCCGAGAAGCGATGTGCGGTGTTTCGTCCTTTCCACAAGATATATAAAGCC-3'. To generate the tetracycline-inducible lentiviral shRNA delivery system targeting TUFM, we obtained Expression Arrest™ non-silencing TripZ control bacteria stock (Cat. RHS4743, Thermo Scientific Open Biosystems, Huntsville, AL) and TUFM-targeting shRNA-containing construct bacteria stock (Oligo ID V2THS\_222080, Cat. RHS4696-99362407, Thermo Scientific Open Biosystems, Huntsville, AL). The ON-TARGETplus SMARTpool of 4 siRNA targeting TUFM (Cat. L-016741-01-0005, Thermo Scientific, Huntsville, AL) and the control pool of 4 siRNA (Cat. D-001810-10-05, Thermo Scientific, Huntsville, AL) were transfected into the cells according to the manual. The TUFM-targeting siRNA sequences are as following: 5'-AGACUUACGUGCGCGACAA-3', 5'-GAACAAGGCUGACGCUGUC-3', 5'-CGAGAUGGCAACCGGACUA-3', 5'-CAGCUUCCCUUGCGUUUAA-3'.

**AACT-based mass spectrometry.** HA-tagged NLRX1 full-length and NLRX1 $\Delta$ LRR truncation sequences were cloned into a retroviral pHSPG vector containing a GFP selection marker according to standard molecular cloning procedure. The primers pairs are as following: for NLRX1 full length construct, 5'-GTGGAATTCATGTACCCATACGATGTTCCCTGACTATG-3', 5'-CCGCTCGAGTCAGCTTCCAGAGCTTCCCAGC-3'; for NLRX1 $\Delta$ LRR construct, 5'-GTGGAATTCATGTACCCATACGATGTTCCCTGACTATG-3', 5'-CCGCTCGAGTCAGGTCTGCCAGCAGGCGTG-3'. The retroviruses were made by transfecting the empty vector or expression construct together with gag-pol and VSVg plasmids into the packaging cells. HEK293T cells were transduced with these three retroviruses respectively and sorted by FACS based on GFP-positivity. Cells with empty vector were grown in DMEM L-Leucine-deficient medium (Cat. D9816, US Biological, Swampscott, MA) supplemented with L-Leucine-5,5,5-d3 (Cat. 486825, Sigma-Aldrich, St.Louis, MO), 10% FBS, 110mg/L sodium pyruvate, 2mM L-glutamine, 1% penicillin and 100 $\mu$ g/ml streptomycin. NLRX1-expressing or NLRX1 $\Delta$ LRR-expressing cells were cultured in regular medium. One billion cells expressing either NLRX1 or NLRX1 $\Delta$ LRR and equal number of control group cells were lysed and immunoprecipitated with anti-HA affinity matrix (Cat. 11815016001, Roche, Indianapolis, IN). Equal amount of beads from both control group and protein expression group were mixed together and eluted with HA peptide (Protein Chemistry core facility, UNC-CH). The elutes were subjected to SDS-PAGE and Coomassie

staining.

The Coomassie-stained gel lanes were continuously excised, and each slice was cut into ca. 1mm cubes and subsequently subjected to in-gel digestion. The gel pieces and trypsin solution (10ng/ $\mu$ L in 25mM ammonium bicarbonate) were pre-chilled at 4 °C for 2h to ensure complete absorbance of enzyme into the gel, and then incubated overnight at 37 °C with gentle shaking. Following extraction of the peptides with the extraction buffer (50% acetonitrile, 50% water, 0.1% formic acid), the peptides were lyophilized and then resuspended in buffer A (2% acetonitrile, 98% water and 0.1% formic acid). LC-MS/MS analysis was performed on a nanoAcquity UPLC - QTOF API US system (Waters, UK). A 5 $\mu$ L sample was loaded onto a reversed phase C18 column (75 $\mu$ m $\times$ 25cm, 1.7 $\mu$ m particle, Waters Company). Linear gradient was run from 100% buffer A to 40% buffer B (98% acetonitrile, 2% water and 0.1% formic acid) in 150min, and then to 80% B in another 30min. Eluted peptides were acquired in the data-dependent mode using MassLynx software (version 4.0, Waters). Top five parent ions of each cycle were selected for further MS/MS analysis.

All the raw files acquired on QTOF were processed using Mascot Distiller software (version 2.3, Matrix Science, UK) and then searched against human International Protein Index (IPI) protein database (version 3.26, 67665 sequences). SILAC quantification was automatically done using Quantitation Toolbox in Distiller. Decoy database search function was also enabled, which ensured the false discovery rate was less than 0.01. Only proteins that had at least two unique peptides achieving an ion score above 39 and

contained at least five consecutive amino acids matching the data base peptides sequences were considered to be positive identifications. All the raw spectrum and SILAC ratios were manually evaluated. Gene Ontology annotation analysis was performed using DAVID Bioinformatics Resources (<http://david.abcc.ncifcrf.gov/>).

**Transfections and viral infections.** HEK293T cells were plated so that they could reach about 80% confluence the next day for transfections. FuGENE<sup>®</sup> 6 (Cat. 11814443001, Roche, Indianapolis, IN) was diluted in serum-free DMEM medium, and corresponding amount of plasmids DNA was added to the transfection reagent so that the DNA:FuGENE<sup>®</sup> 6 ratio was 1:3. The mixture was incubated at room temperature for 20min and then added to the cell culture medium. VSV-GFP virus was generously provided by Dr. John Hiscott at McGill University, Canada. The virus was propagated in VERO cells (ATCC, Manassas, VA). VSV was propagated in Vero cells (ATCC, Manassas, VA). For VSV titering by plaque assays, ten-fold dilutions of virus-infected cell supernatants were made in serum-free DMEM medium in duplicates or triplicates, and added to each well of a 6-well dish plated with confluent VERO cells in monolayer. VERO cells were incubated at 37 °C for 1 h, after which the inoculum was removed and an overlay of 1% methyl cellulose in DMEM supplemented with 10% FBS was added to each well. Three days later, the methyl cellulose overlay was aspirated and cells were fixed in 4% formaldehyde and stained with 0.2% crystal violet for plaque counting. Cell lines or primary cells were plated 24h prior to infection so that HEK293T cells and MEFs could reach about 80% confluence the next day. Virus inoculum was prepared in

pre-warmed serum free DMEM and incubated with cells for 1h at 37 °C. Then the virus inoculum was removed and cells were replenished with complete media.

**Co-immunoprecipitation and Western blots.** Cells were lysed in RIPA buffer (1% Triton X-100, 0.25% DOC, 0.05% SDS, 50mM Tris-HCl pH8.0, 150mM NaCl and 50mM NaF) or NP-40-based lysis buffer (1% NP-40, 50mM Tris-HCl pH8.0, 150mM NaCl) containing complete protease inhibitor cocktail (Cat. 11873580001, Roche, Indianapolis, IN). For the endogenous co-immunoprecipitation experiments, whole cell lysates were pre-cleared with protein A resin (Cat. L00210, GenScript, Piscataway, NJ) and protein G resin (Cat. L00209, GenScript, Piscataway, NJ) for 1h at 4 °C, and then incubated with primary antibody overnight. The protein A/G UltraLink<sup>®</sup> resin (Cat. 53132, Thermo Scientific, Huntsville, AL) was added the next day and incubated for 2h at 4 °C. Beads were washed 5 times before resuspension and boiling in the Laemmli's sample buffer. Protein samples were separated by NuPAGE Bis-Tris 4-12% precast gels (Cat. NP0322BOX, Invitrogen, Carlsbad, CA) or Tris-Glycine 16% precast gels (Cat. EC64952BOX, Invitrogen, Carlsbad, CA). The antibodies used in this study are as following: High-affinity anti-HA-peroxidase (Cat. 12013819001, Roche, Indianapolis, IN), Anti-FLAG<sup>®</sup> M2 affinity gel (Cat. A2220, Sigma-Aldrich, St.Louis, MO), anti-LC3B (Cat. 2775, Cell Signaling, Danvers, MA), anti-TUFM (Cat. ab67991, abcam, Cambridge, MA), anti-TUFM (Cat. HPA018991, Sigma-Aldrich, St. Louis, MO), anti-eEF1 $\alpha$ 1 (Cat. sc-28578, Santa Cruz, Santa Cruz, CA), anti-Bcl-x<sub>L</sub> (Cat. 2762, Cell Signaling, Danvers, MA), anti-Atg5 (Cat. 2630, Cell Signaling, Danvers, MA), anti-

calreticulin (Cat. 2891S, Cell Signaling, Danvers, MA), anti-Actin-HRP (Cat. sc-1615HRP, Santa Cruz, Santa Cruz, CA).

**Luciferase assays.** HEK293T cells were plated in 96-well plate at the density of  $1.0 \times 10^4$  per well 24h prior to transfection. The firefly luciferase reporter plasmids for NF- $\kappa$ B, ISRE and IFNB were transfected together with  $\Delta$ IRIG-I/MITA and increasing doses of TUFM according to the experimental templates. Empty vector plasmid was added so that each well contained 250ng DNA. Cells were lysed with passive lysis buffer (Cat. E194A, Promega, Madison, WI) compatible with luciferase assays. Readings were recorded by a luminometer (Molecular Devices, Sunnyvale, CA) that is capable of injecting luciferase assay buffer (25mM Gly-Gly, 15mM potassium phosphate buffer, 15mM MgSO<sub>4</sub>, 4mM EGTA, 2mM ATP, 1mM DTT) and substrate (0.2mM luciferin, 20mM Gly-Gly, 1mM DTT).

**Laser confocal imaging analysis.** *Nlr1<sup>+/+</sup>* or *Nlr1<sup>-/-</sup>* MEFs were seeded on 8-well glass slide (Cat. 154534, Thermo Fisher Scientific, Rochester, NY) 24h prior to treatments. The next day cells were incubated with VSV-GFP at the MOI of 0.1 for 1h in serum-free DMEM, and then the virus inoculum was removed. Cells were replenished with complete medium and incubated for 4h. Cells were fixed and permeabilized with 4% paraformaldehyde containing 0.1% Triton-X 100 for 20min at room temperature. The cells were washed 3 times with  $1 \times$  PBS. Samples were incubated with blocking buffer (7% BSA, 1% FBS, 2% goat serum, 1% Fc block) for 1h at room temperature. LC3B antibody was diluted at 1:400 in the blocking buffer. The samples were incubated with

primary antibody overnight at 4°C followed by the 2h incubation with Alexa Fluor<sup>®</sup> 647 goat anti-rabbit antibody (Cat. A-21244, Invitrogen, Carlsbad, CA) diluted at 1:2000 ratio in the blocking buffer. Images were acquired with an Olympus FV500 confocal microscope.

**Size Exclusion Chromatography.**  $2 \times 10^7$  HEK293T cells were transfected with either control dsRNA or 5'-ppp dsRNA (Invivogen, San Diego, CA). Cells were harvested 16h post-transfection and lysed in hypotonic lysis buffer with a Dounce homogenizer. The homogenate was centrifuged at 500g for 15min to separate nuclei. The supernatants were filtered and loaded onto Superose 6 HR-10/30 columns (GE Healthcare). 500 µl of each fraction was collected and separated by SDS-PAGE.

## **CHAPTER FOUR**

### **DISCUSSION AND FUTURE DIRECTION**

#### 4.1 Viruses can subvert MAVS-dependent type 1 IFN production

Given the broad consequences of type 1 IFN production in the viral life cycles, MAVS pathway has been heavily targeted by different viruses to abrogate such response. Three simplified models have been proposed to explain how viruses subvert MAVS-mediated antiviral responses: 1) abrogating MAVS function by cleaving the protein off the mitochondria; 2) imposing steric hindrance by interfering with the association between MAVS and upstream RLRs; 3) destabilizing MAVS by polyubiquitination-based mechanisms.

Several viral proteins have been identified to cleave MAVS. HCV encodes a serine protease NS3/4A to cleave MAVS at the residue Cys508, dislodging MAVS from mitochondria<sup>37, 185</sup>. Similarly a closely related virus GB virus B (GBV-B) employs NS3/4A to cleave MAVS<sup>238</sup>. A picornavirus HAV uses the 3ABC precursor of its 3C(pro) cysteine protease to cleave MAVS at the Gln428 site<sup>186</sup>.

In addition to cleaving MAVS, association with MAVS or upstream RLR to compete with their signaling-activating engagement is another widely used strategy by different classes of viruses. The non-structural protein NS1 encoded by influenza A virus inhibits host type 1 IFN response by not only binding to dsRNA to sequester activating RNA species from RLR but also directly associating with RIG-I to prevent IRF3 nuclear translocation<sup>239-241</sup>. The PB2 subunit of influenza RNA polymerase can associate with MAVS and inhibits type 1 IFN production. Although the mitochondrial localization of PB2 is not essential for viral growth *in vitro*, non-mitochondrial PB2-encoding virus

induces higher level of type 1 IFN<sup>242, 243</sup>. The non-structural protein NS2 encoded by human Respiratory Syncytial Virus interacts with the CARD domain of RIG-I and blocks its association with MAVS to inhibit IFN promoter activation<sup>244</sup>. The Z proteins encoded by four New World arenaviruses including Guanarito virus (GTOV), Junin virus (JUNV), Machupo virus (MAVC), and Sabia virus (SABV) have been found to interact with RIG-I and interferes with RIG-I:MAVS association<sup>245</sup>. The LCMV nucleoprotein interacts with both RIG-I and MDA5 to inhibit type 1 IFN signaling triggered by LCMV RNA or other RLR ligands<sup>246</sup>. V proteins encoded by paramyxoviruses associate with MDA5 and abrogate downstream type 1 IFN activation<sup>247</sup>. A recent report demonstrated that V proteins target a region within the MDA5 helicase domain to interrupt dsRNA binding and its homotypic dimerization<sup>248</sup>.

Destablizing MAVS is not only a host strategy to keep immune activation in-check, but also hijacked by viruses to evade immune surveillance. In a clinical samples analysis, MAVS was downregulated in hepatocellular carcinomas of Hepatitis B Virus (HBV) origin<sup>249</sup>. In fact the protein HBX encoded by HBV has been found to associate with MAVS and facilitate its proteosomal degradation through PUb at the Lys136 site. Consistently, the HBX knock-in transgenic mice display enhanced susceptibility to VSV infection<sup>249</sup>. MAVS can also be disrupted by non-proteosomal pathway. For example, Human Rhinovirus 1a (HRV1a) infection can result in degradation of MAVS 7h post-infection. Ectopic expression of HRV1a and polioviral 2A(pro) and 3C(pro) results in the destabilization of MAVS<sup>250</sup>.

## 4.2 Viruses target apoptotic signaling

In addition to being a critical adaptor for type 1 IFN signaling induced by RLR engagement, we demonstrate that MAVS mediates virus-induced apoptosis in an IFN-independent fashion. After our findings were published, two other groups reported similar results regarding the pro-apoptotic function of MAVS<sup>251, 252</sup>. Overexpression of MAVS is similarly found to induce apoptosis in a caspase-3, -8, and -9 dependent manner. Anoikis is a type of apoptosis induced by the detachment of epithelial cells from the extracellular matrix. Not only can anoikis induce the upregulation of MAVS but also recruit caspase-8. Furthermore, MAVS binds to death-associated protein 3 (DAP3); and reduction of MAVS protein level inhibits DAP3-mediated anoikis<sup>251</sup>. We demonstrate MAVS is essential for SeV-induced apoptosis. Another group reported MAVS is similarly critical for Dengue Virus (DENV)-induced apoptosis. RNAi-based reduction of MAVS results in delayed caspases activation and attenuated cell death<sup>252</sup>. Dislocated MAVS not only loses its function in activating type 1 IFN, but becomes inert in activating the apoptotic pathway.

The MAVS-mediated apoptotic signaling is targeted by different classes of viruses. By either truncating the transmembrane domain of MAVS or cleaving it by co-transfecting NS3/4A completely abolishes its pro-apoptotic capacity. In addition, we identified the NSP15 protein encoded by SARS-CoV as an inhibitor of this pathway. NSP15 does not affect staurosporin-induced apoptosis. However, the detailed molecular mechanism of its inhibitory function remains unclear; and further investigation is needed

to understand how MAVS-centered apoptosis is regulated by viral proteins.

Viruses utilize a wide variety of strategies to target host apoptotic signaling. Depending on the stages of viral infection, apoptosis induction or inhibition will benefit the viruses in their spreading and intracellular replication. Thus viruses of diverse families encode pro-survival inhibitors to induce apoptosis, or on the other hand, express viral Bcl-2 homologues to antagonize cell death.

Based on the origins of stimuli, distinct molecular complex that is involved, apoptosis is generally categorized into extrinsic and intrinsic apoptotic signaling. The extrinsic apoptotic pathway, also known as death-receptor pathway is induced by the engagement of death receptors such as TNF receptor-1 (TNFR1) or Fas with their corresponding ligands <sup>253</sup>. This pathway is Bcl-2 protein-independent and functions by recruiting caspase-8 through the death domain of the death receptors. Fas deficiency has been implicated in many autoimmune lymphoproliferative syndrome cases, in which double-negative T cells accumulate in the peripheral <sup>254</sup>. Upon activation, Fas binds to FADD to form a molecular platform DISC (death-inducing signaling complex) for caspase-8 and -10 activation. The activation of caspase-8 will eventually activate downstream effector caspases such as caspase-3, -6 or -7. FLICE is a critical adaptor protein that shares homology to both FADD and caspases. It can bind to the death domain of FADD and induce apoptosis, treatment of caspases inhibitors can block its function <sup>255</sup>. The intrinsic apoptotic pathway, also known as mitochondrial apoptotic pathway, involves the proper function of Bcl-2 family members. Diverse insults, such

as UV irradiation, chemotherapeutic drugs, unfolded protein response and microbial infections etc, could result in the release of cytochrome c, SMAC/Diablo and HtrA2/Omi into the cytosol, which facilitates the assembly of apoptosome and activation of caspase-9<sup>256</sup>.

The extrinsic pathway is targeted by different classes of viruses that employ similar strategies such as DISC formation interference, TNF receptor mimicry and caspase inhibition<sup>253, 257</sup>. Some  $\gamma$ -herpesviruses including Kaposi's-sarcoma-associated human herpesvirus-8 (KSHV) and Molluscum Contagiosum Virus (MCV) express vFLIPs, which contain two DED domains and interacts with FADD. Such interaction blocks the recruitment and activation of FLICE<sup>258</sup>. In addition, TNFR receptors have been identified in both Leporipoxviruses and Orthopoxviruses<sup>259</sup>. Cowpox virus encodes several cytokine response modifier CrmB, -C, -D and -E to bind to TNF and attenuate host TNF signaling<sup>260-263</sup>.

The mitochondrial apoptosis pathway has also been harnessed by viruses belonging to various families in favor of their replication at the early stage of infection or dissemination at later stages. Inhibition of apoptosis facilitates the establishment of viral replication niche within the host, many viruses have evolved homologs of mammalian Bcl-2 proteins to antagonize host apoptotic signaling. Some viral Bcl-2 proteins (vBcl-2s) do not share sequence homology with mammalian Bcl-2, however, their protein structures demonstrate remarkable similarity to their host counterparts. One of the earliest vBcl-2s identified is the E1B-19K protein encoded by adenovirus<sup>264</sup>.

A significant portion of this protein is located on the mitochondria and sequesters pro-apoptotic proteins Bax and Bak from facilitating MOMP<sup>264</sup>. Similar mechanisms are also shared by many other viral proteins such as vaccinia virus F1L protein, Myxoma virus M11L protein, Fowlpox virus FPV039, parapoxvirus ORF virus ORFV125, Epstein-Barr virus (EBV) BALF1 and BHRF1 proteins etc<sup>265</sup>.

Viruses also have evolved proteins activating the mitochondrial apoptotic signaling pathway, possibly facilitating their dissemination to adjacent cells. These proteins function by directly forming a channel on mitochondrial membranes or interacting with host factors to promote MOMP. For example, the Vpr protein encoded by Human Immunodeficiency Virus 1 (HIV-1) directly binds to ANT and VDAC via its C-terminus, promoting MOMP<sup>266</sup>. Such effects could be efficiently blocked by Bcl-2 and ANT/VDAC inhibitors<sup>266</sup>.

### **4.3 Tu translation elongation factors are versatile proteins**

In the current study, we identified TUFM as an interacting partner of NLRX1. TUFM recruits Atg5-Atg12 conjugate to the NLRX1-containing mitochondrial complex to negatively regulate type 1 IFN. TUFM is an evolutionarily conserved protein with sequence homologous to EF-Tu in bacteria. In mammalian cells, there are two forms of EF-Tu: one is eEF1A which is primarily located within the cytosol; and the other one is TUFM, which resides within mitochondria. Besides its well known function in translation elongation, this protein has been implicated in carcinogenesis, oxidative phosphorylation and immune elicitation.

One of the best characterized functions of EF-Tu is its role in peptide elongation. EF-Tu delivers aminoacyl-tRNA to the A-site of the ribosome when a match between codon and anticodon is detected. Then the peptidyl-tRNA mRNA complex moves from the A site to the P site, allowing A site to accept deposit of next amino acid. This amino acid delivery process is GTP-dependent, which explains the high degree of conservation of the GTPase domain of mammalian EF-Tu and that of its bacterial counterpart. Crystal structure analysis of EF-Tu revealed three well defined domains. The N-terminal domain I is responsible for GTP hydrolysis, domain II is responsible for aminoacyl-tRNA binding, the function of the C-terminal domain III is less clear<sup>267</sup>.

Among one of the initial identifications of TUFM, one report demonstrated upregulation of TUFM in a variety of tumors of human or animal origin<sup>234</sup>. Similarly, in a more recent two-dimensional electrophoresis proteomics on the mitochondria-enriched fraction indicated TUFM was highly expressed in human gastric carcinoma cell line AGS<sup>268</sup>. In fact, this protein is also found to be accountable for tumor cell resistance to chemotherapeutic drug Artesunate (ART)<sup>269</sup>. However, the molecular mechanisms of its function underlying carcinogenesis remain unclear. It is possible that more proteins need to be synthesized due to the active life cycle of cancer cells, thus the proteins involved in protein synthesis are upregulated. Interestingly, not all translation elongation factors are upregulated during carcinogenesis, which indicates alternative explanations of the overexpression of TUFM in tumor cells. We found reduction of TUFM resulted in compromised autophagy. Recent evidence highlights the

significance of autophagy in cancer development. Cancer cells could exploit this conserved host cellular function to sustain their viability in the nutrient-poor tumor environment<sup>154, 270</sup>. Further investigation will be essential to elucidate whether the functions of TUFM in autophagy underlie its roles in carcinogenesis.

A point mutation in the domain II of TUFM R339Q has been reported to be associated with the clinical presentation of neonatal lactic acidosis, rapidly progressive encephalopathy and severely compromised mitochondrial protein synthesis as well as deficiency in the mitochondrial respiratory chain<sup>235</sup>. Although this point mutation is unlikely to cause a drastic structural change since its interaction with adjacent amino acid residues is minimal, it is speculated that the mutation may interfere with the proper formation of the TUFM:aminoacyl-tRNA:GTP complex<sup>235</sup>. Notably the oxidative phosphorylation process is defective in the mutant-carrying cells. Galactose is used in lieu of glucose to selectively eliminate oxidative phosphorylation deficient cells. The R339Q-carrying cells were eradicated in this medium, suggesting a possible role of TUFM in oxidative phosphorylation<sup>235</sup>.

In addition, TUFM has also been shown to possess chaperone properties *in vitro* in a GTP-dependent fashion. Protein thermal aggregation is inhibited by recombinant TUFM, and refolding of denatured protein is consistently promoted by TUFM<sup>236</sup>. TUFM is highly similar to its cytoplasmic homologue eEF1 $\alpha$ 1, which displayed very diverse biological functions in addition to peptide elongation as well<sup>267</sup>. Similar to TUFM, eEF1 $\alpha$ 1 also possesses chaperone properties for protein quality control. In fact,

eEF1 $\alpha$ 1 has been shown to be essential for ubiquitin-dependent degradation of N<sup>α</sup>-acetylated proteins <sup>271, 272</sup>. eEF1 $\alpha$ 1 was firstly identified as an actin-associating protein <sup>273</sup>. Its ability to bind and bundle actin filaments has also been confirmed *in vitro* <sup>274</sup>. With an *in vivo* assay in the yeast *Saccharomyces cerevisiae*, eEF1 $\alpha$ 1 displayed significance in cytoskeleton organization, which is independent of its function in protein translation <sup>275</sup>. Given the significance and abundance of eEF1 $\alpha$ 1 within the cells, it has been hijacked by various viruses for their replication and propagation <sup>267</sup>. The conserved 3'-terminal stem-loop (3' SL) of the WNV genomic RNA has been found to associate with eEF1 $\alpha$ 1, dephosphorylation of which abolished such interaction <sup>276</sup>. Mutations that disturb its association with eEF1A1 negatively impacted viral growth. However, viral polyprotein translation efficiency was not altered upon these mutation. Instead, the minus-strand RNA synthesis was closely correlated with the binding efficiency to eEF1A1. Such association between viral RNA was also observed in other flaviviruses <sup>277</sup>.

The function of TUFM in antiviral signaling remains largely unknown, in the current study, we identified TUFM as a potent inhibitor of host type 1 IFN signaling, which is mediated by its interaction with the Atg5-Atg12 conjugate. We found TUFM inhibited NF- $\kappa$ B-, ISRE-dependent and IFNB1 promoter activities in a dose-dependent manner. Overexpression of TUFM squelched *IFNB1* mRNA transcription. Consistently, reduction of TUFM resulted in enhanced immune activation, which depends on the integrity of its N-terminus. Interestingly, although the function of TUFM in the immune

system has not been demonstrated before, its bacterial homologue EF-Tu has been shown to be a potent immune-activating PAMP in the plant immune system<sup>228, 229</sup>. EF-Tu is conserved across bacterial kingdom, thus its recognition by host cells warrants rapid and accurate detection of invading microorganisms. The immune-eliciting activity depends on its N-terminus, as a matter of fact, a short polypeptide comprising of the N-terminal 12 amino acids of EF-Tu plus an N-terminal acetylation is sufficient to activate immune system to its full potential. The sequence acetyl-xKxKFxRxxxxxxxxx has been found to be the minimally required elicitor in *Arabidopsis thaliana* immune system<sup>228</sup>. A later reverse-genetic approach identified the transmembrane protein EFR (Elongation Factor Tu Receptor) as the receptor of EF-Tu. EFR contains a LRR-rich extracellular domain, a single transmembrane domain and an intracellular domain, which displays typical features of a serine-threonine protein kinase. In the *Nicotiana benthamiana* plants that are resistant to EF-Tu signaling, transformation of cells with EFR delivered the capacity of specific binding to the N-terminus of EF-Tu; in addition, transformed cells gained responsiveness to EF-Tu challenge<sup>229</sup>. The endosymbiosis theory hypothesized that mitochondrion originated from the integration of alphaproteobacteria into the host cells, in which host factors constantly interact with the endosymbiont. When bacterial EF-Tu gradually evolves to host TUFM, its function has been transformed from being immune-activating to immune-suppressive. In our sequence homology comparison analysis, the N-terminus of EF-Tu is the only region that undergoes drastic changes, which generates a mitochondrial-targeting sequence in the mammalian homologue.

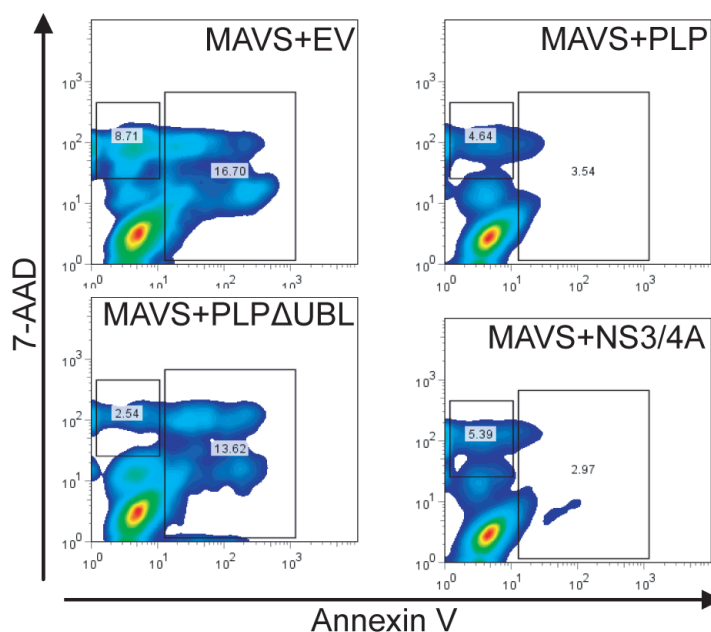
Notably the sequence essential for immune-activation no longer exists in TUFM. The biological functions of TUFM have been implicated in protein translation elongation, oncogenesis, oxidative phosphorylation, protein quality control as well as host antiviral immunity. More investigations are necessary to elucidate the molecular complexes involved in these distinct functions.

#### **4.4 Future directions**

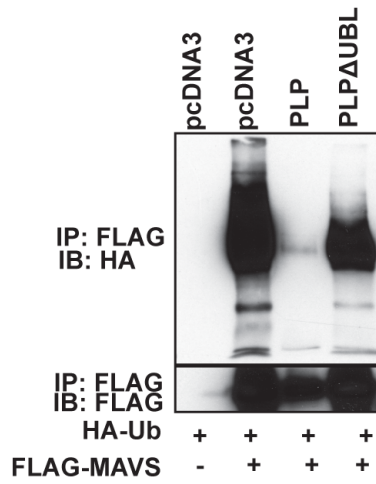
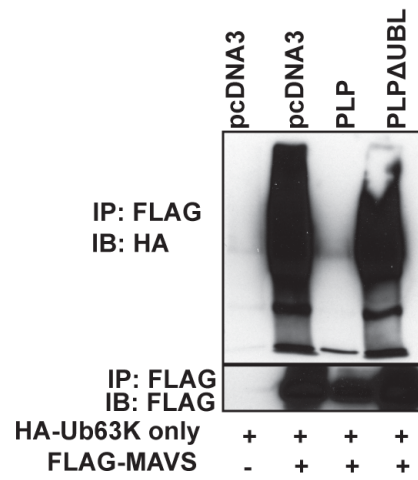
The adaptor proteins could form different macromolecular complexes in response to insults of distinct nature. Our group and others have shown that MAVS activate caspase-3 and -9, the activity of which depends on the formation of apoptosome. However, it's not yet clear whether MAVS-mediated apoptosis induce the oligomerization of Apaf-1. It would be necessary to perform SEC (size exclusion chromatography) to analyze apoptosome in wildtype and MAVS-deficient cells. In addition to caspases cleavage induction, activated caspases can also cleave MAVS, however, a pan-caspase inhibitor zVAD does not inhibit the cleavage<sup>250, 278</sup>. The physiological role of cleaved MAVS is still unclear, it might be possible that cleavage of MAVS could activate the cell death pathway. Further research is needed to elucidate the mechanism underlying the pro-apoptotic function of MAVS. For example, MAVS activation could result in the dissipation of mitochondrial membrane potential  $\Delta\psi_m$ , what molecular complex is involved in the MAVS-induced MOMP remains unknown. A proteomics approach to identify MAVS-interacting protein in response to apoptotic stimuli will generate more clues. We have identified SARS-CoV NSP15 as a potent

inhibitor of MAVS-mediated apoptosis, the exact inhibitory mechanism is still elusive. Notably the inhibitory function is specific to SARS-CoV yet not shared by other CoV. SARS-CoV replication is mostly restricted to the first two weeks of disease onset, the temporal regulation of NSP15 is critical in abrogating host apoptotic responses and thus benefiting the viruses. As an important strategy to evade host surveillance, it is possible that SARS-CoV designates multiple proteins to interfere with host apoptotic signaling. In fact, we have found another protein encoded by SARS-CoV that strongly inhibits MAVS-mediated apoptosis as well. The Papain-like Protease (PLP) can process the SARS-CoV replicase polyprotein. We found when co-transfected with MAVS, PLP abrogated MAVS-mediated apoptosis (Fig. 4.1). PLP contains an ubiquitin-like domain (UBL), which was essential to its inhibitory function. It has previously been shown that PLP possesses deubiquitinating enzyme activity<sup>279-282</sup>, it is possible that this enzymatic activity underlies its inhibitory effect on apoptotic signaling. Ectopic expression of MAVS activates both type 1 IFN and apoptotic signaling, we found that MAVS was heavily ubiquitinated when activated (Fig. 4.2A). PLP potently inhibited MAVS polyubiquitination, while the truncation of its UBL completely abolished such inhibition (Fig. 4.2A). Polyubiquitination is generally categorized into K63-linked and K48-linked modification, with the former being more involved in signaling alteration and the latter being related to proteosomal-mediated protein degradation. We found when we coexpressed MAVS with K63-only ubiquitin, which adds polyubiquitin chain exclusively in a K63-linked manner, PLP also completely deubiquitinated the modified

MAVS and UBL domain was essential for such function (Fig. 4.2B). However, it is unclear how polyubiquitination of MAVS modulates its pro-apoptotic function and which lysine residue is primarily responsible for such modification.



**Figure 4.1** Papain-like protease inhibits MAVS-mediated apoptosis.  $1.0 \times 10^6$  HEK293T cells were transfected with  $1.5 \mu\text{g}$  MAVS with either  $1.5 \mu\text{g}$  control empty vector or PLpro, PLpro $\Delta$ UBL, NS3/4A expression plasmids. Cells were harvested 48h post-transfection for 7-AAD and Annexin V staining. All samples were then subjected to flow cytometry analysis.

**A****B**

**Figure 4.2 PLP inhibits polyubiquitination of MAVS.** (A) HEK293T cells were transfected with HA-ubiquitin, FLAG-MAVS together with PLP or its truncation mutant. Cells were harvested 24h post-transfection and MAVS was immuno-precipitated with anti-FLAG agarose beads, all samples were then subjected to SDS-PAGE. (B) HEK293T cells were transfected with K63-only HA-ubiquitin, FLAG-MAVS together with PLP or its truncation mutant. Cells were harvested 24h post-transfection and analyzed as described in (A).

MAVS protein contains 14 lysine residues (Fig. 4.3), future studies are needed to identify the ones that are primarily responsible for polyubiquitination and delineate the functional significance.

1 mpfaedktyk yicrnfsnfc nvdvveilpy lpeltardqd rlractlsg nrtdlwhlfn  
61 tlqrrpgwve yfiaalrgce lvdladevas vyqsyqprts drppdplepp slpaerpgpp  
121 tpaahsipy nscrekepsy pmpvqetqap espgenseqa lqtlspiraip rnpdggples  
181 ssdlaalspl tssghqeqdt elgsthtaga tssltpsrgp vspsvsfqpl arstprasrl  
241 pgptgsvvst gtsfssspg lasagaaegk qgaesdqaep iicssgaeap ansllskvpt  
301 tlmvntval kvpanpasvs tvpsklptss kppgavpsna ltnpapsklp instragmvp  
361 skvptsmvlt kvsastvptd gssrneetpa aptpagatgg ssawldsse nrglgselsk  
421 pgvlasqvds pfsgcfedla isastslmg pchgpeeney ksegftgihv aenpsiqle  
481 gnpqppadpd ggprpqadrk fqerevchr pspgalwlqv avtgvlvvtl lvlyrrrlh

**Figure 4.3 MAVS contains 14 lysine residues.** MAVS protein sequence contains 14 lysine residues, which are highlighted.

In the current study, we found NLRX1 associated with TUFM to form a molecular platform for RLR signaling modulation. In our proteomics study, we have identified multiple interacting proteins (Table 4.1), many of which might suggest the biological significance of NLRX1 in both antiviral immune signaling and other pathways. For example, NLRX1 could interact with translocon-associated protein; and translocon components have been suggested in the STING-mediated antiviral responses<sup>69</sup>, although we did not find any regulatory effects of NLRX1 on STING-induced ISRE activation, it is possible that NLRX1 might affect other STING-related functions such as intracellular DNA recognition pathways. We have also noticed that NLRX1 is associating with HSP70, the peptide sequence coverage of which is approximately 30%. HSP70 has been documented in regulating immune responses, protein quality control and ER-stress

regulation<sup>283-285</sup>. It suggests NLRX1 might be involved in other signaling pathways other than innate immune responses. Interestingly some proteins involved in the oxidative phosphorylation, such as Peroxiredoxin and Thioredoxin, have also been found in the interacting partners list. To further our understanding in the functions of NLRX1 in disease pathogenesis, it is necessary to develop *in vivo* animal models as well. It is possible that NLRX1 may have very diverse functions in different tissues and disease models. The TUFM genetic deletion animal model is not yet available, generation and a full characterization of this strain would provide deeper insight into this multimeric regulatory complex.

As a novel nodular check-point of RLR signaling, the studies of post-translational modifications of NLRX1 and TUFM are not currently available. A proteomics approach to identify potential modification sites on these proteins will provide valuable tools to further analyze the RLR regulatory network.

Accession	NLRX1-interacting Proteins
IPI00000643	BAG family molecular chaperone regulator 2
IPI00000690	Isoform 1 of Apoptosis-inducing factor 1, mitochondrial precursor
IPI00000816	14-3-3 protein epsilon
IPI00000874	Peroxiredoxin-1
IPI00003362	HSPA5 protein
IPI00003865	Isoform 1 of Heat shock cognate 71 kDa protein
IPI00007188	ADP/ATP translocase 2
IPI00007702	Heat shock-related 70 kDa protein 2
IPI00007765	Stress-70 protein, mitochondrial precursor
IPI00009104	RuvB-like 2
IPI00011134	Heat shock 70 kDa protein 7 (Fragment)
IPI00019385	Translocon-associated protein, delta subunit precursor
IPI00024145	Isoform 1 of Voltage-dependent anion-selective channel protein 2
IPI00025156	Isoform 1 of STIP1 homology and U box-containing protein 1
IPI00025874	Dolichyl-diphosphooligosaccharide--protein glycosyltransferase 67 kDa subunit precursor
IPI00027107	Tu translation elongation factor, mitochondrial
IPI00030275	Heat shock protein 75 kDa, mitochondrial precursor
IPI00216298	Thioredoxin
IPI00220644	Isoform M1 of Pyruvate kinase isozymes M1/M2
IPI00291467	ADP/ATP translocase 3
IPI00293276	Macrophage migration inhibitory factor
IPI00299904	Isoform 1 of DNA replication licensing factor MCM7
IPI00302927	T-complex protein 1 subunit delta
IPI00303476	ATP synthase subunit beta, mitochondrial precursor
IPI00304925	Heat shock 70 kDa protein 1
IPI00306301	Pyruvate dehydrogenase E1 component alpha subunit, somatic form, mitochondrial precursor
IPI00329629	DnaJ homolog subfamily C member 7
IPI00339269	Heat shock 70 kDa protein 6
IPI00376005	Isoform 2 of Eukaryotic translation initiation factor 5A-1
IPI00382470	Heat shock protein HSP 90-alpha 2
IPI00419585	Peptidyl-prolyl cis-trans isomerase A
IPI00456762	Protein TMEM142B
IPI00465248	Isoform alpha-enolase of Alpha-enolase
IPI00465260	GARS protein
IPI00646779	TUBB6 protein

**Table 4.1 NLRX1 interactome.** NLRX1 interacts with multiple proteins involved in antiviral signaling, oxidative phosphorylation and protein quality control etc.

#### 4.5 Concluding remarks

The mitochondrial immune signaling protein complex plays pivotal roles in the host antiviral innate immune responses. The adaptor MAVS associates with upstream PRRs, such as RIG-I and MDA5 when they are engaged in their respective ligands, and activates NF- $\kappa$ B and IRF3 to mount type 1 IFN production<sup>34-37</sup>, which together with apoptosis constitutes the first line of host defense against viruses. Here we identified a novel mitochondrial complex that potently modulates host innate antiviral responses. MAVS has dual roles in mounting type 1 IFN production and initiating virus-induced apoptosis. Both functions have been targeted by a variety of viral proteins for modulation. A closely associated inhibitory complex, which is composed of NLRX1, TUFM and the Atg5-Atg12 conjugate, potently modulates MAVS-mediated type 1 IFN activation and virus-induced autophagy. We have established the first physical link between an NLR protein and the virus-induced autophagic machinery via an intermediary protein TUFM. Although to decipher how a single protein can be involved in different molecular complexes and their exquisite structural basis remains to be a major challenge, the results in this study shed light on the future identification of critical antiviral therapeutic targets to activate innate immune system to its full potential.

## REFERENCES

1. Gray, M.W., Burger, G. & Lang, B.F. Mitochondrial evolution. *Science (New York, N.Y)* **283**, 1476-1481 (1999).
2. Moore, C.B. & Ting, J.P. Regulation of mitochondrial antiviral signaling pathways. *Immunity* **28**, 735-739 (2008).
3. Starkov, A.A. The role of mitochondria in reactive oxygen species metabolism and signaling. *Annals of the New York Academy of Sciences* **1147**, 37-52 (2008).
4. Hailey, D.W. *et al.* Mitochondria supply membranes for autophagosome biogenesis during starvation. *Cell* **141**, 656-667 (2010).
5. Brenner, D. & Mak, T.W. Mitochondrial cell death effectors. *Curr Opin Cell Biol* **21**, 871-877 (2009).
6. Oberst, A., Bender, C. & Green, D.R. Living with death: the evolution of the mitochondrial pathway of apoptosis in animals. *Cell death and differentiation* **15**, 1139-1146 (2008).
7. Kleine, T., Maier, U.G. & Leister, D. DNA transfer from organelles to the nucleus: the idiosyncratic genetics of endosymbiosis. *Annual review of plant biology* **60**, 115-138 (2009).
8. Dolezal, P., Likic, V., Tachezy, J. & Lithgow, T. Evolution of the molecular machines for protein import into mitochondria. *Science (New York, N.Y)* **313**, 314-318 (2006).
9. Hayashi, T., Rizzuto, R., Hajnoczky, G. & Su, T.P. MAM: more than just a housekeeper. *Trends in cell biology* **19**, 81-88 (2009).
10. Hettema, E.H. & Motley, A.M. How peroxisomes multiply. *Journal of cell science* **122**, 2331-2336 (2009).
11. Kroemer, G. & Reed, J.C. Mitochondrial control of cell death. *Nature medicine* **6**, 513-519 (2000).
12. Green, D.R. & Kroemer, G. The pathophysiology of mitochondrial cell death. *Science (New York, N.Y)* **305**, 626-629 (2004).

13. Liu, X., Kim, C.N., Yang, J., Jemmerson, R. & Wang, X. Induction of apoptotic program in cell-free extracts: requirement for dATP and cytochrome c. *Cell* **86**, 147-157 (1996).
14. Li, K. *et al.* Cytochrome c deficiency causes embryonic lethality and attenuates stress-induced apoptosis. *Cell* **101**, 389-399 (2000).
15. Li, P. *et al.* Cytochrome c and dATP-dependent formation of Apaf-1/caspase-9 complex initiates an apoptotic protease cascade. *Cell* **91**, 479-489 (1997).
16. Bernardi, P., Scorrano, L., Colonna, R., Petronilli, V. & Di Lisa, F. Mitochondria and cell death. Mechanistic aspects and methodological issues. *European journal of biochemistry / FEBS* **264**, 687-701 (1999).
17. Kokoszka, J.E. *et al.* The ADP/ATP translocator is not essential for the mitochondrial permeability transition pore. *Nature* **427**, 461-465 (2004).
18. Galluzzi, L. & Kroemer, G. Mitochondrial apoptosis without VDAC. *Nature cell biology* **9**, 487-489 (2007).
19. Nakagawa, T. *et al.* Cyclophilin D-dependent mitochondrial permeability transition regulates some necrotic but not apoptotic cell death. *Nature* **434**, 652-658 (2005).
20. Wei, M.C. *et al.* Proapoptotic BAX and BAK: a requisite gateway to mitochondrial dysfunction and death. *Science (New York, N.Y)* **292**, 727-730 (2001).
21. Danial, N.N. & Korsmeyer, S.J. Cell death: critical control points. *Cell* **116**, 205-219 (2004).
22. Scorrano, L. *et al.* A distinct pathway remodels mitochondrial cristae and mobilizes cytochrome c during apoptosis. *Developmental cell* **2**, 55-67 (2002).
23. Janeway, C.A., Jr. Approaching the asymptote? Evolution and revolution in immunology. *Cold Spring Harbor symposia on quantitative biology* **54 Pt 1**, 1-13 (1989).
24. Medzhitov, R., Preston-Hurlburt, P. & Janeway, C.A., Jr. A human homologue of the *Drosophila* Toll protein signals activation of adaptive immunity. *Nature* **388**, 394-397 (1997).

25. Medzhitov, R. & Janeway, C.A., Jr. Innate immunity: the virtues of a nonclonal system of recognition. *Cell* **91**, 295-298 (1997).
26. Akira, S., Uematsu, S. & Takeuchi, O. Pathogen recognition and innate immunity. *Cell* **124**, 783-801 (2006).
27. Lopez, C.B. *et al.* TLR-independent induction of dendritic cell maturation and adaptive immunity by negative-strand RNA viruses. *J Immunol* **173**, 6882-6889 (2004).
28. Edelmann, K.H. *et al.* Does Toll-like receptor 3 play a biological role in virus infections? *Virology* **322**, 231-238 (2004).
29. Sparwasser, T. *et al.* Bacterial DNA causes septic shock. *Nature* **386**, 336-337 (1997).
30. Stockinger, S. *et al.* IFN regulatory factor 3-dependent induction of type I IFNs by intracellular bacteria is mediated by a TLR- and Nod2-independent mechanism. *J Immunol* **173**, 7416-7425 (2004).
31. Cortez-Gonzalez, X. *et al.* TLR9-independent activation of B lymphocytes by bacterial DNA. *DNA and cell biology* **25**, 253-261 (2006).
32. Hochrein, H. *et al.* Herpes simplex virus type-1 induces IFN-alpha production via Toll-like receptor 9-dependent and -independent pathways. *Proceedings of the National Academy of Sciences of the United States of America* **101**, 11416-11421 (2004).
33. Yoneyama, M. *et al.* The RNA helicase RIG-I has an essential function in double-stranded RNA-induced innate antiviral responses. *Nature immunology* **5**, 730-737 (2004).
34. Seth, R.B., Sun, L., Ea, C.K. & Chen, Z.J. Identification and characterization of MAVS, a mitochondrial antiviral signaling protein that activates NF-kappaB and IRF 3. *Cell* **122**, 669-682 (2005).
35. Kawai, T. *et al.* IPS-1, an adaptor triggering RIG-I- and Mda5-mediated type I interferon induction. *Nature immunology* **6**, 981-988 (2005).
36. Xu, L.G. *et al.* VISA is an adapter protein required for virus-triggered IFN-beta signaling. *Molecular cell* **19**, 727-740 (2005).

37. Meylan, E. *et al.* Cardif is an adaptor protein in the RIG-I antiviral pathway and is targeted by hepatitis C virus. *Nature* **437**, 1167-1172 (2005).
38. Takahashi, K. *et al.* Nonself RNA-sensing mechanism of RIG-I helicase and activation of antiviral immune responses. *Molecular cell* **29**, 428-440 (2008).
39. Cui, S. *et al.* The C-terminal regulatory domain is the RNA 5'-triphosphate sensor of RIG-I. *Molecular cell* **29**, 169-179 (2008).
40. Kato, H. *et al.* Differential roles of MDA5 and RIG-I helicases in the recognition of RNA viruses. *Nature* **441**, 101-105 (2006).
41. Myong, S. *et al.* Cytosolic viral sensor RIG-I is a 5'-triphosphate-dependent translocase on double-stranded RNA. *Science (New York, N.Y)* **323**, 1070-1074 (2009).
42. Nallagatla, S.R. *et al.* 5'-triphosphate-dependent activation of PKR by RNAs with short stem-loops. *Science* **318**, 1455-1458 (2007).
43. Hornung, V. *et al.* 5'-Triphosphate RNA is the ligand for RIG-I. *Science* **314**, 994-997 (2006).
44. Schlee, M. *et al.* Recognition of 5' triphosphate by RIG-I helicase requires short blunt double-stranded RNA as contained in panhandle of negative-strand virus. *Immunity* **31**, 25-34 (2009).
45. Schmidt, A. *et al.* 5'-triphosphate RNA requires base-paired structures to activate antiviral signaling via RIG-I. *Proceedings of the National Academy of Sciences of the United States of America* **106**, 12067-12072 (2009).
46. Kato, H. *et al.* Length-dependent recognition of double-stranded ribonucleic acids by retinoic acid-inducible gene-I and melanoma differentiation-associated gene 5. *The Journal of experimental medicine* **205**, 1601-1610 (2008).
47. Malathi, K., Dong, B., Gale, M., Jr. & Silverman, R.H. Small self-RNA generated by RNase L amplifies antiviral innate immunity. *Nature* **448**, 816-819 (2007).
48. Rehwinkel, J. *et al.* RIG-I detects viral genomic RNA during negative-strand RNA virus infection. *Cell* **140**, 397-408 (2010).
49. Pichlmair, A. *et al.* Activation of MDA5 requires higher-order RNA structures generated during virus infection. *Journal of virology* **83**, 10761-10769 (2009).

50. Takeuchi, O. & Akira, S. Pattern recognition receptors and inflammation. *Cell* **140**, 805-820 (2010).
51. Loo, Y.M. *et al.* Distinct RIG-I and MDA5 signaling by RNA viruses in innate immunity. *Journal of virology* **82**, 335-345 (2008).
52. Fredericksen, B.L., Keller, B.C., Fornek, J., Katze, M.G. & Gale, M., Jr. Establishment and maintenance of the innate antiviral response to West Nile Virus involves both RIG-I and MDA5 signaling through IPS-1. *Journal of virology* **82**, 609-616 (2008).
53. Chiu, Y.H., Macmillan, J.B. & Chen, Z.J. RNA polymerase III detects cytosolic DNA and induces type I interferons through the RIG-I pathway. *Cell* **138**, 576-591 (2009).
54. Ablasser, A. *et al.* RIG-I-dependent sensing of poly(dA:dT) through the induction of an RNA polymerase III-transcribed RNA intermediate. *Nat Immunol* **10**, 1065-1072 (2009).
55. Takaoka, A. *et al.* DAI (DLM-1/ZBP1) is a cytosolic DNA sensor and an activator of innate immune response. *Nature* **448**, 501-505 (2007).
56. Wang, Z. *et al.* Regulation of innate immune responses by DAI (DLM-1/ZBP1) and other DNA-sensing molecules. *Proceedings of the National Academy of Sciences of the United States of America* **105**, 5477-5482 (2008).
57. Kaiser, W.J., Upton, J.W. & Mocarski, E.S. Receptor-interacting protein homotypic interaction motif-dependent control of NF-kappa B activation via the DNA-dependent activator of IFN regulatory factors. *J Immunol* **181**, 6427-6434 (2008).
58. Rebsamen, M. *et al.* DAI/ZBP1 recruits RIP1 and RIP3 through RIP homotypic interaction motifs to activate NF-kappaB. *EMBO reports* **10**, 916-922 (2009).
59. Ishii, K.J. *et al.* TANK-binding kinase-1 delineates innate and adaptive immune responses to DNA vaccines. *Nature* **451**, 725-729 (2008).
60. Yanai, H. *et al.* HMGB proteins function as universal sentinels for nucleic-acid-mediated innate immune responses. *Nature* **462**, 99-103 (2009).
61. Unterholzner, L. *et al.* IFI16 is an innate immune sensor for intracellular DNA. *Nature immunology* **11**, 997-1004 (2010).

62. Burckstummer, T. *et al.* An orthogonal proteomic-genomic screen identifies AIM2 as a cytoplasmic DNA sensor for the inflammasome. *Nature immunology* **10**, 266-272 (2009).
63. Fernandes-Alnemri, T., Yu, J.W., Datta, P., Wu, J. & Alnemri, E.S. AIM2 activates the inflammasome and cell death in response to cytoplasmic DNA. *Nature* **458**, 509-513 (2009).
64. Hornung, V. *et al.* AIM2 recognizes cytosolic dsDNA and forms a caspase-1-activating inflammasome with ASC. *Nature* **458**, 514-518 (2009).
65. Roberts, T.L. *et al.* HIN-200 proteins regulate caspase activation in response to foreign cytoplasmic DNA. *Science (New York, N.Y)* **323**, 1057-1060 (2009).
66. Kim, T. *et al.* Aspartate-glutamate-alanine-histidine box motif (DEAH)/RNA helicase A helicases sense microbial DNA in human plasmacytoid dendritic cells. *Proceedings of the National Academy of Sciences of the United States of America* **107**, 15181-15186 (2010).
67. Ting, J.P., Duncan, J.A. & Lei, Y. How the noninflammasome NLRs function in the innate immune system. *Science (New York, N.Y)* **327**, 286-290 (2010).
68. Yang, P. *et al.* The cytosolic nucleic acid sensor LRRFIP1 mediates the production of type I interferon via a beta-catenin-dependent pathway. *Nature immunology* **11**, 487-494 (2010).
69. Ishikawa, H. & Barber, G.N. STING is an endoplasmic reticulum adaptor that facilitates innate immune signalling. *Nature* **455**, 674-678 (2008).
70. Zhong, B. *et al.* The adaptor protein MITA links virus-sensing receptors to IRF3 transcription factor activation. *Immunity* **29**, 538-550 (2008).
71. Sun, W. *et al.* ERIS, an endoplasmic reticulum IFN stimulator, activates innate immune signaling through dimerization. *Proceedings of the National Academy of Sciences of the United States of America* **106**, 8653-8658 (2009).
72. Ishikawa, H., Ma, Z. & Barber, G.N. STING regulates intracellular DNA-mediated, type I interferon-dependent innate immunity. *Nature* **461**, 788-792 (2009).
73. Dixit, E. *et al.* Peroxisomes are signaling platforms for antiviral innate immunity. *Cell* **141**, 668-681 (2010).

74. Onoguchi, K. *et al.* Virus-infection or 5'ppp-RNA activates antiviral signal through redistribution of IPS-1 mediated by MFN1. *PLoS pathogens* **6**, e1001012 (2010).
75. Zhong, B. *et al.* The ubiquitin ligase RNF5 regulates antiviral responses by mediating degradation of the adaptor protein MITA. *Immunity* **30**, 397-407 (2009).
76. DeYoung, B.J. & Innes, R.W. Plant NBS-LRR proteins in pathogen sensing and host defense. *Nat Immunol* **7**, 1243-1249 (2006).
77. Ting, J.P., Willingham, S.B. & Bergstralh, D.T. NLRs at the intersection of cell death and immunity. *Nat Rev Immunol* **8**, 372-379 (2008).
78. Davis, B.K., Wen, H. & Ting, J.P. The Inflammasome NLRs in Immunity, Inflammation, and Associated Diseases. *Annual review of immunology* (2011).
79. Jha, S. & Ting, J.P. Inflammasome-associated nucleotide-binding domain, leucine-rich repeat proteins and inflammatory diseases. *J Immunol* **183**, 7623-7629 (2009).
80. Pedra, J.H., Cassel, S.L. & Sutterwala, F.S. Sensing pathogens and danger signals by the inflammasome. *Current opinion in immunology* **21**, 10-16 (2009).
81. Bao, Q. & Shi, Y. Apoptosome: a platform for the activation of initiator caspases. *Cell death and differentiation* **14**, 56-65 (2007).
82. Martinon, F., Burns, K. & Tschopp, J. The inflammasome: a molecular platform triggering activation of inflammatory caspases and processing of proIL-beta. *Molecular cell* **10**, 417-426 (2002).
83. Faustin, B. *et al.* Reconstituted NALP1 inflammasome reveals two-step mechanism of caspase-1 activation. *Molecular cell* **25**, 713-724 (2007).
84. Boyden, E.D. & Dietrich, W.F. Nalp1b controls mouse macrophage susceptibility to anthrax lethal toxin. *Nature genetics* **38**, 240-244 (2006).
85. Wu, W. *et al.* Resistance of human alveolar macrophages to Bacillus anthracis lethal toxin. *J Immunol* **183**, 5799-5806 (2009).
86. Mariathasan, S. *et al.* Cryopyrin activates the inflammasome in response to toxins and ATP. *Nature* **440**, 228-232 (2006).

87. Sutterwala, F.S. *et al.* Critical role for NALP3/CIAS1/Cryopyrin in innate and adaptive immunity through its regulation of caspase-1. *Immunity* **24**, 317-327 (2006).
88. Marina-Garcia, N. *et al.* Pannexin-1-mediated intracellular delivery of muramyl dipeptide induces caspase-1 activation via cryopyrin/NLRP3 independently of Nod2. *J Immunol* **180**, 4050-4057 (2008).
89. Yamasaki, K. *et al.* NLRP3/cryopyrin is necessary for interleukin-1beta (IL-1beta) release in response to hyaluronan, an endogenous trigger of inflammation in response to injury. *The Journal of biological chemistry* **284**, 12762-12771 (2009).
90. Gurcel, L., Abrami, L., Girardin, S., Tschopp, J. & van der Goot, F.G. Caspase-1 activation of lipid metabolic pathways in response to bacterial pore-forming toxins promotes cell survival. *Cell* **126**, 1135-1145 (2006).
91. Craven, R.R. *et al.* Staphylococcus aureus alpha-hemolysin activates the NLRP3-inflammasome in human and mouse monocytic cells. *PloS one* **4**, e7446 (2009).
92. Halle, A. *et al.* The NALP3 inflammasome is involved in the innate immune response to amyloid-beta. *Nature immunology* **9**, 857-865 (2008).
93. Martinon, F., Petrilli, V., Mayor, A., Tardivel, A. & Tschopp, J. Gout-associated uric acid crystals activate the NALP3 inflammasome. *Nature* **440**, 237-241 (2006).
94. Dostert, C. *et al.* Innate immune activation through Nalp3 inflammasome sensing of asbestos and silica. *Science (New York, N.Y)* **320**, 674-677 (2008).
95. Hornung, V. *et al.* Silica crystals and aluminum salts activate the NALP3 inflammasome through phagosomal destabilization. *Nature immunology* **9**, 847-856 (2008).
96. Eisenbarth, S.C., Colegio, O.R., O'Connor, W., Sutterwala, F.S. & Flavell, R.A. Crucial role for the Nalp3 inflammasome in the immunostimulatory properties of aluminium adjuvants. *Nature* **453**, 1122-1126 (2008).
97. Kool, M. *et al.* Cutting edge: alum adjuvant stimulates inflammatory dendritic cells through activation of the NALP3 inflammasome. *J Immunol* **181**, 3755-3759 (2008).

98. Li, H., Willingham, S.B., Ting, J.P. & Re, F. Cutting edge: inflammasome activation by alum and alum's adjuvant effect are mediated by NLRP3. *J Immunol* **181**, 17-21 (2008).
99. Chu, J. *et al.* Cholesterol-dependent cytolysins induce rapid release of mature IL-1beta from murine macrophages in a NLRP3 inflammasome and cathepsin B-dependent manner. *Journal of leukocyte biology* **86**, 1227-1238 (2009).
100. Duewell, P. *et al.* NLRP3 inflammasomes are required for atherogenesis and activated by cholesterol crystals. *Nature* **464**, 1357-1361 (2010).
101. Rajamaki, K. *et al.* Cholesterol crystals activate the NLRP3 inflammasome in human macrophages: a novel link between cholesterol metabolism and inflammation. *PloS one* **5**, e11765 (2010).
102. Pelegrin, P. & Surprenant, A. Pannexin-1 couples to maitotoxin- and nigericin-induced interleukin-1beta release through a dye uptake-independent pathway. *The Journal of biological chemistry* **282**, 2386-2394 (2007).
103. Pelegrin, P. & Surprenant, A. Pannexin-1 mediates large pore formation and interleukin-1beta release by the ATP-gated P2X7 receptor. *The EMBO journal* **25**, 5071-5082 (2006).
104. Tschopp, J. & Schroder, K. NLRP3 inflammasome activation: The convergence of multiple signalling pathways on ROS production? *Nature reviews* **10**, 210-215 (2010).
105. Martinon, F. Signaling by ROS drives inflammasome activation. *European journal of immunology* **40**, 616-619 (2010).
106. Bolwell, G.P. Role of active oxygen species and NO in plant defence responses. *Current opinion in plant biology* **2**, 287-294 (1999).
107. Zhou, R., Tardivel, A., Thorens, B., Choi, I. & Tschopp, J. Thioredoxin-interacting protein links oxidative stress to inflammasome activation. *Nature immunology* **11**, 136-140 (2010).
108. Zhou, R., Yazdi, A.S., Menu, P. & Tschopp, J. A role for mitochondria in NLRP3 inflammasome activation. *Nature* **469**, 221-225 (2011).
109. Franchi, L. *et al.* Cytosolic flagellin requires Ipaf for activation of caspase-1 and interleukin 1beta in salmonella-infected macrophages. *Nature immunology* **7**,

- 576-582 (2006).
110. Mariathasan, S. *et al.* Differential activation of the inflammasome by caspase-1 adaptors ASC and Ipaf. *Nature* **430**, 213-218 (2004).
  111. Miao, E.A. *et al.* Cytoplasmic flagellin activates caspase-1 and secretion of interleukin 1beta via Ipaf. *Nature immunology* **7**, 569-575 (2006).
  112. Suzuki, T. *et al.* Differential regulation of caspase-1 activation, pyroptosis, and autophagy via Ipaf and ASC in Shigella-infected macrophages. *PLoS pathogens* **3**, e111 (2007).
  113. Amer, A. *et al.* Regulation of Legionella phagosome maturation and infection through flagellin and host Ipaf. *The Journal of biological chemistry* **281**, 35217-35223 (2006).
  114. Sutterwala, F.S. *et al.* Immune recognition of Pseudomonas aeruginosa mediated by the IPAF/NLRC4 inflammasome. *The Journal of experimental medicine* **204**, 3235-3245 (2007).
  115. Molofsky, A.B. *et al.* Cytosolic recognition of flagellin by mouse macrophages restricts Legionella pneumophila infection. *The Journal of experimental medicine* **203**, 1093-1104 (2006).
  116. Ren, T., Zamboni, D.S., Roy, C.R., Dietrich, W.F. & Vance, R.E. Flagellin-deficient Legionella mutants evade caspase-1- and Naip5-mediated macrophage immunity. *PLoS pathogens* **2**, e18 (2006).
  117. Zamboni, D.S. *et al.* The BirA cytosolic pattern-recognition receptor contributes to the detection and control of Legionella pneumophila infection. *Nature immunology* **7**, 318-325 (2006).
  118. Miao, E.A., Ernst, R.K., Dors, M., Mao, D.P. & Aderem, A. Pseudomonas aeruginosa activates caspase 1 through Ipaf. *Proceedings of the National Academy of Sciences of the United States of America* **105**, 2562-2567 (2008).
  119. Franchi, L. *et al.* Critical role for Ipaf in Pseudomonas aeruginosa-induced caspase-1 activation. *European journal of immunology* **37**, 3030-3039 (2007).
  120. Kanneganti, T.D., Lamkanfi, M. & Nunez, G. Intracellular NOD-like receptors in host defense and disease. *Immunity* **27**, 549-559 (2007).

121. Philpott, D.J. & Girardin, S.E. Nod-like receptors: sentinels at host membranes. *Current opinion in immunology* **22**, 428-434 (2010).
122. Barnich, N., Aguirre, J.E., Reinecker, H.C., Xavier, R. & Podolsky, D.K. Membrane recruitment of NOD2 in intestinal epithelial cells is essential for nuclear factor- $\kappa$ B activation in muramyl dipeptide recognition. *The Journal of cell biology* **170**, 21-26 (2005).
123. Kufer, T.A., Kremmer, E., Adam, A.C., Philpott, D.J. & Sansonetti, P.J. The pattern-recognition molecule Nod1 is localized at the plasma membrane at sites of bacterial interaction. *Cellular microbiology* **10**, 477-486 (2008).
124. Moore, C.B. *et al.* NLRX1 is a regulator of mitochondrial antiviral immunity. *Nature* **451**, 573-577 (2008).
125. Yasukawa, K. *et al.* Mitofusin 2 inhibits mitochondrial antiviral signaling. *Science signaling* **2**, ra47 (2009).
126. Arnoult, D. *et al.* An N-terminal addressing sequence targets NLRX1 to the mitochondrial matrix. *Journal of cell science* **122**, 3161-3168 (2009).
127. Abdul-Sater, A.A. *et al.* Enhancement of reactive oxygen species production and chlamydial infection by the mitochondrial Nod-like family member, NLRX1. *The Journal of biological chemistry* (2010).
128. Tattoli, I. *et al.* NLRX1 is a mitochondrial NOD-like receptor that amplifies NF- $\kappa$ B and JNK pathways by inducing reactive oxygen species production. *EMBO reports* **9**, 293-300 (2008).
129. Sabbah, A. *et al.* Activation of innate immune antiviral responses by Nod2. *Nature immunology* **10**, 1073-1080 (2009).
130. Allen, I.C. *et al.* The NLRP3 inflammasome mediates in vivo innate immunity to influenza A virus through recognition of viral RNA. *Immunity* **30**, 556-565 (2009).
131. Ichinohe, T., Lee, H.K., Ogura, Y., Flavell, R. & Iwasaki, A. Inflammasome recognition of influenza virus is essential for adaptive immune responses. *The Journal of experimental medicine* **206**, 79-87 (2009).
132. Benko, S., Magalhaes, J.G., Philpott, D.J. & Girardin, S.E. NLRC5 limits the activation of inflammatory pathways. *J Immunol* **185**, 1681-1691 (2010).

133. Cui, J. *et al.* NLRC5 negatively regulates the NF-kappaB and type I interferon signaling pathways. *Cell* **141**, 483-496 (2010).
134. Kuenzel, S. *et al.* The nucleotide-binding oligomerization domain-like receptor NLRC5 is involved in IFN-dependent antiviral immune responses. *J Immunol* **184**, 1990-2000 (2010).
135. Meissner, T.B. *et al.* NLR family member NLRC5 is a transcriptional regulator of MHC class I genes. *Proceedings of the National Academy of Sciences of the United States of America* **107**, 13794-13799 (2010).
136. Neerinx, A. *et al.* A role for the human nucleotide-binding domain, leucine-rich repeat-containing family member NLRC5 in antiviral responses. *The Journal of biological chemistry* **285**, 26223-26232 (2010).
137. Kuenzel, S. *et al.* The nucleotide-binding oligomerization domain-like receptor NLRC5 is involved in IFN-dependent antiviral immune responses. *J Immunol* **184**, 1990-2000 (2009).
138. Davis, B.K. *et al.* Cutting Edge: NLRC5-Dependent Activation of the Inflammasome. *J Immunol* (2011).
139. Kumar, H. *et al.* NLRC5 deficiency does not influence cytokine induction by virus and bacteria infections. *J Immunol* **186**, 994-1000 (2011).
140. Poeck, H. *et al.* Recognition of RNA virus by RIG-I results in activation of CARD9 and inflammasome signaling for interleukin 1 beta production. *Nature immunology* **11**, 63-69 (2009).
141. Jounai, N. *et al.* The Atg5 Atg12 conjugate associates with innate antiviral immune responses. *Proceedings of the National Academy of Sciences of the United States of America* **104**, 14050-14055 (2007).
142. Tal, M.C. *et al.* Absence of autophagy results in reactive oxygen species-dependent amplification of RLR signaling. *Proceedings of the National Academy of Sciences of the United States of America* **106**, 2770-2775 (2009).
143. Xu, L., Xiao, N., Liu, F., Ren, H. & Gu, J. Inhibition of RIG-I and MDA5-dependent antiviral response by gC1qR at mitochondria. *Proc Natl Acad Sci U S A* **106**, 1530-1535 (2009).
144. Jia, Y. *et al.* Negative regulation of MAVS-mediated innate immune response by

- PSMA7. *J Immunol* **183**, 4241-4248 (2009).
145. Komuro, A. & Horvath, C.M. RNA- and virus-independent inhibition of antiviral signaling by RNA helicase LGP2. *Journal of virology* **80**, 12332-12342 (2006).
  146. Lin, R. *et al.* Negative regulation of the retinoic acid-inducible gene I-induced antiviral state by the ubiquitin-editing protein A20. *The Journal of biological chemistry* **281**, 2095-2103 (2006).
  147. Friedman, C.S. *et al.* The tumour suppressor CYLD is a negative regulator of RIG-I-mediated antiviral response. *EMBO reports* **9**, 930-936 (2008).
  148. You, F. *et al.* PCBP2 mediates degradation of the adaptor MAVS via the HECT ubiquitin ligase AIP4. *Nature immunology* **10**, 1300-1308 (2009).
  149. Nakhaei, P. *et al.* The E3 ubiquitin ligase Triad3A negatively regulates the RIG-I/MAVS signaling pathway by targeting TRAF3 for degradation. *PLoS pathogens* **5**, e1000650 (2009).
  150. Rothenfusser, S. *et al.* The RNA helicase Lgp2 inhibits TLR-independent sensing of viral replication by retinoic acid-inducible gene-I. *J Immunol* **175**, 5260-5268 (2005).
  151. Satoh, T. *et al.* LGP2 is a positive regulator of RIG-I- and MDA5-mediated antiviral responses. *Proceedings of the National Academy of Sciences of the United States of America* **107**, 1512-1517 (2010).
  152. Lad, S.P. *et al.* Identification of MAVS splicing variants that interfere with RIGI/MAVS pathway signaling. *Molecular immunology* **45**, 2277-2287 (2008).
  153. Shintani, T. & Klionsky, D.J. Autophagy in health and disease: a double-edged sword. *Science (New York, N.Y)* **306**, 990-995 (2004).
  154. Levine, B. & Kroemer, G. Autophagy in the pathogenesis of disease. *Cell* **132**, 27-42 (2008).
  155. Kanazawa, T. *et al.* Amino acids and insulin control autophagic proteolysis through different signaling pathways in relation to mTOR in isolated rat hepatocytes. *The Journal of biological chemistry* **279**, 8452-8459 (2004).
  156. Ravikumar, B. *et al.* Inhibition of mTOR induces autophagy and reduces toxicity of polyglutamine expansions in fly and mouse models of Huntington disease.

- Nature genetics* **36**, 585-595 (2004).
157. Sugawara, K. *et al.* The crystal structure of microtubule-associated protein light chain 3, a mammalian homologue of *Saccharomyces cerevisiae* Atg8. *Genes Cells* **9**, 611-618 (2004).
  158. Suzuki, N.N., Yoshimoto, K., Fujioka, Y., Ohsumi, Y. & Inagaki, F. The crystal structure of plant ATG12 and its biological implication in autophagy. *Autophagy* **1**, 119-126 (2005).
  159. Geng, J. & Klionsky, D.J. The Atg8 and Atg12 ubiquitin-like conjugation systems in macroautophagy. 'Protein modifications: beyond the usual suspects' review series. *EMBO reports* **9**, 859-864 (2008).
  160. Klionsky, D.J. *et al.* Guidelines for the use and interpretation of assays for monitoring autophagy in higher eukaryotes. *Autophagy* **4**, 151-175 (2008).
  161. Lee, H.K., Lund, J.M., Ramanathan, B., Mizushima, N. & Iwasaki, A. Autophagy-dependent viral recognition by plasmacytoid dendritic cells. *Science (New York, N.Y)* **315**, 1398-1401 (2007).
  162. Yousefi, S. *et al.* Calpain-mediated cleavage of Atg5 switches autophagy to apoptosis. *Nature cell biology* **8**, 1124-1132 (2006).
  163. Reggiori, F., Shintani, T., Nair, U. & Klionsky, D.J. Atg9 cycles between mitochondria and the pre-autophagosomal structure in yeasts. *Autophagy* **1**, 101-109 (2005).
  164. Takahashi, Y. *et al.* Bif-1 interacts with Beclin 1 through UVRAG and regulates autophagy and tumorigenesis. *Nature cell biology* **9**, 1142-1151 (2007).
  165. Lee, I.H. *et al.* A role for the NAD-dependent deacetylase Sirt1 in the regulation of autophagy. *Proceedings of the National Academy of Sciences of the United States of America* **105**, 3374-3379 (2008).
  166. Skaug, B., Jiang, X. & Chen, Z.J. The role of ubiquitin in NF-kappaB regulatory pathways. *Annual review of biochemistry* **78**, 769-796 (2009).
  167. Isaacson, M.K. & Ploegh, H.L. Ubiquitination, ubiquitin-like modifiers, and deubiquitination in viral infection. *Cell host & microbe* **5**, 559-570 (2009).
  168. Gack, M.U. *et al.* TRIM25 RING-finger E3 ubiquitin ligase is essential for

- RIG-I-mediated antiviral activity. *Nature* **446**, 916-920 (2007).
169. Gack, M.U., Nistal-Villan, E., Inn, K.S., Garcia-Sastre, A. & Jung, J.U. Phosphorylation-mediated negative regulation of RIG-I antiviral activity. *Journal of virology* **84**, 3220-3229 (2010).
  170. Kayagaki, N. *et al.* DUBA: a deubiquitinase that regulates type I interferon production. *Science (New York, N.Y)* **318**, 1628-1632 (2007).
  171. Arimoto, K. *et al.* Polyubiquitin conjugation to NEMO by tripartite motif protein 23 (TRIM23) is critical in antiviral defense. *Proceedings of the National Academy of Sciences of the United States of America* **107**, 15856-15861 (2010).
  172. Zeng, W. *et al.* Reconstitution of the RIG-I pathway reveals a signaling role of unanchored polyubiquitin chains in innate immunity. *Cell* **141**, 315-330 (2010).
  173. Lei, Y. *et al.* MAVS-mediated apoptosis and its inhibition by viral proteins. *PLoS one* **4**, e5466 (2009).
  174. Besch, R. *et al.* Proapoptotic signaling induced by RIG-I and MDA-5 results in type I interferon-independent apoptosis in human melanoma cells. *J Clin Invest* **119**, 2399-2411 (2009).
  175. Sun, Q. *et al.* The specific and essential role of MAVS in antiviral innate immune responses. *Immunity* **24**, 633-642 (2006).
  176. Cuconati, A. & White, E. Viral homologs of BCL-2: role of apoptosis in the regulation of virus infection. *Genes & development* **16**, 2465-2478 (2002).
  177. Bouchier-Hayes, L. & Martin, S.J. CARD games in apoptosis and immunity. *EMBO reports* **3**, 616-621 (2002).
  178. Zou, H., Henzel, W.J., Liu, X., Lutschg, A. & Wang, X. Apaf-1, a human protein homologous to *C. elegans* CED-4, participates in cytochrome c-dependent activation of caspase-3. *Cell* **90**, 405-413 (1997).
  179. Ting, J.P. *et al.* The NLR gene family: a standard nomenclature. *Immunity* **28**, 285-287 (2008).
  180. Inohara, N. *et al.* Nod1, an Apaf-1-like activator of caspase-9 and nuclear factor-kappaB. *The Journal of biological chemistry* **274**, 14560-14567 (1999).

181. Ogura, Y. *et al.* Nod2, a Nod1/Apaf-1 family member that is restricted to monocytes and activates NF-kappaB. *The Journal of biological chemistry* **276**, 4812-4818 (2001).
182. Sadasivam, S. *et al.* Caspase-1 activator Ipaf is a p53-inducible gene involved in apoptosis. *Oncogene* **24**, 627-636 (2005).
183. Poyet, J.L. *et al.* Identification of Ipaf, a human caspase-1-activating protein related to Apaf-1. *The Journal of biological chemistry* **276**, 28309-28313 (2001).
184. Potter, J.A., Randall, R.E. & Taylor, G.L. Crystal structure of human IPS-1/MAVS/VISA/Cardif caspase activation recruitment domain. *BMC structural biology* **8**, 11 (2008).
185. Li, X.D., Sun, L., Seth, R.B., Pineda, G. & Chen, Z.J. Hepatitis C virus protease NS3/4A cleaves mitochondrial antiviral signaling protein off the mitochondria to evade innate immunity. *Proceedings of the National Academy of Sciences of the United States of America* **102**, 17717-17722 (2005).
186. Yang, Y. *et al.* Disruption of innate immunity due to mitochondrial targeting of a picornaviral protease precursor. *Proceedings of the National Academy of Sciences of the United States of America* **104**, 7253-7258 (2007).
187. Griffin, D.E. & Hardwick, J.M. Regulators of apoptosis on the road to persistent alphavirus infection. *Annual review of microbiology* **51**, 565-592 (1997).
188. Chen, C.Y. *et al.* Open reading frame 8a of the human severe acute respiratory syndrome coronavirus not only promotes viral replication but also induces apoptosis. *The Journal of infectious diseases* **196**, 405-415 (2007).
189. Tan, Y.X. *et al.* Induction of apoptosis by the severe acute respiratory syndrome coronavirus 7a protein is dependent on its interaction with the Bcl-XL protein. *Journal of virology* **81**, 6346-6355 (2007).
190. Fouchier, R.A. *et al.* Aetiology: Koch's postulates fulfilled for SARS virus. *Nature* **423**, 240 (2003).
191. Drosten, C. *et al.* Identification of a novel coronavirus in patients with severe acute respiratory syndrome. *The New England journal of medicine* **348**, 1967-1976 (2003).
192. Ksiazek, T.G. *et al.* A novel coronavirus associated with severe acute respiratory

- syndrome. *The New England journal of medicine* **348**, 1953-1966 (2003).
193. Chan-Yeung, M. & Xu, R.H. SARS: epidemiology. *Respirology (Carlton, Vic)* **8 Suppl**, S9-14 (2003).
  194. Rota, P.A. *et al.* Characterization of a novel coronavirus associated with severe acute respiratory syndrome. *Science (New York, N.Y)* **300**, 1394-1399 (2003).
  195. Marra, M.A. *et al.* The Genome sequence of the SARS-associated coronavirus. *Science (New York, N.Y)* **300**, 1399-1404 (2003).
  196. Peiris, J.S. *et al.* Clinical progression and viral load in a community outbreak of coronavirus-associated SARS pneumonia: a prospective study. *Lancet* **361**, 1767-1772 (2003).
  197. Frieman, M., Heise, M. & Baric, R. SARS coronavirus and innate immunity. *Virus research* **133**, 101-112 (2008).
  198. Schaecher, S.R., Touchette, E., Schriewer, J., Buller, R.M. & Pekosz, A. Severe acute respiratory syndrome coronavirus gene 7 products contribute to virus-induced apoptosis. *Journal of virology* **81**, 11054-11068 (2007).
  199. Ye, Z., Wong, C.K., Li, P. & Xie, Y. A SARS-CoV protein, ORF-6, induces caspase-3 mediated, ER stress and JNK-dependent apoptosis. *Biochimica et biophysica acta* (2008).
  200. Lau, Y.L. & Peiris, J.S. Pathogenesis of severe acute respiratory syndrome. *Current opinion in immunology* **17**, 404-410 (2005).
  201. Nicholls, J.M. *et al.* Time course and cellular localization of SARS-CoV nucleoprotein and RNA in lungs from fatal cases of SARS. *PLoS medicine* **3**, e27 (2006).
  202. Adrain, C. & Martin, S.J. The mitochondrial apoptosome: a killer unleashed by the cytochrome seas. *Trends in biochemical sciences* **26**, 390-397 (2001).
  203. Lamkanfi, M., Festjens, N., Declercq, W., Vanden Berghe, T. & Vandennebeele, P. Caspases in cell survival, proliferation and differentiation. *Cell death and differentiation* **14**, 44-55 (2007).
  204. Hacker, G. The morphology of apoptosis. *Cell and tissue research* **301**, 5-17 (2000).

205. Heylbroeck, C. *et al.* The IRF-3 transcription factor mediates Sendai virus-induced apoptosis. *Journal of virology* **74**, 3781-3792 (2000).
206. Zamzami, N. *et al.* Sequential reduction of mitochondrial transmembrane potential and generation of reactive oxygen species in early programmed cell death. *The Journal of experimental medicine* **182**, 367-377 (1995).
207. Zamzami, N. *et al.* Reduction in mitochondrial potential constitutes an early irreversible step of programmed lymphocyte death in vivo. *The Journal of experimental medicine* **181**, 1661-1672 (1995).
208. Chawla-Sarkar, M. *et al.* Apoptosis and interferons: role of interferon-stimulated genes as mediators of apoptosis. *Apoptosis* **8**, 237-249 (2003).
209. Yoneyama, M. *et al.* Shared and unique functions of the DExD/H-box helicases RIG-I, MDA5, and LGP2 in antiviral innate immunity. *J Immunol* **175**, 2851-2858 (2005).
210. Silverman, N. & Maniatis, T. NF-kappaB signaling pathways in mammalian and insect innate immunity. *Genes & development* **15**, 2321-2342 (2001).
211. Miagkov, A.V. *et al.* NF-kappaB activation provides the potential link between inflammation and hyperplasia in the arthritic joint. *Proceedings of the National Academy of Sciences of the United States of America* **95**, 13859-13864 (1998).
212. Holm, G.H. *et al.* Retinoic acid-inducible gene-I and interferon-beta promoter stimulator-1 augment proapoptotic responses following mammalian reovirus infection via interferon regulatory factor-3. *The Journal of biological chemistry* **282**, 21953-21961 (2007).
213. Peters, K., Chattopadhyay, S. & Sen, G.C. IRF-3 activation by Sendai virus infection is required for cellular apoptosis and avoidance of persistence. *Journal of virology* **82**, 3500-3508 (2008).
214. Ivanov, K.A. *et al.* Major genetic marker of nidoviruses encodes a replicative endoribonuclease. *Proceedings of the National Academy of Sciences of the United States of America* **101**, 12694-12699 (2004).
215. Green, D.R. Apoptotic pathways: ten minutes to dead. *Cell* **121**, 671-674 (2005).
216. Reeves, M.B., Davies, A.A., McSharry, B.P., Wilkinson, G.W. & Sinclair, J.H. Complex I binding by a virally encoded RNA regulates mitochondria-induced cell

- death. *Science (New York, N.Y)* **316**, 1345-1348 (2007).
217. van Deventer, H.W. *et al.* C-C chemokine receptor 5 on pulmonary fibrocytes facilitates migration and promotes metastasis via matrix metalloproteinase 9. *The American journal of pathology* **173**, 253-264 (2008).
218. Rehwinkel, J. & Reis e Sousa, C. RIGorous detection: exposing virus through RNA sensing. *Science (New York, N.Y)* **327**, 284-286 (2010).
219. Harton, J.A., Linhoff, M.W., Zhang, J. & Ting, J.P. Cutting edge: CATERPILLER: a large family of mammalian genes containing CARD, pyrin, nucleotide-binding, and leucine-rich repeat domains. *J Immunol* **169**, 4088-4093 (2002).
220. Schroder, K. & Tschopp, J. The inflammasomes. *Cell* **140**, 821-832 (2010).
221. Rajan, J.V., Rodriguez, D., Miao, E.A. & Aderem, A. The NLRP3 inflammasome detects EMCV and VSV infection. *Journal of virology* (2011).
222. Thomas, P.G. *et al.* The intracellular sensor NLRP3 mediates key innate and healing responses to influenza A virus via the regulation of caspase-1. *Immunity* **30**, 566-575 (2009).
223. Sanjuan, M.A. & Green, D.R. Eating for good health: linking autophagy and phagocytosis in host defense. *Autophagy* **4**, 607-611 (2008).
224. Virgin, H.W. & Levine, B. Autophagy genes in immunity. *Nature immunology* **10**, 461-470 (2009).
225. Chen, X., Smith, L.M. & Bradbury, E.M. Site-specific mass tagging with stable isotopes in proteins for accurate and efficient protein identification. *Analytical chemistry* **72**, 1134-1143 (2000).
226. Ong, S.E. *et al.* Stable isotope labeling by amino acids in cell culture, SILAC, as a simple and accurate approach to expression proteomics. *Mol Cell Proteomics* **1**, 376-386 (2002).
227. Ye, Z. & Ting, J.P. NLR, the nucleotide-binding domain leucine-rich repeat containing gene family. *Current opinion in immunology* **20**, 3-9 (2008).
228. Kunze, G. *et al.* The N terminus of bacterial elongation factor Tu elicits innate immunity in Arabidopsis plants. *The Plant cell* **16**, 3496-3507 (2004).

229. Zipfel, C. *et al.* Perception of the bacterial PAMP EF-Tu by the receptor EFR restricts *Agrobacterium*-mediated transformation. *Cell* **125**, 749-760 (2006).
230. Shelly, S., Lukinova, N., Bambina, S., Berman, A. & Cherry, S. Autophagy is an essential component of *Drosophila* immunity against vesicular stomatitis virus. *Immunity* **30**, 588-598 (2009).
231. Mizushima, N., Yoshimori, T. & Levine, B. Methods in mammalian autophagy research. *Cell* **140**, 313-326 (2010).
232. Kabeya, Y. *et al.* LC3, a mammalian homologue of yeast Apg8p, is localized in autophagosome membranes after processing. *The EMBO journal* **19**, 5720-5728 (2000).
233. Chan, D.C. Mitochondrial fusion and fission in mammals. *Annual review of cell and developmental biology* **22**, 79-99 (2006).
234. Wells, J., Henkler, F., Leversha, M. & Koshy, R. A mitochondrial elongation factor-like protein is over-expressed in tumours and differentially expressed in normal tissues. *FEBS letters* **358**, 119-125 (1995).
235. Valente, L. *et al.* Infantile encephalopathy and defective mitochondrial DNA translation in patients with mutations of mitochondrial elongation factors EFG1 and EFTu. *American journal of human genetics* **80**, 44-58 (2007).
236. Suzuki, H., Ueda, T., Taguchi, H. & Takeuchi, N. Chaperone properties of mammalian mitochondrial translation elongation factor Tu. *The Journal of biological chemistry* **282**, 4076-4084 (2007).
237. Zhou, R., Yazdi, A.S., Menu, P. & Tschopp, J. A role for mitochondria in NLRP3 inflammasome activation. *Nature* (2010).
238. Chen, Z. *et al.* GB virus B disrupts RIG-I signaling by NS3/4A-mediated cleavage of the adaptor protein MAVS. *Journal of virology* **81**, 964-976 (2007).
239. Mibayashi, M. *et al.* Inhibition of retinoic acid-inducible gene I-mediated induction of beta interferon by the NS1 protein of influenza A virus. *Journal of virology* **81**, 514-524 (2007).
240. Opitz, B. *et al.* IFNbeta induction by influenza A virus is mediated by RIG-I which is regulated by the viral NS1 protein. *Cellular microbiology* **9**, 930-938 (2007).

241. Guo, Z. *et al.* NS1 protein of influenza A virus inhibits the function of intracytoplasmic pathogen sensor, RIG-I. *American journal of respiratory cell and molecular biology* **36**, 263-269 (2007).
242. Graef, K.M. *et al.* The PB2 subunit of the influenza virus RNA polymerase affects virulence by interacting with the mitochondrial antiviral signaling protein and inhibiting expression of beta interferon. *Journal of virology* **84**, 8433-8445 (2010).
243. Iwai, A. *et al.* Influenza A virus polymerase inhibits type I interferon induction by binding to interferon beta promoter stimulator 1. *The Journal of biological chemistry* **285**, 32064-32074 (2010).
244. Ling, Z., Tran, K.C. & Teng, M.N. Human respiratory syncytial virus nonstructural protein NS2 antagonizes the activation of beta interferon transcription by interacting with RIG-I. *Journal of virology* **83**, 3734-3742 (2009).
245. Fan, L., Briese, T. & Lipkin, W.I. Z proteins of New World arenaviruses bind RIG-I and interfere with type I interferon induction. *Journal of virology* **84**, 1785-1791 (2010).
246. Zhou, S. *et al.* Induction and inhibition of type I interferon responses by distinct components of lymphocytic choriomeningitis virus. *Journal of virology* **84**, 9452-9462 (2010).
247. Andrejeva, J. *et al.* The V proteins of paramyxoviruses bind the IFN-inducible RNA helicase, mda-5, and inhibit its activation of the IFN-beta promoter. *Proceedings of the National Academy of Sciences of the United States of America* **101**, 17264-17269 (2004).
248. Childs, K.S., Andrejeva, J., Randall, R.E. & Goodbourn, S. Mechanism of mda-5 Inhibition by paramyxovirus V proteins. *Journal of virology* **83**, 1465-1473 (2009).
249. Wei, C. *et al.* The hepatitis B virus X protein disrupts innate immunity by downregulating mitochondrial antiviral signaling protein. *J Immunol* **185**, 1158-1168 (2010).
250. Drahos, J. & Racaniello, V.R. Cleavage of IPS-1 in cells infected with human rhinovirus. *Journal of virology* **83**, 11581-11587 (2009).
251. Li, H.M. *et al.* IPS-1 is crucial for DAP3-mediated anoikis induction by caspase-8

- activation. *Cell death and differentiation* **16**, 1615-1621 (2009).
252. Yu, C.Y., Chiang, R.L., Chang, T.H., Liao, C.L. & Lin, Y.L. The interferon stimulator mitochondrial antiviral signaling protein facilitates cell death by disrupting the mitochondrial membrane potential and by activating caspases. *Journal of virology* **84**, 2421-2431 (2010).
  253. Lamkanfi, M. & Dixit, V.M. Manipulation of host cell death pathways during microbial infections. *Cell host & microbe* **8**, 44-54 (2010).
  254. Straus, S.E., Sneller, M., Lenardo, M.J., Puck, J.M. & Strober, W. An inherited disorder of lymphocyte apoptosis: the autoimmune lymphoproliferative syndrome. *Annals of internal medicine* **130**, 591-601 (1999).
  255. Muzio, M. *et al.* FLICE, a novel FADD-homologous ICE/CED-3-like protease, is recruited to the CD95 (Fas/APO-1) death--inducing signaling complex. *Cell* **85**, 817-827 (1996).
  256. Youle, R.J. & Strasser, A. The BCL-2 protein family: opposing activities that mediate cell death. *Nat Rev Mol Cell Biol* **9**, 47-59 (2008).
  257. Chen, Y.B. *et al.* Alternate functions of viral regulators of cell death. *Cell death and differentiation* **13**, 1318-1324 (2006).
  258. Thome, M. *et al.* Viral FLICE-inhibitory proteins (FLIPs) prevent apoptosis induced by death receptors. *Nature* **386**, 517-521 (1997).
  259. Rahman, M.M. & McFadden, G. Modulation of tumor necrosis factor by microbial pathogens. *PLoS pathogens* **2**, e4 (2006).
  260. Hu, F.Q., Smith, C.A. & Pickup, D.J. Cowpox virus contains two copies of an early gene encoding a soluble secreted form of the type II TNF receptor. *Virology* **204**, 343-356 (1994).
  261. Loparev, V.N. *et al.* A third distinct tumor necrosis factor receptor of orthopoxviruses. *Proceedings of the National Academy of Sciences of the United States of America* **95**, 3786-3791 (1998).
  262. Saraiva, M. & Alcami, A. CrmE, a novel soluble tumor necrosis factor receptor encoded by poxviruses. *Journal of virology* **75**, 226-233 (2001).
  263. Smith, C.A. *et al.* Cowpox virus genome encodes a second soluble homologue of

- cellular TNF receptors, distinct from CrmB, that binds TNF but not LT alpha. *Virology* **223**, 132-147 (1996).
264. White, E., Cipriani, R., Sabbatini, P. & Denton, A. Adenovirus E1B 19-kilodalton protein overcomes the cytotoxicity of E1A proteins. *Journal of virology* **65**, 2968-2978 (1991).
265. Galluzzi, L., Brenner, C., Morselli, E., Touat, Z. & Kroemer, G. Viral control of mitochondrial apoptosis. *PLoS pathogens* **4**, e1000018 (2008).
266. Jacotot, E. *et al.* Control of mitochondrial membrane permeabilization by adenine nucleotide translocator interacting with HIV-1 viral protein rR and Bcl-2. *The Journal of experimental medicine* **193**, 509-519 (2001).
267. Mateyak, M.K. & Kinzy, T.G. eEF1A: thinking outside the ribosome. *The Journal of biological chemistry* **285**, 21209-21213 (2010).
268. Kim, H.K. *et al.* Mitochondrial alterations in human gastric carcinoma cell line. *American journal of physiology* **293**, C761-771 (2007).
269. Sertel, S. *et al.* Factors determining sensitivity or resistance of tumor cell lines towards artesunate. *Chemico-biological interactions* **185**, 42-52 (2010).
270. Rabinowitz, J.D. & White, E. Autophagy and metabolism. *Science (New York, N.Y)* **330**, 1344-1348 (2010).
271. Gonen, H., Dickman, D., Schwartz, A.L. & Ciechanover, A. Protein synthesis elongation factor EF-1 alpha is an isopeptidase essential for ubiquitin-dependent degradation of certain proteolytic substrates. *Advances in experimental medicine and biology* **389**, 209-219 (1996).
272. Gonen, H. *et al.* Protein synthesis elongation factor EF-1 alpha is essential for ubiquitin-dependent degradation of certain N alpha-acetylated proteins and may be substituted for by the bacterial elongation factor EF-Tu. *Proceedings of the National Academy of Sciences of the United States of America* **91**, 7648-7652 (1994).
273. Yang, F., Demma, M., Warren, V., Dharmawardhane, S. & Condeelis, J. Identification of an actin-binding protein from Dictyostelium as elongation factor 1a. *Nature* **347**, 494-496 (1990).
274. Demma, M., Warren, V., Hock, R., Dharmawardhane, S. & Condeelis, J. Isolation

- of an abundant 50,000-dalton actin filament bundling protein from Dictyostelium amoebae. *The Journal of biological chemistry* **265**, 2286-2291 (1990).
275. Gross, S.R. & Kinzy, T.G. Translation elongation factor 1A is essential for regulation of the actin cytoskeleton and cell morphology. *Nature structural & molecular biology* **12**, 772-778 (2005).
276. Blackwell, J.L. & Brinton, M.A. Translation elongation factor-1 alpha interacts with the 3' stem-loop region of West Nile virus genomic RNA. *Journal of virology* **71**, 6433-6444 (1997).
277. Davis, W.G., Blackwell, J.L., Shi, P.Y. & Brinton, M.A. Interaction between the cellular protein eEF1A and the 3'-terminal stem-loop of West Nile virus genomic RNA facilitates viral minus-strand RNA synthesis. *Journal of virology* **81**, 10172-10187 (2007).
278. Scott, I. & Norris, K.L. The mitochondrial antiviral signaling protein, MAVS, is cleaved during apoptosis. *Biochem Biophys Res Commun* **375**, 101-106 (2008).
279. Barretto, N. *et al.* Deubiquitinating activity of the SARS-CoV papain-like protease. *Advances in experimental medicine and biology* **581**, 37-41 (2006).
280. Barretto, N. *et al.* The papain-like protease of severe acute respiratory syndrome coronavirus has deubiquitinating activity. *Journal of virology* **79**, 15189-15198 (2005).
281. Lindner, H.A. *et al.* The papain-like protease from the severe acute respiratory syndrome coronavirus is a deubiquitinating enzyme. *Journal of virology* **79**, 15199-15208 (2005).
282. Ratia, K. *et al.* Severe acute respiratory syndrome coronavirus papain-like protease: structure of a viral deubiquitinating enzyme. *Proceedings of the National Academy of Sciences of the United States of America* **103**, 5717-5722 (2006).
283. Chen, T. & Cao, X. Stress for maintaining memory: HSP70 as a mobile messenger for innate and adaptive immunity. *European journal of immunology* **40**, 1541-1544 (2010).
284. Salminen, A., Paimela, T., Suuronen, T. & Kaarniranta, K. Innate immunity meets with cellular stress at the IKK complex: regulation of the IKK complex by HSP70 and HSP90. *Immunology letters* **117**, 9-15 (2008).

285. Gotoh, T., Terada, K., Oyadomari, S. & Mori, M. hsp70-DnaJ chaperone pair prevents nitric oxide- and CHOP-induced apoptosis by inhibiting translocation of Bax to mitochondria. *Cell death and differentiation* **11**, 390-402 (2004).